

an informal report intended for use as a preliminary or working document

END

All Public Utilities • Electric Power Research Institute • U.S. Nuclear Regulatory Commission • U.S. Department of Energy

LYSIS OF THE TMI-2
E RADIATION MONITOR

Revised by OSTI

NOV 08 1985

Michael B. Murphy
Jeffrey M. Mueller
William C. Jernigan

pared for the
Department of Energy
> Mile Island Operations Office
Contract No. DE-AC07-76ID01570

DISCLAIMER

This report was prepared as an account of work sponsored by an agency of the United States Government. Neither the United States Government nor any agency thereof, nor any of their employees, makes any warranty, express or implied, or assumes any legal liability or responsibility for the accuracy, completeness, or usefulness of any information, apparatus, product, or process disclosed, or represents that its use would not infringe privately owned rights. Reference herein to any specific commercial product, process, or service by trade name, trademark, manufacturer, or otherwise does not necessarily constitute or imply its endorsement, recommendation, or favoring by the United States Government or any agency thereof. The views and opinions of authors expressed herein do not necessarily state or reflect those of the United States Government or any agency thereof.

ANALYSIS OF THE TMI-2 DOME RADIATION MONITOR

**Michael B. Murphy
Geoffrey M. Mueller
William C. Jernigan**

Published August 1985

**Sandia National Laboratories
Albuquerque, New Mexico 87185**

**Prepared for EG&G Idaho, Inc.
and the U.S. Department of Energy
Three Mile Island Operations Office
Under DOE Contract No. DE-AC07-76ID01570**

ABSTRACT

Questions have been raised regarding the accuracy of the in-containment radiation readings from the LOCA qualified, dome radiation monitor, HP-R-214 during the March 28, 1979 accident at the Three Mile Island Unit 2 Reactor. This report discusses the accuracy of the readings, gives the results of examining the radiation monitor itself, and estimates the radiation environment inside containment during the accident.

**Prepared for the U.S. Department of Energy
Three Mile Island Operations Office
Under DOE B and R No. AG-35-30-10**

ACKNOWLEDGMENTS

The authors would like to thank the EG&G staff at the Three Mile Island Technical Integration Office for their efforts in obtaining the removal of the HP-R-214 from containment and for providing the authors with many details regarding accident events and other items. Dick Meininger and Lori Hecker were instrumental in this regard. We are also grateful to Willis Bixby of the U.S DOE and numerous individuals at General Public Utilities for their help and cooperation. Thanks also to Bill Hopkins of Bechtel, Inc. and Charles Mayo of SAI for their helpful comments and work regarding radiation sources and rates as well as their review of this report.

At Sandia, Ralph Trujillo did much of the chemical analysis and testing of elastomeric materials. Lloyd Bonzon and Frank Thome both assisted in our planning and examinations. Bill O'Neal performed the radioisotope analyses. Ray Alls provided many technical suggestions on how to proceed in the analysis and was our primary advisor on such matters. Betty J. Tolman was the editor of this report.

CONTENTS

I.	Summary and Recommendations	7
	A. Failure Modes	8
	B. Design Improvement Recommendations	9
	C. Gamma Total Dose Estimates	9
	D. Radiation Time History	10
II.	Introduction	15
III	Dome Monitor Description	19
	A. Physical Location and Container	19
	B. Channel Description	23
	C. Specifications and Operation	23
IV.	Examination Findings	27
	A. Handling and Decontamination	27
	B. Pressure Vessel Seals	29
	1. Leak Rate	29
	2. Stainless Steel Vessel Internal Contamination	29
	C. Detector Evaluation and Failure Modes	33
	1. Methods	33
	2. SS Vessel Attenuation	33
	3. Initial Detector Checkout and Examination	34
	4. Capacitor C17 Failure	36
	5. MOS Transistor Degradation	36
	6. Humidity Effects	36
	7. Radiation Measurement Characterization	40
V.	Radiation Total Dose	45
VI.	TMI-2 Radiation Time History	53
	A. Dome Monitor Stripchart Correction	53
	B. Two Hypotheses Regarding Radiation Levels	54
	C. Discussion of Stripchart Features	57
	D. Radiation Levels Outside the Vessel, Hypothesis 1	68
	E. Radiation Levels Outside the Vessel, Hypothesis 2	73
	F. Conclusions Regarding Hypotheses 1 and 2	73

APPENDICES

A.	Radiation Detector Operation	79
B.	SS Vessel Contaminant Levels and Chemical Analyses	92
C.	Ratemeter Readout Accuracy	119
D.	HP-UR-1901 Stripchart Recorder Accuracy and Corrected Data	121
E.	HP-R-214 Line-of-Sight to "Candy Canes"	135
F.	HP-R-212 and HP-R-213 Stripcharts	138
G.	Radiation Total Dose Information	140
H.	Gamma Transport Calculations and Results	154

FIGURES

1	HP-R-214 Corrected Stripchart	11
2	TMI-2 Gamma Radiation Time History	12
3	Dome Monitor Detector, Victoreen Model 847-1	16
4	Dome Monitor, Stainless Steel Container	17
5	TMI Unit 2, 345 Foot Plan Layout	20
6	Area Radiation Monitors at TMI-2	21

7	HP-R-214 Dome Monitor.21
8	Dome Monitor HP-R-214 Vessel22
9	Closeup of Two Vessel Holes.22
10	Cabling and Interconnect Diagram23
11	Exploded View of Dome Monitor Detector25
12	HP-R-214 Ratemeter, Victoreen Model 846-1.26
13	HP-R-214 and Shipping Container.28
14	HP-R-214 After Decontamination and Sealing28
15	Leak Rates29
16	Stainless Steel Container Rim.30
17	Stainless Steel Container Opened31
18	HP-R-214 Detector Readout Vs. Co 60 Source Strength.35
19	Humidity Effects37
20	HP-R-214 Detector Lo Amp Board38
21	End View of Detector Electrode Pin39
22	HP-R-214 Detector Pre-Amp Equivalent Circuit40
23	HP-R-214 Detector Readout on the Sandia Vertical Range41
24	HP-R-214 Readout Vs. Source Level.42
25	HP-R-214 Lo Amp and Hi Amp Outputs43
26	2N3565 Fairchild NPN Transistor Gain Degradation46
27	Transistor Annealing Characteristics48
28	HP-R-214 Cable49
29	Cable Silicone Insulation Degradation Characteristics.49
30	HP-R-214 Stripchart.55
31	Expanded Scale Stripchart, 1 to 30 hours58
32	Expanded Scale Stripchart, 20 to 1400 hours.59
33	Multivalued Response62
34	Actual HP-R-214 Stripchart Recording63
35	HP-R-214 Detector Block Diagram.66
36	TMI-2 Gamma Rate History, Hypothesis 170
37	Effects of Radioactive Gas Inside the SS Vessel.71
38	Moisture Correction.72

TABLES

I. SUMMARY AND RECOMMENDATIONS

The Dome Radiation Monitor at TMI-2 is the only instrument inside containment capable of measuring the high radiation levels which might be present during a loss-of-cooling accident (LOCA). As such, plant technical specifications (Reference 1) require it to be operative throughout a LOCA. The Dome Monitor provides operators with radiation level information which can be used to assess population exposure hazards in the event of a containment failure and the attendant radiation release. The Dome Monitor reading by itself can be used to declare a General Emergency. Since the accident at TMI-2, the Dome Monitor has been assigned a more important role in Regulatory Guide 1.97 (Reference 2) which addresses post accident monitoring equipment. It has been recognized that a high range monitor can be useful in controlling an accident by providing operators with one more useful bit of information regarding plant status.

During the accident at TMI-2, operators used the Dome Monitor readings as required and declared a General Emergency based on an 8 R/hr high alarm. Later, they calculated off-site radiation exposure levels based on a 300 R/hr reading. Our examination of the Dome Monitor has revealed that, while the declaration of a General Emergency was proper, the radiation levels measured were probably inaccurate at that time. Much later in the accident, they were certainly inaccurate. We show in this report that circuit failures occurred at various times during and following the first days of the accident. The accuracy of the monitor was also decreased by the presence of a thick lead and stainless steel shield used to protect the detector and its electronics.

Failures in the in-containment detector electronics package as well as chart scaling and other problems encountered in the control room confused operators during the accident and have severely complicated attempts by accident investigators to determine the true radiation levels inside containment. Our analysis of this radiation monitoring channel has led us through a labyrinth of possibilities and thus through often conflicting data. In our attempts to determine failure causes and to reconstruct the radiation time history inside containment, we have had to collect data ranging from the characterization of light transmittance properties of irradiated mylar to the effects of humidity on electrical circuits. It has been a most difficult and complex task.

In this report we present findings on our primary objective--that of determining the Dome Monitor detector failure modes and our best estimates of when they occurred. In conjunction with this we make specific recommendations for design improvements. Our secondary objective has been that of determining radiation levels inside containment, both total integrated gamma dose and gamma dose rate as a function of time. While we are highly confident

in most of our findings, we have reservations regarding the accuracy of our estimated gamma dose rate time history.

In general, however, the accident at TMI-2 demonstrates the need for improving radiation measurements during a loss-of-coolant accident. The Dome Monitor failures indicate that similar systems should be reconsidered. Finally, the accident indicates that equipment used in containment should undergo more extensive environmental testing prior to installation. A summary of our specific findings follows.

A. FAILURE MODES

The Dome Monitor detector consists of dual ion chambers and a fairly complex electronics package. These two components are housed inside a sealed container which is itself inside a sealed, lead-lined pressure vessel. The failure modes described below were generally the result of the severe, but not unreasonable, containment environment.

1. Moisture intrusion into the detector electronics package.

The protective stainless steel, pressurized vessel seal leaked and allowed moisture from the containment atmosphere to enter the vessel. This moisture easily permeated into the detector electronics package because of an inadvertent error in sealing the detector mounting bracket to the detector. This moisture reduced the resistance to ground in the high impedance ion chamber circuit and thus degraded the detector radiation measurement accuracy significantly. Moisture may have entered the electronics sometime within the first 3 hours of the accident.

2. DC feedback in the preamplifier. The effects of moisture were further accentuated by dc feedback paths in the two preamplifier circuits. The lowering of preamplifier input impedances by the presence of moisture coupled with the dc feedback paths caused the detector to, at times, indicate higher and lower levels of radiation than were actually present.

3. MOS transistor degradation. Both ion chambers use 3N163 Solitron MOS transistors to form high input impedance circuits. These MOS transistors were severely degraded by radiation exposure and eventually caused irregular jumps in radiation readings.

4. Electrolytic capacitor failure. Capacitor C17 leaked electrolyte onto the circuit board sometime after 416 days from the start of the accident. This leakage not only reduced the capacitance of C17, but also corroded completely through a transistor lead.

5. Reed switch reliability. We do not think that either reed switch in the preamplifier circuits failed during the accident; however, during our failure analysis both actually broke in half.

Either they were both degraded, or they were unacceptably fragile.

B. DESIGN IMPROVEMENT RECOMMENDATIONS

Our examination results strongly indicate the following design changes to improve high level radiation monitoring.

1. Fabricate the detector to be more nearly hermetically sealed. A single O-ring gasket of such a large circumference and with the particular sealing arrangement on HP-R-214 is not sufficient. Periodically seal and leak test the device to verify that it is sealed.
2. Do not use the detector inside a thick, lead-shielded vessel since it is impossible to predict levels outside such a shield. If this recommendation is implemented, the detector electronics must either be redesigned to operate after accumulating extremely high total radiation doses or must be removed from containment altogether. It is quite difficult to design a radiation-hardened circuit to operate in the Mrad region; therefore, we recommend placing the electronics outside of containment. (The proper seals are still required for the ion chambers.) If this is done, the maximum detection level should be increased from 10 KR/hr to at least 1 MR/hr. The minimum detection level can be increased from 0.1 mR/hr to 100 mR/hr. This can be done because this instrument is intended to operate in a LOCA and not simply to monitor normal low levels of radiation.
3. Do not use MOS transistors or MOS integrated circuits in any application where radiation exposure is a possibility. Most MOS devices are abnormally radiation sensitive and degrade dramatically at reasonably low doses.
4. Use military grade, or better, components in the electronics package. Mil Standard 883 Class B components should be sufficient for this application. These components undergo rigorous inspection and testing procedures and have a much improved reliability over standard commercial grade components. The electrolytic capacitors, plastic-encapsulated transistors, and reed switches are not suited for use in such an important piece of equipment, particularly where severe environments are possible.
5. Conformally coat all printed wiring boards. This minimizes effects in the event that moisture is able to circumvent a hermetic seal.

C. GAMMA TOTAL DOSE ESTIMATES

Using transistor current gain (HFE) degradation and elastomeric material degradation properties, we have estimated the total

gamma radiation dose received by the Dome Monitor (HP-R-214) electronics inside the stainless steel vessel and the dose in the multiconductor cable outside the vessel. We analyzed both at Sandia National Laboratories (SNL). In addition, we have summarized the doses received by other radiation detectors which have been analyzed at SNL. These doses, shown below in Table 1, are indicative of levels seen by other instruments and cables inside containment. These estimates refer only to gamma-induced damage and not beta damage since beta damage is generally a surface phenomenon.

Table 1. Total Gamma Radiation Doses Received by TMI-2 Radiation Detectors.

<u>Containment Elevation (Feet)</u>	<u>Instrument</u>	<u>Dose (rads)</u>
305	HP-R-211	2.5 X 10E5
305	HP-R-212	4.5 X 10E5
347	HP-R-213	9.9 X 10E5
372	HP-R-214	7.9 X 10E6
	Cable	
372	HP-R-214 Detector	2.2 X 10E5

D. RADIATION TIME HISTORY

The original Dome Monitor stripchart recording is erroneous because the output was plotted on five decade log paper rather than on eight decade paper and the recorder was improperly scaled. Figure 1 shows the Dome Monitor output as it should have been recorded, i.e. we have corrected the original stripchart to account for the log paper and scaling errors. This plot presumably gives the radiation levels inside the lead-lined stainless steel vessel. We have found, however, that some, if not all, of these radiation measurements are grossly inaccurate.

Our findings indicate that radiation levels recorded in the time period from 800 hours after the accident began until the monitor was finally turned off are incorrect because of both moisture intrusion into the detector and component failures. During the first 800 hours of the accident, the available data supports the proposition of two hypotheses regarding accuracy. Hypothesis 1 proposes that the Dome Monitor was relatively accurate even though some moisture had probably entered the detector housing. Hypothesis 2 says that the monitor was inaccurate for substantially all of the accident because of moisture intrusion into the detector as early as 7:00 a.m. on the day of the accident.

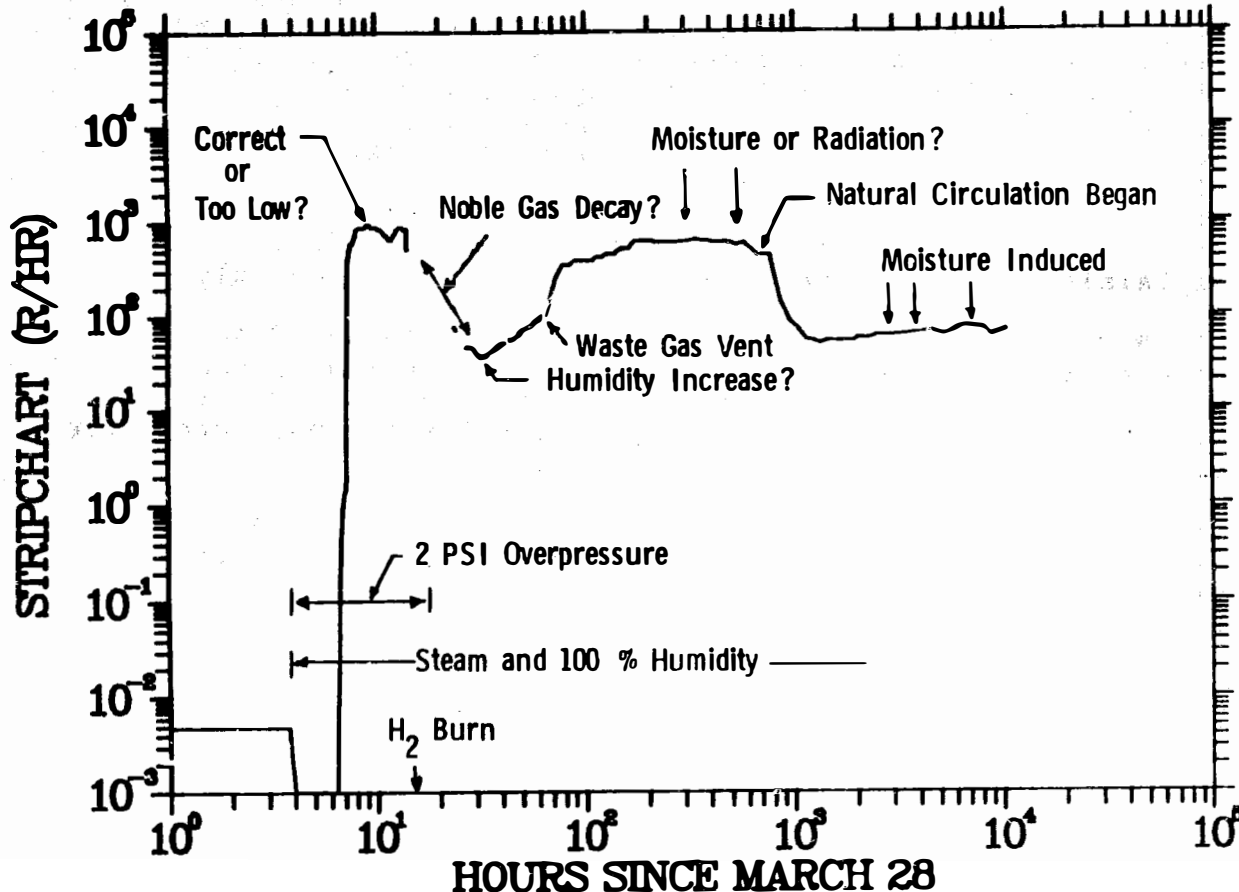


Figure 1. HP-R-214 Corrected Stripchart. The original HP-R-214 stripchart recording has been plotted on the proper log paper and corrected for recorder scaling errors.

If we adjust the peak radiation level based on our confidence in our radiation total dose measurements, the peak level associated with Hypothesis 2 is some 25 times higher than that actually recorded. Hypothesis 1 is supported in part by the fact that the radiation dose received by the detector electronics corresponds closely to the integrated area under the corrected stripchart recording.

The major difficulty with Hypothesis 1 is that the indicated radiation levels in the 60 to 800 hour time frame are much higher than predicted based on the release of noble gas. No plausible radiation source has been found which would produce such high levels so late in the accident, including the shine from the steam generator candy canes.

Hypothesis 2 is plausible since the detector has such an unusual response in the presence of even small amounts of moisture. Our laboratory tests show the detector in the presence of moisture to read too low for high radiation input levels and too high for low radiation input levels. While we have found the detector to be substantially in error in the presence of moisture, the magnitude of the errors are not large enough to fully explain both the peak rate associated with Hypothesis 2 or the rate in the 60 to 800 hour time frame. Another problem with Hypothesis 2 is that of explaining how moisture entered the detector so quickly.

We favor the second hypothesis primarily because of our inability to explain the Dome Monitor stripchart recording in the 60 to 800 hour time frame. Something appears to be wrong. We minimize the difficulties associated with Hypothesis 2 since moisture intrusion and moisture effects are so variable.

Gamma radiation rates as a function of time both inside the vessel shield and in the outside containment atmosphere are estimated in Figure 2. Here, we assume that Hypothesis 2 is

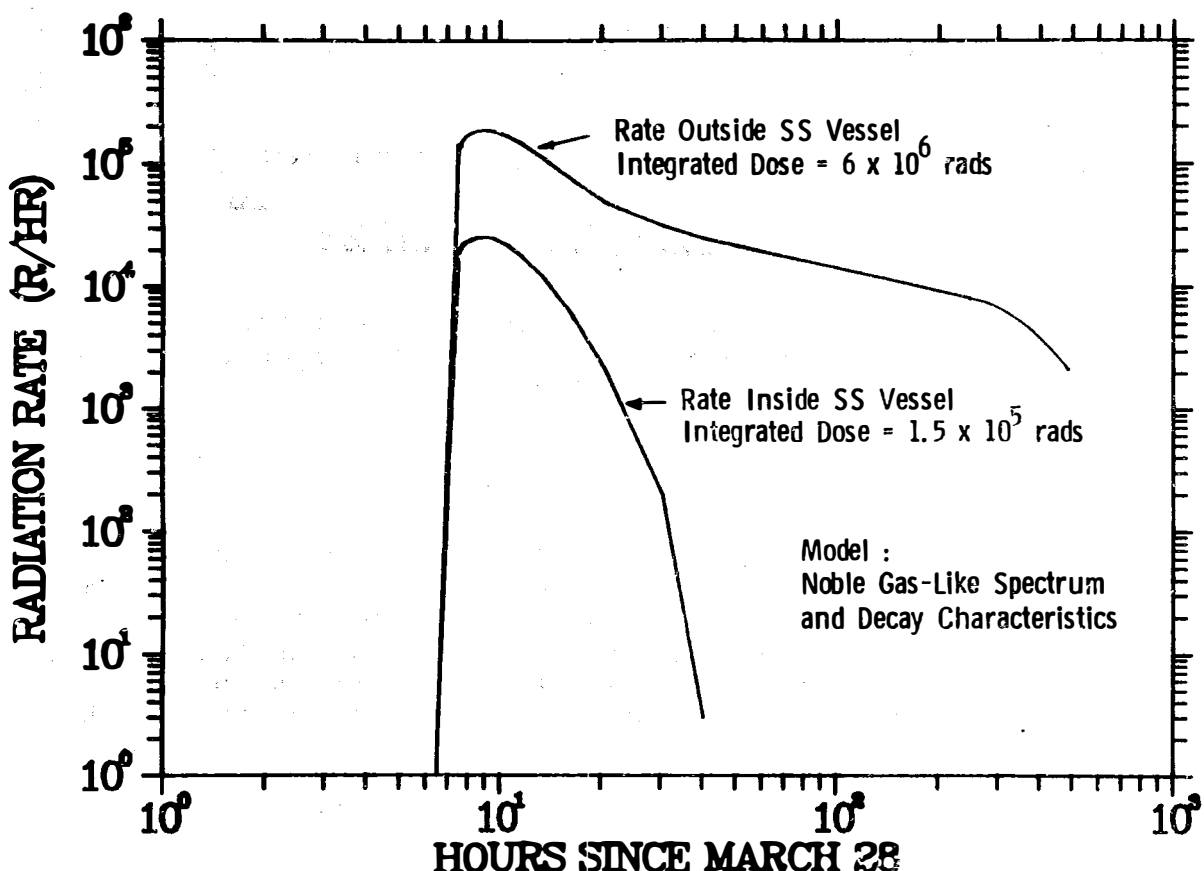


Figure 2. TMI-2 Gamma Radiation Time History. This is our best estimate of radiation history both inside and outside the stainless steel vessel (Hypothesis 2). We have assumed a noble gas spectrum and decay characteristics in order to calculate the level outside the vessel.

II. INTRODUCTION

A Site Emergency at TMI-2 was declared at 6:55 a.m. on March 28, 1979 and was based on high radiation readings from several process and area radiation monitors located inside the TMI-2 Containment Building (Reference 3). Radiation levels had actually begun to rise inside containment at approximately 6:27 a.m. as recorded by a low range area radiation monitor, HP-R-213. This monitor is located at the 347 foot level of containment.

At 6:32 a.m. the high range Dome Radiation Monitor, HP-R-214, also began to show increased levels of radioactivity. At 7:10 a.m. reactor operators made offsite exposure calculations should a containment breach occur. These calculations were made in accordance with regulations to estimate the offsite exposure rate downwind in Goldsboro, Pennsylvania. Goldsboro is situated 1.2 miles west of the plant. Using a 300 R/hr radiation reading from the Dome Monitor, engineers estimated that the whole body exposure rate could be as high as 40 R/hr in Goldsboro. Investigators were later to discover the 300 R/hr reading was incorrect because operators had misread the level off the Dome Monitor readout meter. This error was of no great consequence, however.

At 7:27 a.m. a General Emergency was declared in accordance with licensing provisions, based on a Dome Monitor reading of greater than 8 R/hr. The shift supervisor contacted the Pennsylvania Bureau of Radiological Health and the Civil Defense to inform them of the direction of the wind and suggested they be prepared to evacuate the area west of the plant. However, because of a low Containment Building pressure of only 1 psig and his feeling that the 40 R/hr calculation was unreliable, the supervisor ordered radiation surveys to be made around the plant boundary prior to recommending an evacuation.

By 8:00 a.m. radiation surveys had been made and no significant levels of radioactivity had been detected. The Civil Defense was advised of this and was asked to standby. More radiation surveys were then conducted, and the results of these and the fact that Dome Monitor readings had stabilized and a containment breach was unlikely convinced officials that a large scale evacuation was unnecessary. Eventually, the initial 40 R/hr calculations were shown to be in error. The sequence of events just described demonstrates the way in which Dome Monitor readings can be and were used during an accident.

The Dome Monitor stripchart recording represents the only record available of the radiation levels inside the TMI-2 Containment Building as a function of time. If this record could be interpreted properly, containment release models used in reactor safety studies could be at least partially validated. These models are used to predict LOCA radiation levels likely to be present inside containment, and can thus establish equipment

qualification standards and design guidelines. The stripchart record in the Control Room, however, was in error.

Unfortunately, the Dome Monitor radiation detector appears to have failed over the course of the accident in at least three ways. This report discusses the results of our examinations of the radiation detector (Figure 3) and its stainless-steel, lead-lined container (see the ss vessel in Figure 4), the ratemeter readout module, and the detector signal and power cable. The various failure modes of the detector are described, and these are used to better interpret the stripchart record. Correction factors are applied to the record to account for both failures and recording errors. The result is a "corrected stripchart" recording of the radiation levels inside the shielded ss vessel. Estimates of radiation levels outside the container are then made.

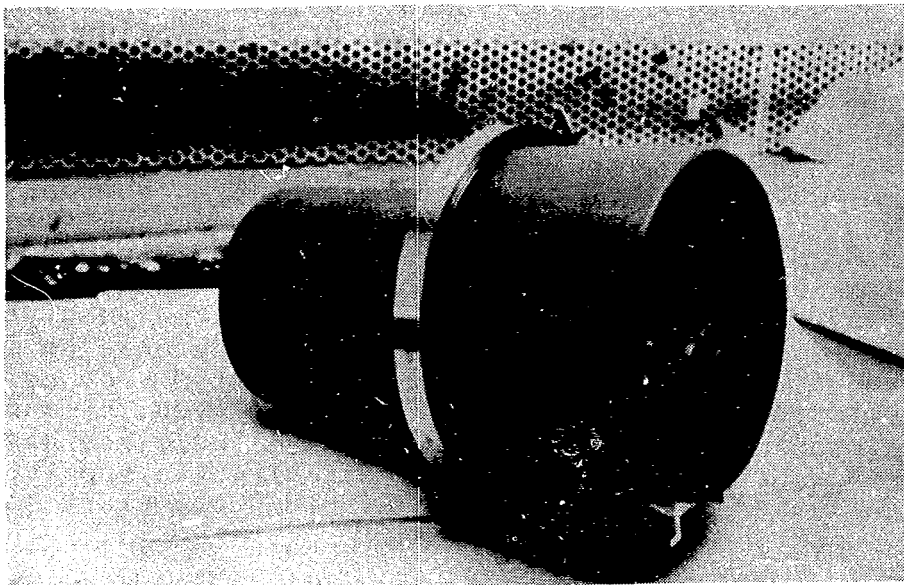


Figure 3. Dome Monitor Detector, Victoreen Model 847-1.

This report will focus on:

- Failure modes of the detector;
- Radiation dose absorbed by the detector and cable;
- Radiation levels as function of time, inside the vessel; and
- Radiation levels as function of time, outside the vessel.

The radiation detector was removed and examined as a part of the DOE TMI-2 Instrumentation and Electrical Equipment Examination Program which is administered by the DOE/EG&G Technical Integration Office (TIO) at Three Mile Island.

correct, and we calculate the time history based on total gamma dose measurements only. To do this, we have assumed the radio-nuclide energy spectrum and decay characteristics to be that of noble gases. Under these conditions the peak gamma rate in the upper part of containment was on the order of 200,000 R/hr. If we assume a 60% noble gas release, other radionuclides must account for about 85% of the level of activity. This seems high; therefore, it is our guess that 200,000 R/hr is an upper bound of the actual rate. We place no error bars on these estimates because of the numerous potential sources of error.

Notice that as time passes and the energy spectrum becomes softer, the rate inside the lead-shielded vessel drops dramatically with respect to that outside the vessel. This shows the importance of having a detector which does not require extensive shielding to survive. This detector is essentially useless after 20 hours, even though external radiation levels are still quite high.

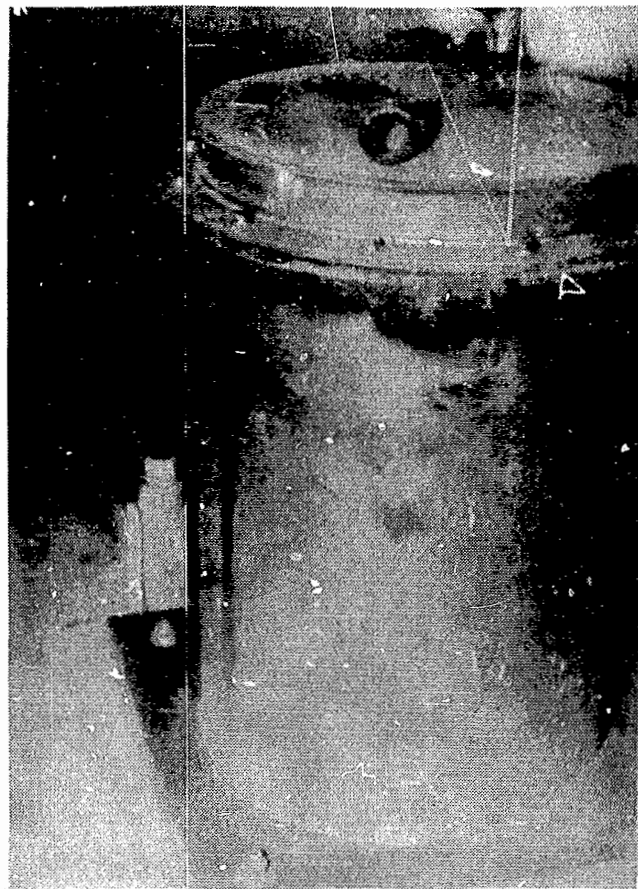


Figure 4. Dome Monitor, Stainless Steel Container. Notice the electrical cable and the hole positions.

III. DOME MONITOR DESCRIPTION

A. PHYSICAL LOCATION AND CONTAINER

The Containment Building Dome Radiation Monitor at TMI-2 is located on top of the elevator shaft enclosure roof at an elevation of 372 feet. Figure 5 shows a plan view of the 345 foot operating level with the Dome Monitor located near the Containment Building wall. Figure 6 shows the placement of the Dome Monitor in containment. This location, although a good distance from the top of the 473 foot dome, provides a good view of the entire upper level. Figure 7 is a photograph of the Dome Monitor before removal; as can be seen, it is in a relatively uncluttered area.

The actual radiation detector is packed in fiberglass insulation and is housed inside the stainless-steel vessel. The vessel (sectional view, Figure 8) has lead between its double walls.

Both the inner and outer walls are ss and each is 3.175 mm thick. Molten lead has been poured into two openings at the top upper rim and completely fills the 3.962 cm gap. The inner and outer steel walls have been welded in such a way as to form an airtight container. The entire container weighs approximately 250 Kg.

The lid-to-container seal is a circular, flat, silicone, rubber gasket 63 mm wide and 3.8 mm thick. When the lid is bolted down in place, the container is meant to be sealed against intrusion by radioactive gas and water. The external connector, through which power and signals are supplied to the detector inside the container, is hermetically sealed and welded to a steel pipe exiting the vessel. The purpose of the lead shield is to attenuate the extremely high gamma levels associated with a LOCA so that the instrument inside can be kept in range. Of course, the attenuation factor is highly energy dependent. For 0.8 MeV gamma energies the shield will reduce the levels (as seen by the detector inside) by a factor of 74.7, whereas for 1.3 MeV gamma energies the attenuation factor is only 17.8.

During a LOCA the first radiation to be released is the radioactive gas which fills the gap between the fuel rod cladding and the fuel pellets. This gas has a major element of the noble gas, XE 133, which emits gamma rays with energies of only 81 KeV. In order to detect XE 133 as early as possible, two holes were drilled through the outer ss wall and through the lead up to (but not through) the inner wall. These holes are on the side of the vessel directly opposite the connector (Figure 9) and are 1.27 cm and 3.175 mm in diameter. The larger hole is situated approximately 12.7 cm up from the baseplate. The vessel is oriented so that the holes point toward the center of the Containment Building.

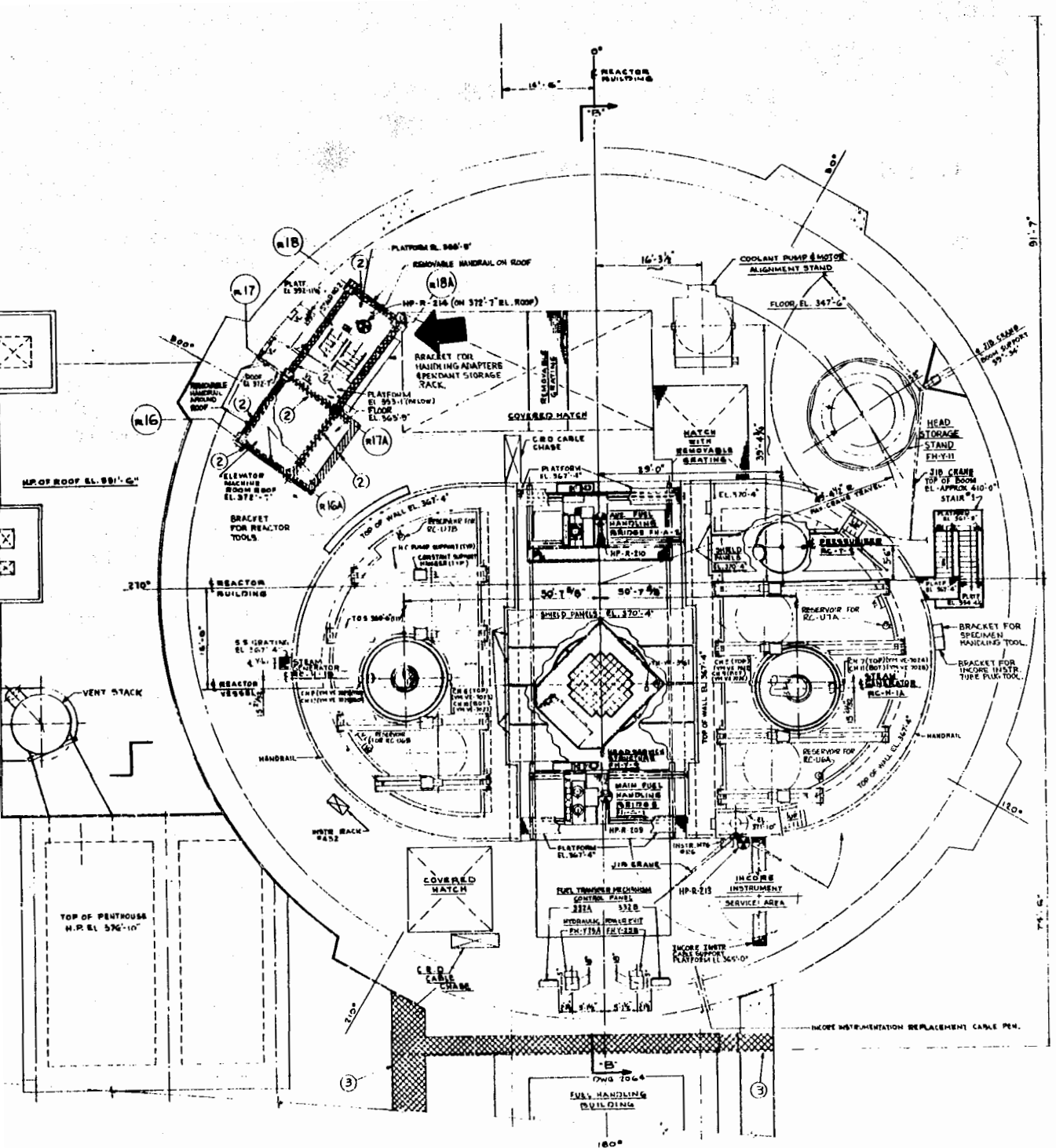


Figure 5. TMI Unit 2, 345-Foot Plan Layout. The Dome Monitor Detector HP-R-214 is located on top of elevator shaft as shown by the bold arrow.

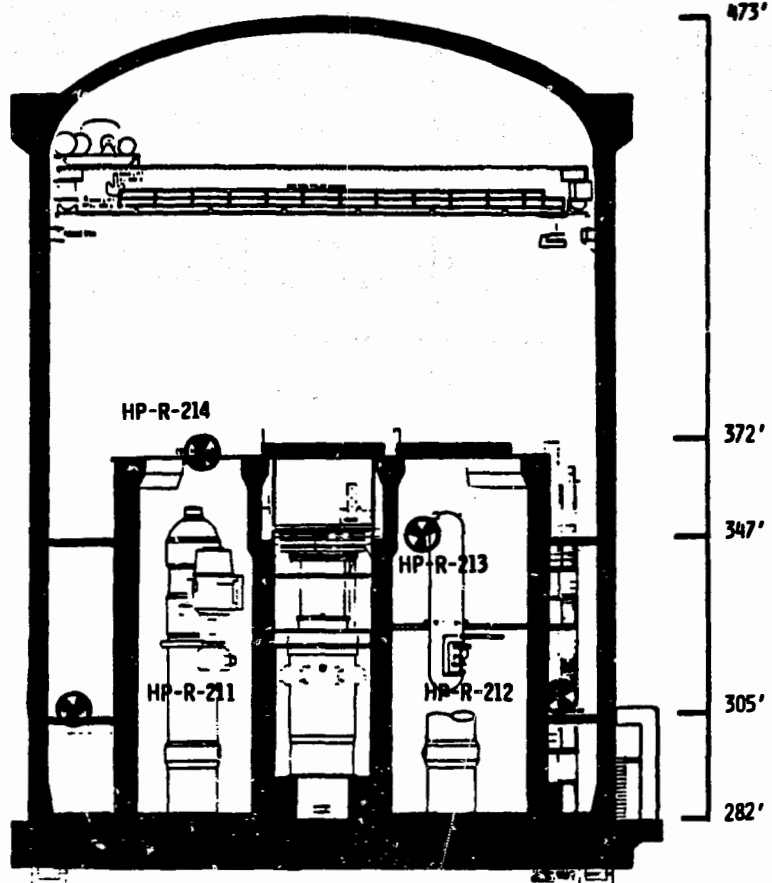


Figure 6. Area Radiation Monitors at TMI-2.

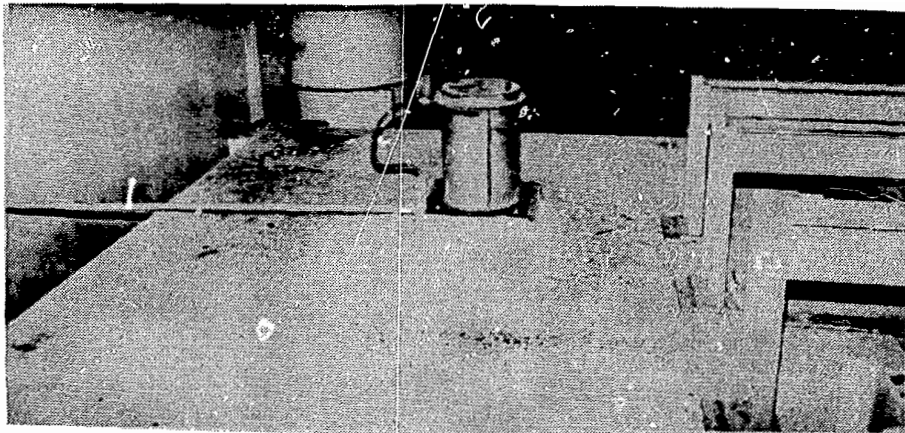
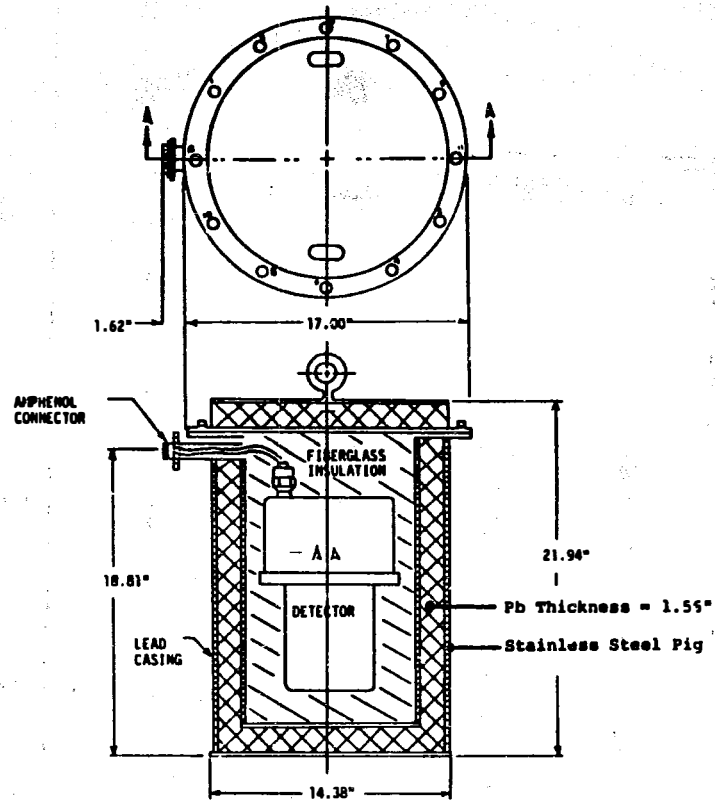


Figure 7. HP-R-214 Dome Monitor. The stainless steel vessel is shown in place on top of the elevator shaft.



**Figure 8. Dome Monitor HP-R-214 Vessel.
Cross section of stainless steel container.**

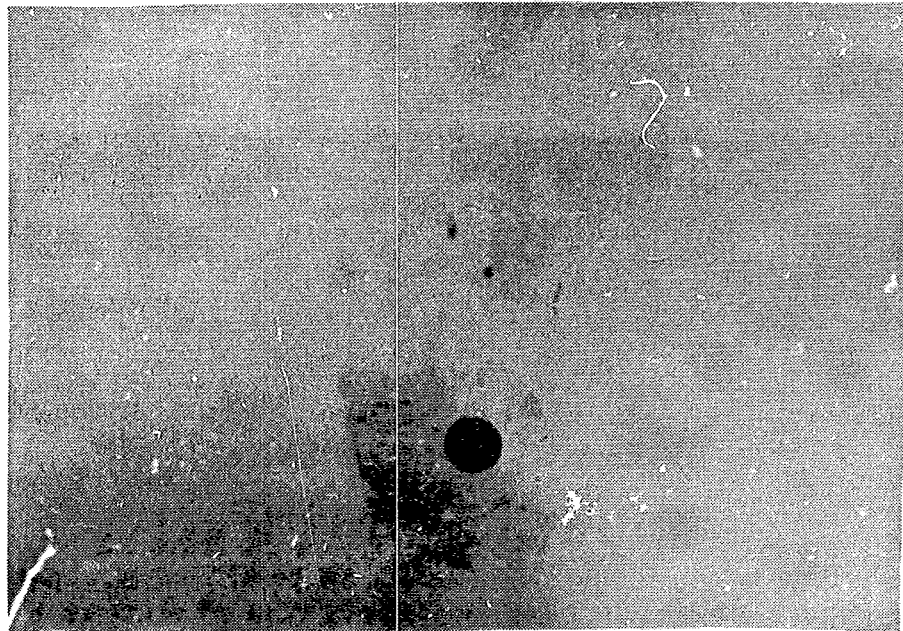


Figure 9. Closeup of the Two Vessel Holes.

B. CHANNEL DESCRIPTION

The Dome Monitor Radiation Measurement Channel consists of the Victoreen Model 847-1 detector which is inside the ss vessel and the Victoreen Model 846-2 readout module which is located in the TMI-2 Control Room. A multichannel stripchart recorder, HP-UR-1901 is connected to the readout module; this recorder is also in a rack in the Control Room. Figure 10 shows the cabling and interconnection diagram of the system. Approximately 130.5 meters of cable separate the two instruments. Victoreen designed the channel and also supplied the ss vessel.

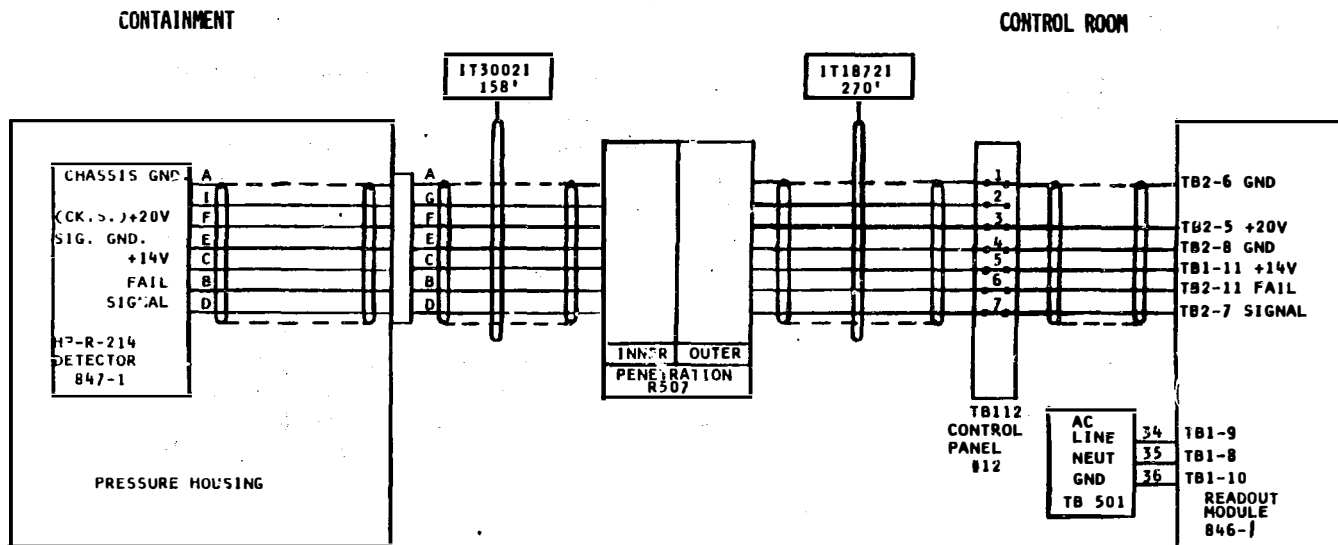


Figure 10. Cabling and Interconnect Diagram. The approximate length in feet of each cable is shown.

C. SPECIFICATIONS AND OPERATION

The detector and readout form a standard Victoreen 845 Area Monitoring System. The specifications for the System (excluding the ss vessel) are given in Table 2. This system is intended to satisfy NRC regulations which require a high range radiation monitor capable of measuring radiation levels as high as $10E7$ R/hr (Reference 2). The radiation monitor is required to withstand the temperatures, pressures, and steam environment associated

Table 2. Specifications for the 845 Area Monitoring System.

Ran e:

Full-Scale.....	8 decades from 0.1 to 10 mR/h
Three-Decade.....	0.1 to 10^2 , 1 to 10^3 , 10 to 10^4 , 10^2 to 10^5 , 10^3 to 10^6 and 10^4 to 10^7 mR/h
Precision.....	+ 10% in any decade
Circuitry.....	All Solid State
Type of Radiation Detected.....	Gamma or X-Ray
Energy Dependence.....	80 keV to 3 MeV + 10%
Directional Dependence.....	Less than 10% in any direction with ^{60}Co
Type of Detector.....	Dual coaxial ionization chamber of atmospheric pressure
Pressure Limits.....	15 psig for both detector and readout module
Temperature Limits:	
Detector.....	-40°F to + 140°F (-20°C to + 60°C)
Readout Module.....	32°F to + 140°F (0°C to + 60°C)
Humidity.....	0 to 95% for both detector and readout module
Alarms.....	ALERT and HIGH, adjustable, set point of either shows on meter when pushbutton is depressed
External Alarm Contacts.....	One set of Form C (SPDT) contacts rated at 115V, 5A dc
Alarm Reset.....	Optional-manual or automatic
Fail Indicator.....	Green light, normally on, goes off to indicate failure of any type
Recorder Output.....	0 to 10 mV + 0.14 mV (always indicates 8 decades)
Computer Output.....	0 to 50 mV + 0.68 mV (always indicates 8 decades)
Internal Power Supply.....	14.0 V + 10 mV

with a full-scale LOCA. Detailed descriptions of how the detector and readout operate is given in Appendix A of this report and in Reference 4.

Briefly, the detector is capable of measuring gamma or x-ray radiation levels ranging from 0.1 mR/hr to $10E4$ R/hr (8 decades). The detector uses dual coaxial ion chambers with high and low range ion current outputs. The larger volume, outer chamber measures the lower four decades; the smaller volume, inner chamber measures the upper four decades.

The electrical circuitry associated with the ion chambers is contained on three printed wiring boards which are mounted on a bracket affixed to the ion chamber assembly. Figure 11 shows an exploded view of the detector assembly. A housing cover is placed over the electronics and seals the electronics enclosure to the ion chamber assembly via a rubber O-ring. Power and signal lines exit the entire assembly through a hermetically sealed connector mounted in the housing. Presumably, the assembly is then hermetically sealed. (We will see later in this report that the seal was violated.)

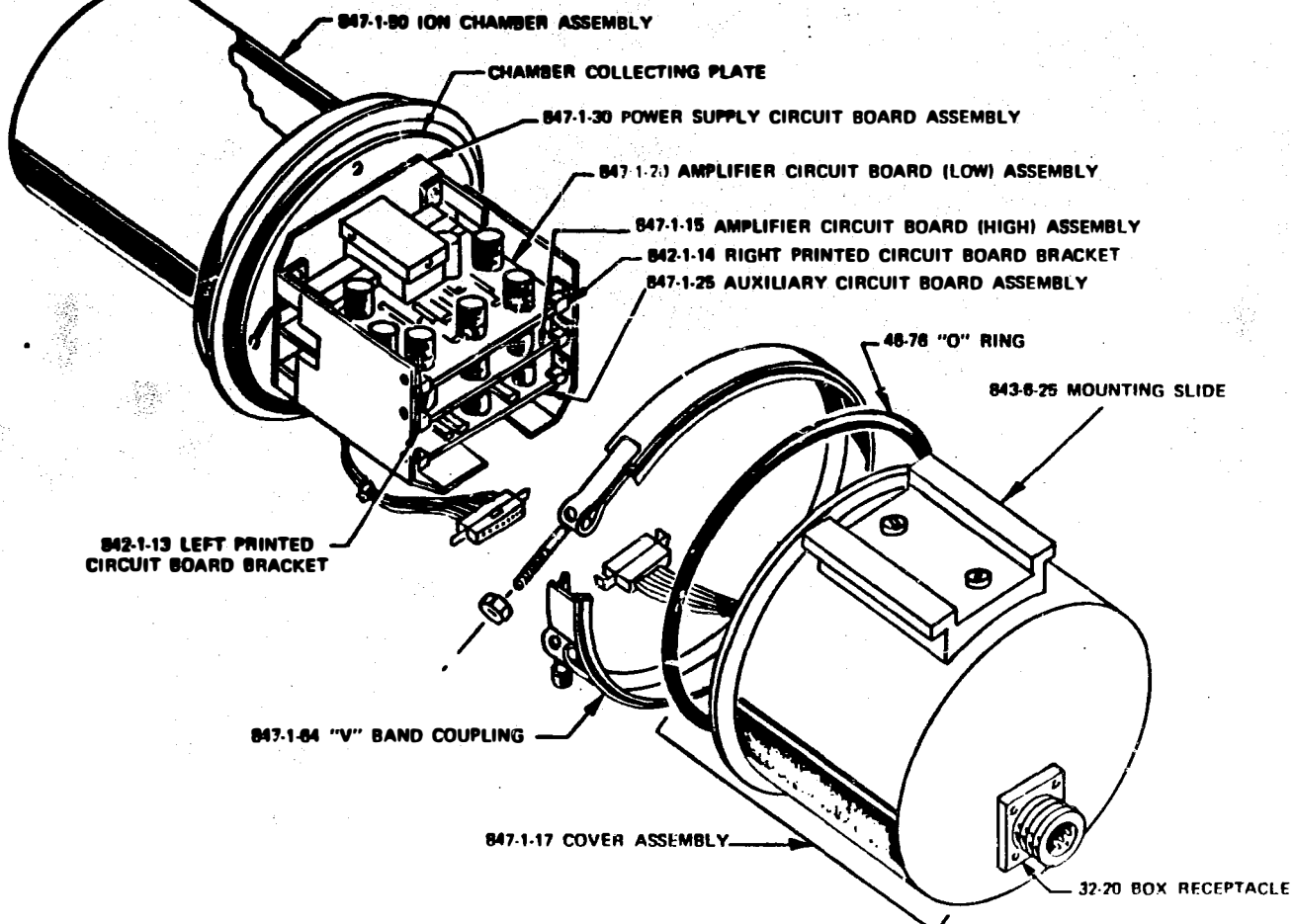
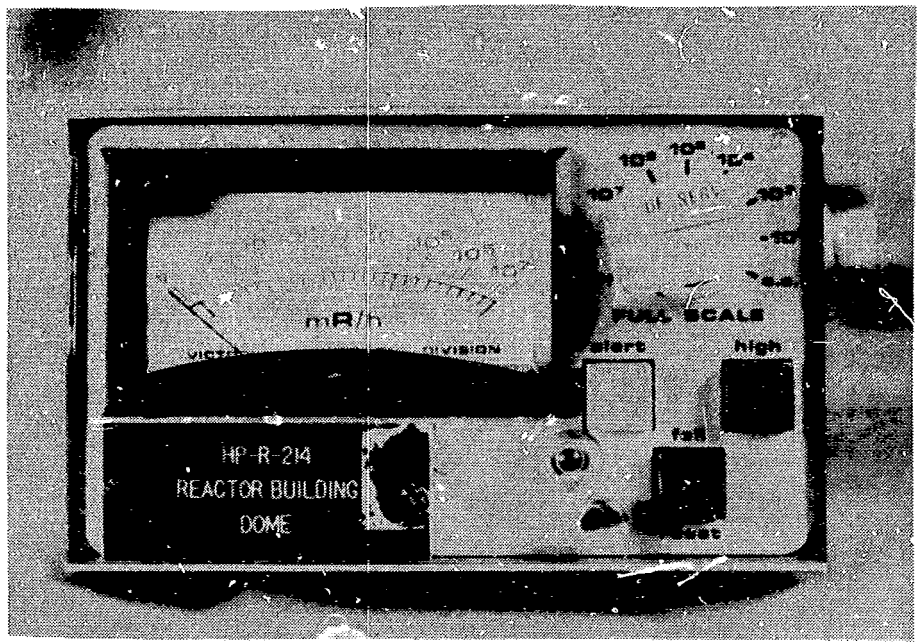


Figure 11. Exploded View of Dome Monitor Detector.

The top two circuit boards are the amplifiers for the two ion chamber outputs, and the third board consists of a power supply, a summing amplifier, a timing signal generator, and miscellaneous circuitry. The two ion current amplifiers are almost identical. The ion current from the chambers is sampled every 333 msec by a reed switch closure. This current sample is converted to a voltage by charging a capacitor in the high impedance input circuit. An MOS transistor forms a source follower in the input circuit to achieve the high impedance required.

The output signal from this circuit is later sampled again and amplified in stages of $x1$, $x9$, $x10$, and $x10$. The outputs from each of these amplifier stages are clipped at 9.5 volts and summed in an amplifier, along with similar outputs from the other ion chamber amplifier string. Thus, an ion current derived signal voltage is multiplied by 900 by the time it reaches the last stage of each amplifier string.

When all eight amplifier outputs are summed, 8 decades of level can be displayed on the meter and the scale is linear between decades. The readout is shown in Figure 12. Both the ion current buffer/preamplifier circuit and the method of summing amplifier outputs play important roles with respect to detector failure modes. These subjects are discussed in detail later in this report.



**Figure 12. HP-R-214 Ratemeter, Victoreen
Model 846-1.**

IV. EXAMINATION FINDINGS*

A. HANDLING AND DECONTAMINATION

The Dome Monitor, HP-R-214, was removed from containment in May, 1982 and was shipped to Sandia National Laboratories; it arrived in Albuquerque, New Mexico on June 24, 1982. At TMI-2 (under the direction of Bechtel, Inc.) the unit was unbolted from the elevator shaft roof and hoisted via a steel-cable belt arrangement (attached to the polar crane rails) to the 347 foot Containment Building level. Subsequently, the unit was moved to the 305 foot level where it was placed into a specially designed, steel box for protection. Unfortunately, while placing the unit into the box it was inadvertently turned 90 degrees from its proper orientation and forcefully jammed into the box. This shattered the hermetically sealed connector and thus violated the container seal. The unfortunate accident is the only damage the unit sustained from its removal to its unpacking. Shock monitors which had been mounted on the unit before its shipment from TMI-2 confirmed that it had received gentle handling in transit. Figure 13 shows the vessel inside the box. Handling the unit at TMI-2 and SNL has been difficult because of its weight.

The damaged connector was removed, and the open pipe was sealed before decontamination could begin. Numerous swipe samples and metal filing samples were taken before decontamination. On June 29, 1982 the unit was decontaminated by repeated washings and scrubbing with Brillo pads. Trifluorethylene, Radiac foam, Turco 4324 and Tide were all used in the process. Average beta/gamma radiation levels measured at a distance of 2.5 cm from the ss vessel surfaces before decontamination using a geiger counter were:

	$\beta\gamma$	γ
Top	35 mR/hr	10 mR/hr
Sides	14 mR/hr	6 mR/hr
Baseplate	170 mR/hr	50 mR/hr

Decontamination reduced these levels by a factor of about two. After decontamination, the stainless steel was bright and shiny and the entire unit was sprayed with Krylon to trap any contaminant particles. Figure 14 shows the unit after decontamination.

*Much of the data presented in this chapter is contained in laboratory notebooks kept during our examination to accurately document our findings. See References 5, 6, and 7.

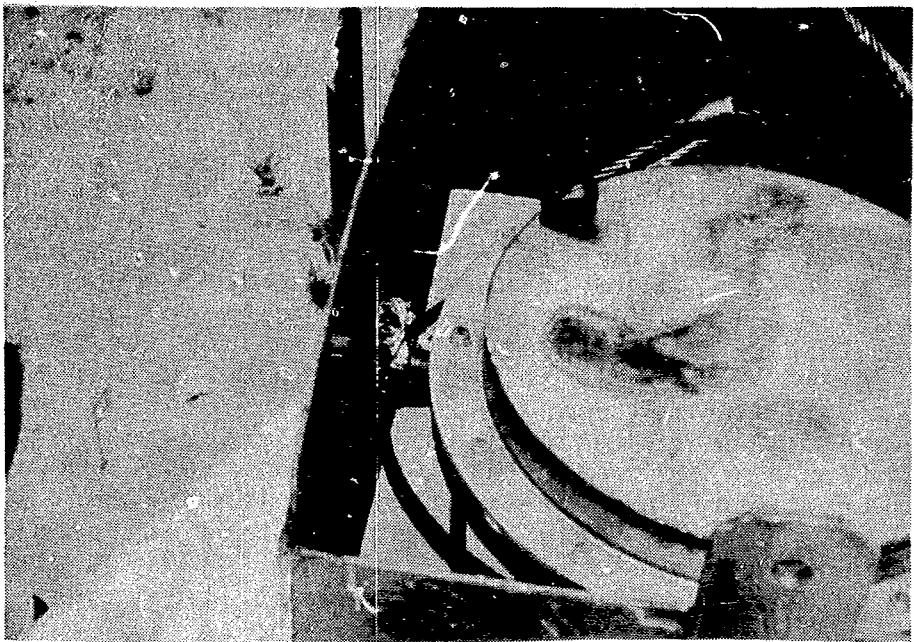


**Figure 13. HP-R-214 and Shipping Container.
The crushed connector is shown on the left.**

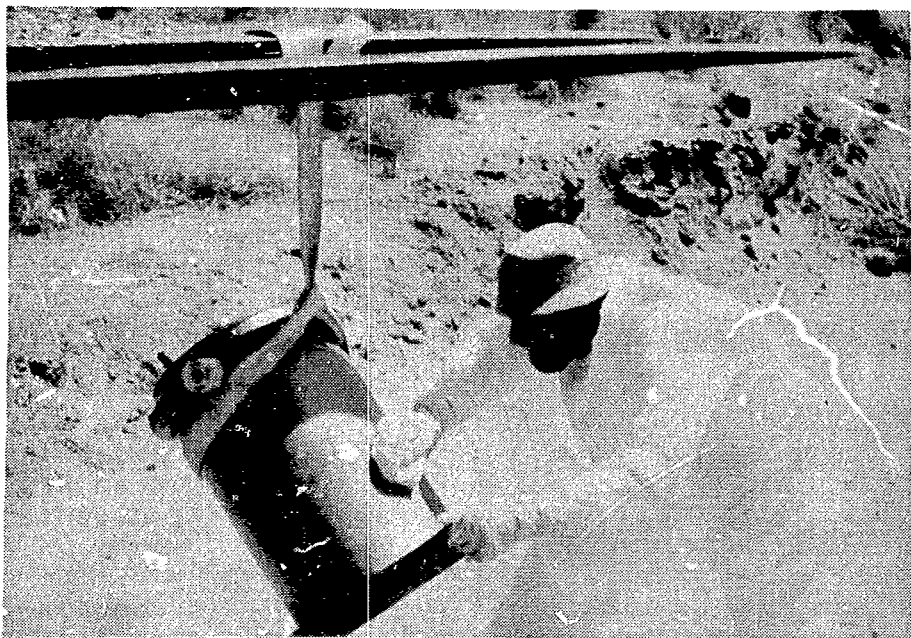


Figure 14. HP-R-214 After Decontamination and Sealing.

B. PRESSURE VESSEL SEALS

1. Leak Rate. A major concern regarding the accuracy of the Dome Monitor readings during the accident was whether or not the lead shield had somehow been circumvented by radioactive gas and suspended or dissolved radioactive particles. The damage to the connector incurred during removal from containment breached the seal and undoubtedly allowed some cesium contamination to penetrate to the inside of the container, making it difficult to determine when contamination occurred. Nevertheless, our examination revealed that probably only a small quantity of contaminants would have been able to enter the container in this way, since the connector still partially covered the 2.5 cm diameter tube end.

We mounted a specially designed fitting to the undamaged tube end which allowed us to leak-test the ss vessel. We then pressurized the container to 10 psig and observed the pressure as a function of time. Later in our examination, we injected air into the detector itself through the hermetic connector and measured the leak rate of the detector. We did this by inserting a hypodermic syringe needle through the rubber center portion of the connector and pumping air into it. The results of both these tests are shown in Figure 15.

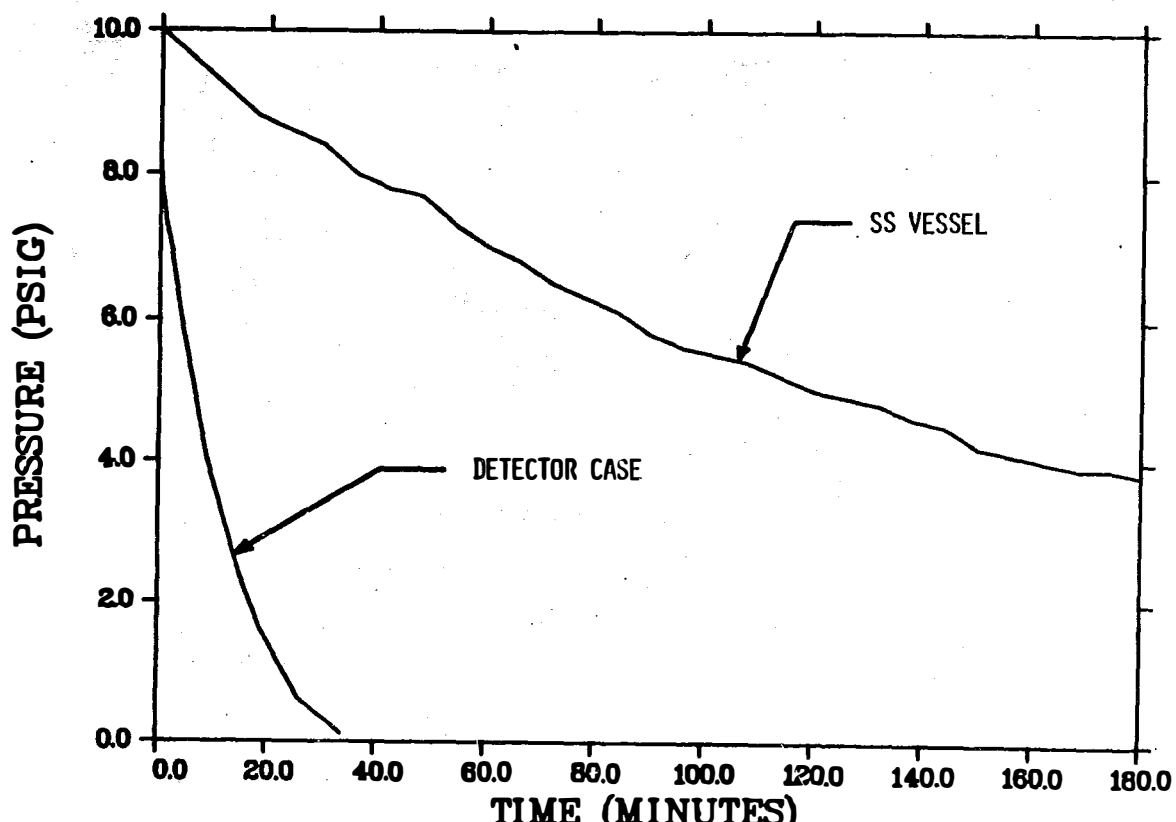


Figure 15. Leak Rates. The stainless steel vessel and detector container leak rates.

The ss vessel is seen to have an approximate exponential leak rate with a time constant of approximately 3.0 hours. The leak rate of the detector case is also approximately exponential with a time constant of 12.5 minutes. We were not able to find precisely where the ss vessel was leaking; however, we feel that the leak was probably under the large, flat gasket which seals the vessel to the lid. The leak in the detector electronics portion was through two unsealed screwholes used to mount the wall-mounting bracket to the detector case. The O-ring seal appeared to be intact. This breach of seal is a serious oversight in the detector mechanical design as will be shown later in this report with reference to a path for humidity to enter the detector electronics package.

2. Stainless Steel Vessel Internal Contamination. As stated earlier, it was very important to determine whether significant radioactive contaminants were able to get inside the ss vessel. Because of this concern, we removed the vessel lid carefully to reduce the possibility that containment "dust" would fall into the vessel. All twelve top retaining bolts were tight, having a minimum of 60 inch-pounds breakaway torque. After the lid was removed, it was apparent from the spreading of the gasket that the top was indeed securely fastened. Figures 16 through 17 show the vessel and detector in various stages of disassembly.



Figure 16. Stainless Steel Container Rim. The lid has just been removed. Notice how "dirty" the rim area which was under the gasket is. The radiation level measured 3 mR/hr in approximately the probe location shown in the photograph.

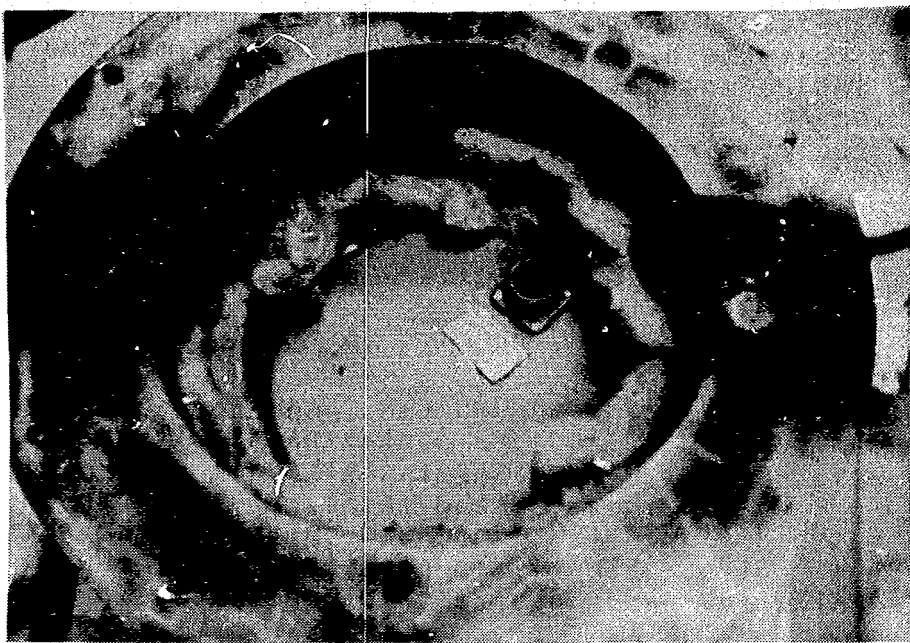


**Figure 17. Stainless Steel Container Opened.
The top layer of insulation has been removed
exposing the detector.**

With the lid off, geiger counter readings showed gamma levels to be 1.3 mR/hr approximately in the center of the inside of the vessel near the top and around 3 mR/hr around the rim under the gasket; this indicates that contaminants were present inside the vessel. The inside surface was somewhat dirty and appeared to be slightly oily. Its appearance suggests that after fabrication, it had not been thoroughly cleaned. Numerous discolorations and precipitant collection points were found on the underside of the lid and underneath the gasket.

A series of radiation and chemical tests were conducted at this point to determine whether contaminants had actually leaked into the vessel during the accident or whether the radiation measured was a result of its entry through the broken connector. These tests are summarized below; detailed data is given in Appendix B.

- a. Swipe samples taken from the various vessel and detector surfaces were counted.
- b. Fiberglass samples taken from various locations inside the vessel were counted.
- c. Chemical analysis of materials on the vessel lid underside were made.
- d. Chemical tests looking for boron on the swipe and cotton swab samples were conducted.

The swipes indicated that Cs 137 was distributed throughout the vessel, but that the distribution was not uniform. The averaged data below indicates that the bottom had substantially higher concentrations of Cs 137 than other parts of the vessel. (Cs 137 was by far the most prevalent radioisotope and was used as an indicator of radiation activity.)

Bottom	.14	uCi/swipe
Lid	.019	uCi/swipe
Sides	.0031	uCi/swipe

Had contaminants diffused through the connector tube after the connector was damaged or had the contaminants simply fallen off the lid during removal, the contaminant levels of the sides would have been larger than those on the vessel bottom. It thus appears as though a liquid was condensed on the inside surfaces and flowed to the bottom. Fiberglass activity measurements summarized below further supports this conclusion.

Middle Bottom	340016	counts/600 sec
Geometric Center	246	counts/600 sec
Outer Top	5133	counts/600 sec

The fiberglass was taped around the detector and came out of the vessel as a single unit. The "middle bottom" sample was in direct contact with the vessel bottom; the "outer top" was in contact with the vessel lid; the "geometric center" was closest to the detector and completely surrounded by other fiberglass. If we postulate that radioactive gas and aerosol with suspended particles in it had freely entered the vessel, we would suspect that plateout and attachment would be somewhat uniform throughout the fiberglass. This was definitely not the case. The portion of the fiberglass which was in direct contact with vessel surfaces (top or bottom) had substantially higher concentrations of contaminants than those portions toward the center of the bundle.

Four samples of particulates on the underside of the lid were examined using a scanning electron microscope and x-ray energy dispersive spectroscopy. This analysis showed major elements to be Si, Ca, and Ti; the minor elements were Al, Pb, and Fe. We would expect these elements on the vessel because of manufacturing; we would also expect these elements if tap water had evaporated and left precipitates.

Boron is an element used in containment sprays and unlike sodium hydroxide is not commonly found in tap water, neither is it a result of the manufacturing process. Emission spectroscopy tests were made on swipe samples and moist cotton swab samples were taken from inside the vessel. These tests showed small but significant amounts of boron (200 ug/sample) in the vessel.

These radiation and chemical tests strongly indicate that containment spray and radioactive liquid entered the ss vessel during the accident. The most probable entry was beneath the flat gasket under the vessel lid. It does not appear as though significant amounts of radioactive gas entered; instead, our guess is that liquid which had accumulated in the lip area gap (between the lid and the vessel) entered the vessel by capillary action and that the liquid ran down both the inner sides of the vessel and on the underside of the lid. The pressure differential (approximately 3 psig at various times) between the containment atmosphere and that inside the vessel helped to force the liquid inside. Radiation levels indicate that only small amounts of liquid (even in the manner just described) actually entered the vessel.

C. DETECTOR EVALUATION AND FAILURE MODES

1. Methods. After the ss vessel was decontaminated, a lengthy series of gamma facility tests were conducted in an effort to characterize the TMI-2 detector's response to a radiation stimulus. These tests were performed at the SNL Vertical Range (VR), Gamma Irradiation Facility (GIF), and the High Intensity Adjustable Cobalt Array (HIACA) facilities.

The VR is calibrated to National Bureau of Standards (NBS) specifications and is capable of producing maximum gamma levels of approximately 600 R/hr. The GIF and HIACA facilities both require that radiation detector probes be used to measure levels. The probes can detect levels as high as 150,000 R/hr. All sources are Co 60 except that GIF can be converted for use with a Cs 137 source. Both the GIF and HIACA sources are immersed in water and are mechanically raised up and out of the water for exposure. Many of our tests used these sources both under and out of the water, using the water as a shield to adjust radiation levels. This method undoubtedly softened and broadened the source spectra; however, we were not able to distinguish a significant difference in detector response between the Co 60 and Cs 137 sources. We conclude that the spectrum softening does not appreciably affect our results.

2. SS Vessel Attenuation. After the TMI-2 detector was removed from the ss vessel, a new Victoreen 847-1 detector was placed inside and exposed at GIF. This was done to get a crude estimate of gamma attenuation by the SS vessel. With the source totally above water and the radiation level at approximately 144,000 R/hr on the outside of the vessel, the detector inside measured 4000 R/hr. The stainless steel and lead vessel thus attenuated the level by a factor of 36. Co 60 source emits 1.17 MeV and 1.33 MeV gammas and the attenuation should be somewhere between 22 and 35. The slightly higher attenuation of the ss vessel measured value is probably a result of the spacial falloff as one moves away from the source.

No appreciable difference in attenuation was found by rotating the vessel by 90 degrees. As long as the source was not shining directly into the 1.27 cm ss vessel hole, essentially no effect of the hole was seen. However, with the source directly opposite the hole (and thereby providing a direct path entry), levels inside were a factor of two higher. No effort was made in these more qualitative measurements to determine precisely the effects of the hole or the vessel attenuation factor, because the behavior in the radioactive gas inside containment would be quite different since the gas unlike the Co 60 source completely surrounds the vessel.

3. Initial Detector Checkout and Examination. The connector that attaches to the detector inside the ss vessel was broken and thus was replaced. A set of electrical measurements were made and compared to those measurements similarly taken using the "new" Victoreen detector and ratemeter. The TMI-2 ratemeter was used with the TMI-2 detector. Table 3 lists those measurements. Voltage levels for HP-R-214 are fairly close to those of the new detector; however, the meter reading was sometimes constant at 20 mR/hr and sometimes varied from 0.8 mR/hr to 500 mR/hr. Resistance measurements between all pins were approximately equal to those measured on the new ratemeter. These levels and the erratic behavior are consistent with those measured by Technology for Energy Inc. (TEC) during in-situ testing at Three Mile Island. (See Reference 8.)

Table 3. Quiescent DC Measurements. The test detector voltage and current characteristics are compared with those of the HP-R-214 detector.

<u>Measured Parameter</u>	<u>Test Detector</u>	<u>Measurement</u> <u>HP-R-214 Detector</u>
(C.S) +20V (V)	20.58	21.88
+24V (V)	13.99	13.35
FAIL IN (V)	2.92	2.67
SIGNAL (V)	0.15	0.87
MTR (mR/hr)	0.20	0.8-500.0
+24V I (ma)	75.00	74.90
(C.S) +20V I (ma)	20.50	18.50

The unopened ss vessel was exposed in the GIF facility; the results are given in Figure 18. The radiation levels measured inside the ss vessel by HP-R-214 are considerably below those of the new detector when it was later placed inside the vessel and similar data taken.

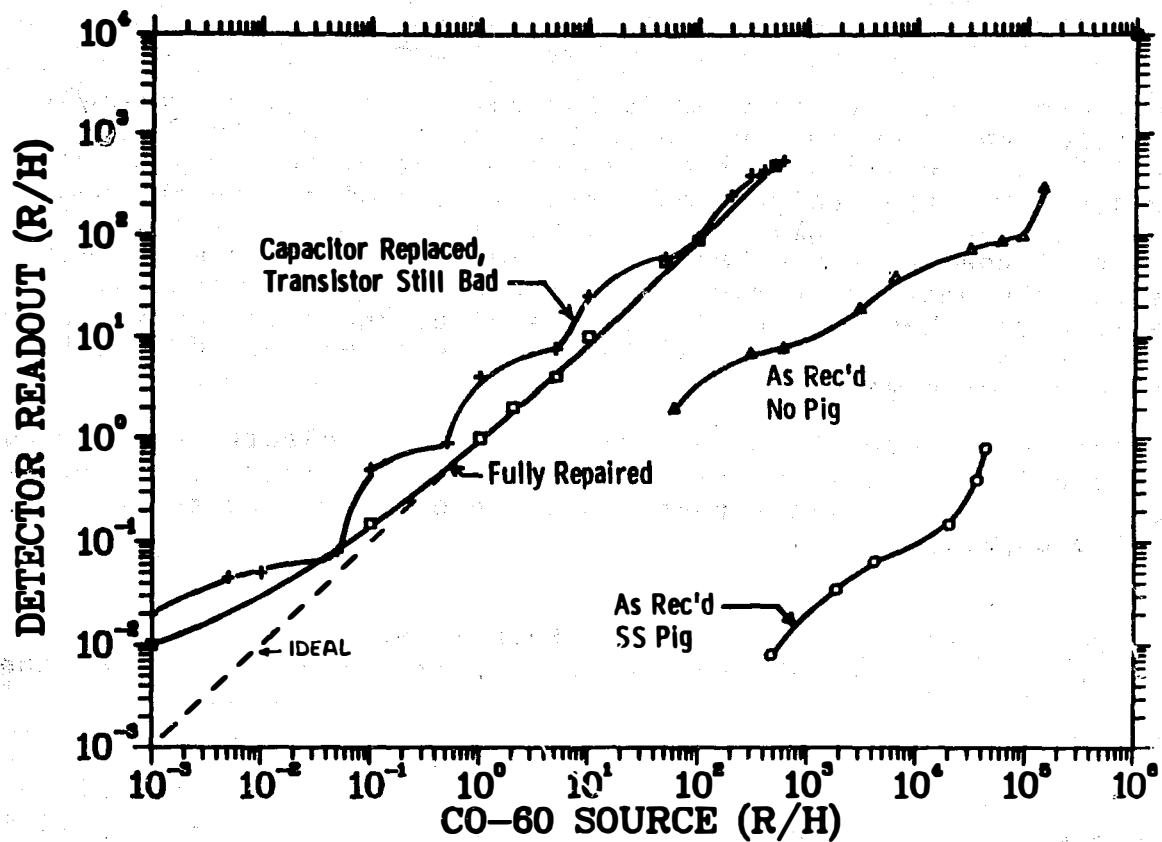


Figure 18. HP-R-214 Detector Readout Vs. Co 60 Source Strength. The curves show the response of the detector in the various stages of disassembly and repair when exposed to a Co 60 source. The curve in the lower right-hand corner is that measured upon receipt at Sandia National Laboratories after decontamination of the outside of the vessel. The curve directly above is the detector response outside the ss vessel but with no repair work done. The somewhat linear curves on the left are those of a partially and a fully repaired unit with low humidity.

The HP-R-214 detector was found to be only slightly contaminated on the outside and virtually uncontaminated inside after it was opened. Rust was evident all around the rubber gasket seating groove. Immediately upon opening, beads of moisture were evident on many of the components on the printed circuit boards. Even the boards were shiny, indicating a thin film of moisture. This water rapidly evaporated.

4. Capacitor C17 Failure. Troubleshooting of the detector at the Vertical Range and in the laboratory revealed an intermittent, low-range amplifier board. The problem was traced to a faulty electrolytic capacitor C17 which is in the reed switch driver circuit. The capacitor is a wet electrolytic 275 uf, 25-

volt capacitor used to provide the energy storage necessary to transfer the reed switch. A portion of the capacitor electrolyte had leaked onto the printed wiring board and was quite evident. The electrolyte had partially corroded away the base lead of transistor Q14. This failure is almost certainly the cause of the erratic behavior noticed during the in-situ tests before the unit was removed from the Containment Building. The failure must have occurred sometime after the unit was taken out of service at TMI-2 on April 16, 1980; this was 384 days after the accident began.

We can only speculate about the cause of the electrolyte leakage since this is a common failure mode for this class of capacitor. However, it is possible that radiation degraded the rubber seal on the capacitor can.

5. MOS Transistor Degradation. Even after C17 and Q14 were replaced, the unit behaved somewhat erratically. We traced the problem to a 3N163 MOS transistor (Q15) in the input circuit of the low-range amplifier board. The transistor nominally should have a gate to source threshold voltage (V_{GSth}) of approximately -4.0 volts. This transistor had a V_{GSth} of -9.0 volts. Since the supply voltage for this portion of the circuit is only 11.8 volts and since the voltage supplied to the source of Q15 is even less, it is probable that Q15 was on occasion operating outside its normal, active region. Q15 was most certainly degraded by radiation dose accumulation.

6. Humidity Effects. Since water droplets were found on the circuit boards inside the detector when it was first opened, we conducted tests to determine what, if any, effect high humidity and/or liquid water might have on detector operation. We found that humidity by itself has a dramatic effect on the detector readout, even in the absence of radiation; moisture condensation is not necessary to cause these effects. Figure 19 shows the results of one of many experiments involving humidity.

For the particular test shown in Figure 19, a wet sponge was placed inside the detector electronics cavity and the unit was clamped shut. The mounting bracket holes had been sealed with RTV adhesive; this ensured a good seal. To simulate temperature conditions inside the TMI-2 reactor at the time of the accident, the unit was placed inside a temperature chamber which maintains a temperature of 130° F. No radiation source was present. After the sponge was placed into the detector, the detector was immediately placed inside the chamber and the chamber was turned on.*

*The purpose of the wet sponge was to establish a known relative humidity (RH) of 100% inside the detector. Earlier, we had conducted tests in a standard humidity chamber but at humidities greater than 90% RH found that accurate control of the level could not be maintained.

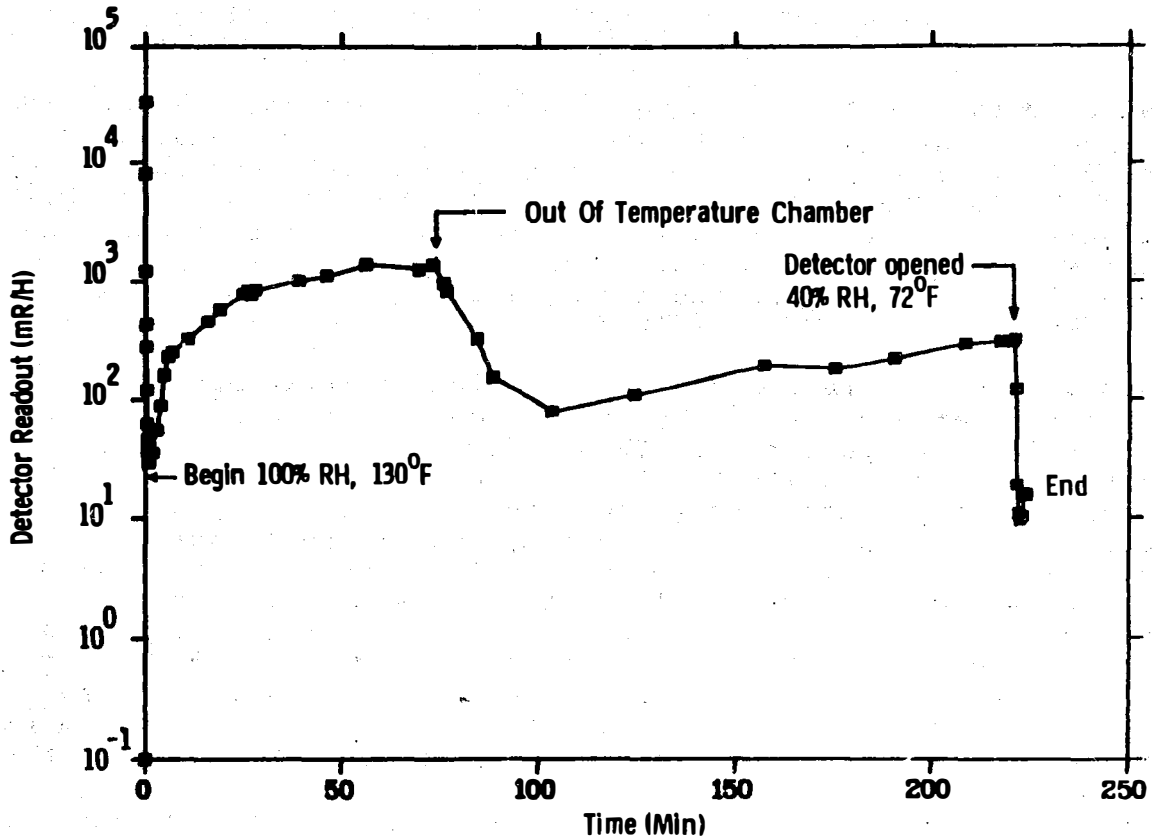


Figure 19. Humidity Effects. The detector was put in a 100% RH environment; it was heated up, allowed to cool, then opened up to room atmosphere. The unit was not exposed to any radiation source.

The readout immediately rose to 3×10^4 mR/hr as is characteristic of the start-up kick. As time passed, the readout level fell at first and then began to rise as the humidity inside the chamber increased, instead of falling to some low background radiation reading. The detector output leveled off at approximately 1000 mR/hr. The detector was removed from the chamber approximately 70 minutes after the test began and was allowed to stabilize at room temperature. The level indication first dipped and then at this temperature rose eventually to 300 mR/hr. At 225 minutes after the test began, the detector was opened. The readout level abruptly fell to 10 mR/hr and remained there.

The test results were repeated in numerous similar tests. In these tests the quiescent readout reading was generally between 300 mR/hr and 5 R/hr at room temperature. In the tests we were never able to determine why HP-R-214 would register anywhere from 5 to 30 mR/hr in the absence of radiation or high levels of humidity. We can only speculate that some current leakage path exists in the pre-amp circuit.

The results of other tests performed to investigate the effects of humidity are given in References 5 and 6. In summary, we found that high humidity affected the high amplifier output more than the low amplifier output. However, the low amplifier was affected also. Humidity affected the new detector in much the same way, but not to the same extent. Humidity causes the readout to rise even if the high voltage to the ion chambers is disconnected.

Each of the Victoreen 847-1 detector ion chambers has a grounded guard ring around the chamber electrode to separate it from the -150 volt plate potential. This is typically done on extremely high impedance circuits to minimize any leakage from the high voltage plate to the output electrode. Surface conduction is a major problem, and it is enhanced by contaminants (notably sodium) and moisture. Resistance from the electrode to a voltage source as high as $10E10$ to $10E12$ ohms is still small enough to typically cause inaccurate readings. With reference to the guard ring, the design of HP-R-214 appears to be proper. We were not able to determine precisely which leakage paths were causing improper readouts from HP-R-214. However, we can state that they were either 1) inside the shielded preamplifier boxes in both the low and high preamplifiers, 2) on the ion chambers where the electrode exits, or 3) in both places. (See Figures 20 and 21.)

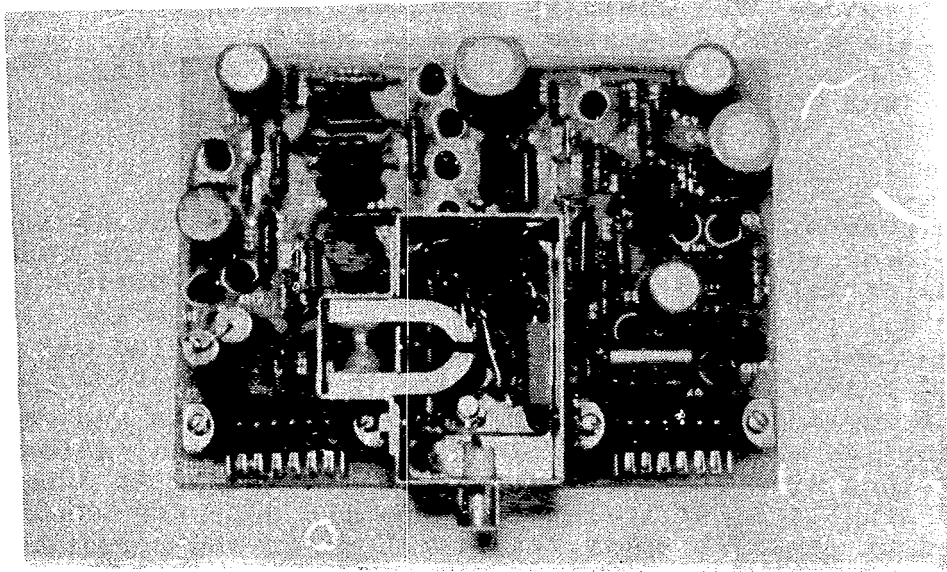


Figure 20. HP-R-214 Detector Lo Amp Board.
The cover has been removed from the preamplifier shield box. The ion chamber electrode enters the box on the down side of the photograph. The application of high humidity in this box or around the electrode plug caused the detector to read high with no radiation present.

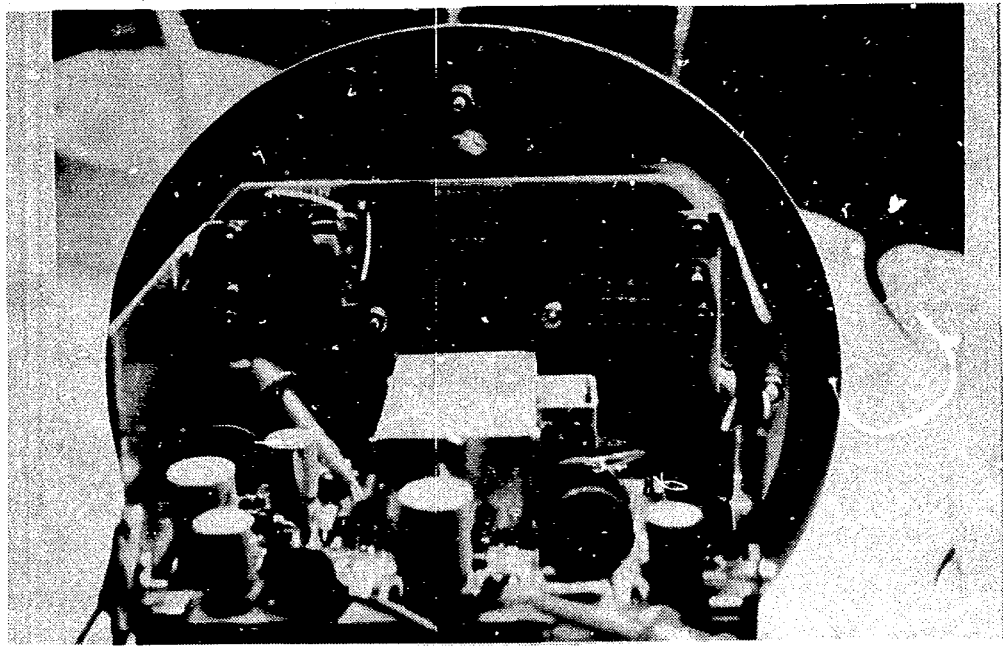


Figure 21. End View of Detector Electrode Pin. The pin exits the chamber assembly and plugs into a receptor jack in the end of the preamplifier shield box. The box is shown as it is mounted on the printed wiring assembly just prior to insertion into the chamber assembly connectors.

In any event, our tests showed that no other circuitry (either on the amplifier boards or the auxillary board) was inordinately sensitive to humidity. The effect of such a leakage path in the high range preamplifier circuit will now be discussed.

Leakage Paths--The circuit diagram shown in Figure 22 is a simplified schematic of the high range preamplifier. Let us assume that a resistive path exists on the electrode side of the reed switch. The DC voltage on the emitter of Q19 is 0.7 volts. A part of this voltage is fed back to the gate of Q15. With the reed switch closed, the gate voltage would have a value set by the resistive divider action of the 10E9 ohm resistor and the moisture-induced resistance. When the reed switch is open, the potential would abruptly change since the moisture resistive path would no longer be there. This change, even though it is small, would appear as an AC signal out of the preamplifier and would be amplified by 900 by the time it reached the output of the last amplifier in the amplifier chain following the preamplifier. The signal could thus cause a significant deflection of the readout meter even in the absence of a radiation field.

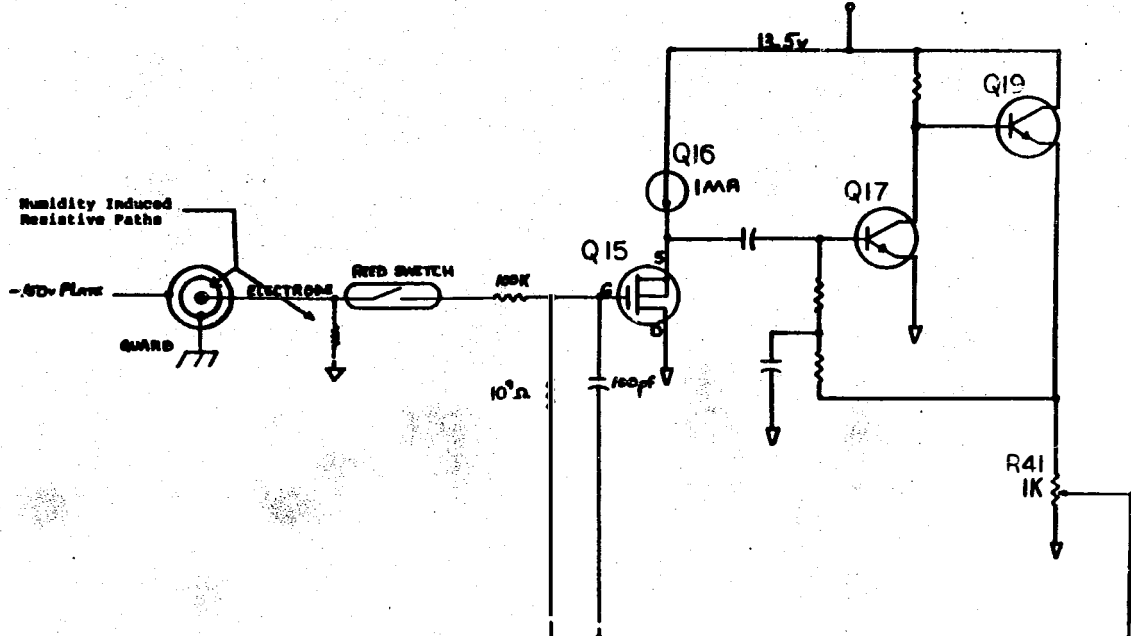


Figure 22. HP-R-214 Detector Pre-Amp Equivalent Circuit.
Feedback from R41 coupled with a humidity-induced resistive path on the ion chamber electrode and reed switch action can produce an AC signal out of the preamplifier. This signal is then amplified by 900. This erroneous signal causes the detector to indicate radiation where there is none.

7. Radiation Measurement Characterization

Figure 18 shows the detector readout as a function of Co 60 radiation level incident on the outside of the ss vessel with the detector still inside. Figure 18 also shows several other plots of detector readout as a function of radiation after the detector had been removed from the ss vessel. Note that the detector as received is in error by more than one order of magnitude. After C17 was replaced, but with the degraded Q15 MOS transistor still in the circuit, the accuracy was greatly improved. The effect of the degraded transistor caused the detector to generally read high in addition to being erratic. Once the unit was fully repaired, the detector (except at very low radiation levels) was quite accurate. As explained earlier, we have been unable to explain fully the quiescent 20 mR reading with no radiation present.

The data using the fully repaired unit was taken at the Vertical Range where 600 R/hr is the maximum achievable level. Figure 23 shows the data under different temperature and humidity conditions. Again, the room temperature, low humidity case is quite linear and accurate. The effect of 100% relative humidity is

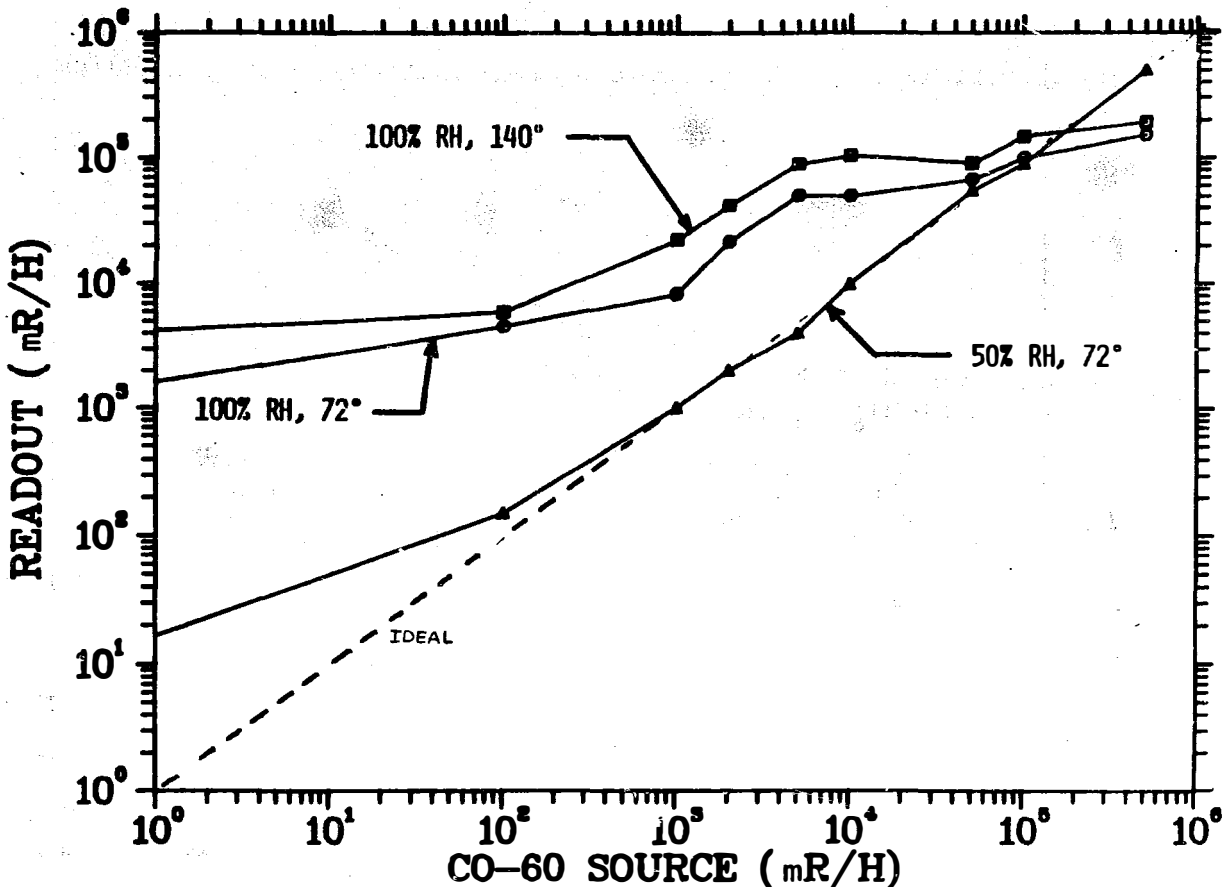


Figure 23. HP-R-214 Detector Readout on the Sandia Vertical Range. The effects of moisture and temperature on the detector accuracy are evident.

pronounced. The background level appears as approximately 1.0 R/hr and the slope of the curve is much lower. In fact, it is somewhat flat over the range of 5 R/hr to 600 R/hr of input radiation level where it ranges from only 50 to 200 R/hr. Raising the temperature from 72° F to 140° F results in an approximate doubling of readout level. A temperature of 140° F was selected for testing because temperatures inside containment fluctuated between 140° F and 120° F for an extended period of time during the accident (Reference 9).

Figure 24 combines the relatively low level radiation data from the Vertical Range with the much higher levels attainable at HIACA. At low radiation levels the "dry" detector is significantly more accurate than when moisture is introduced. At radiation input levels above 100 R/hr, the readout response is substantially below what it should be for both dry and 100% RH cases.

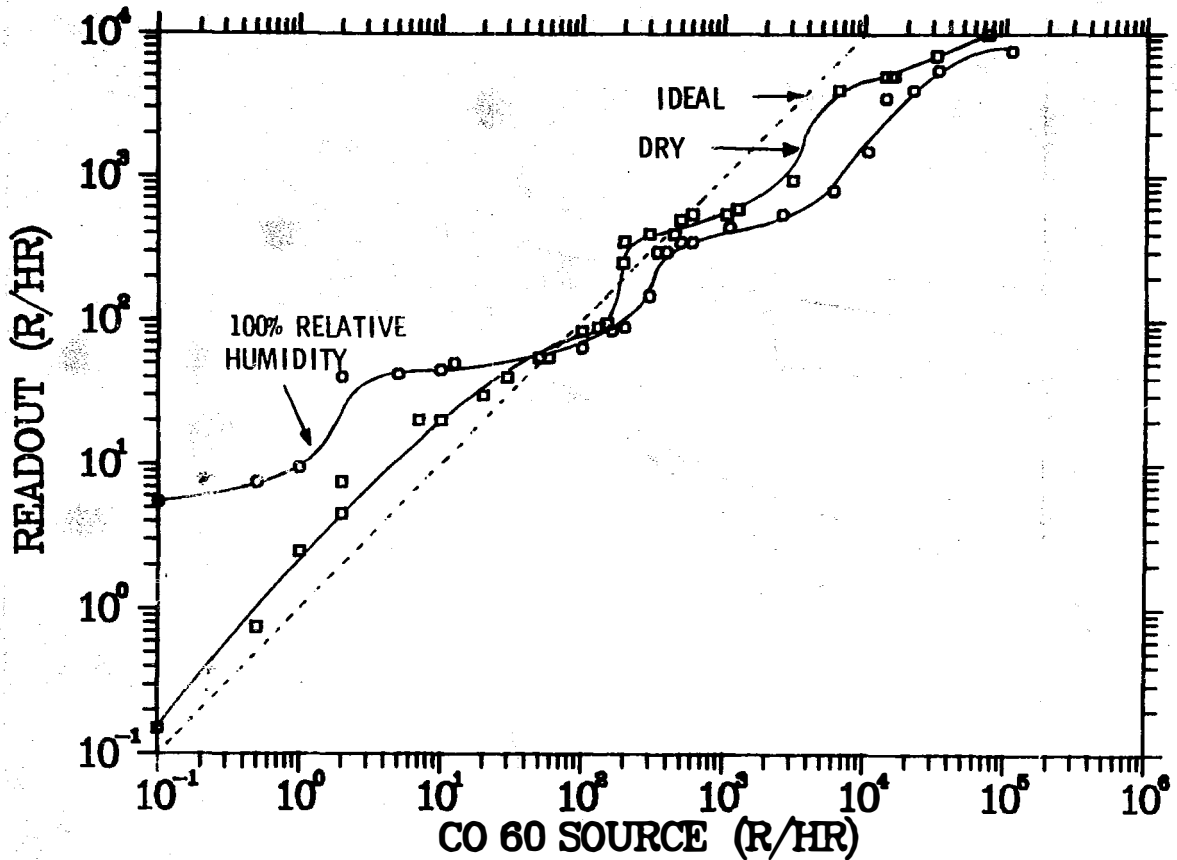
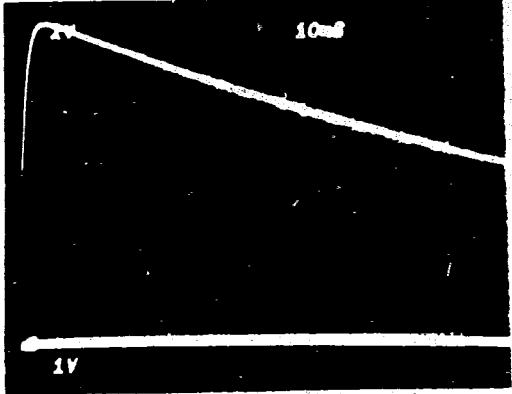
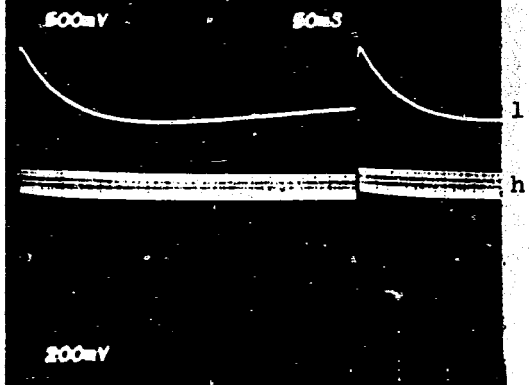


Figure 24. HP-R-214 Readout Vs. Source Level. Vertical range and HIACA data are shown for both dry and high humidity cases.

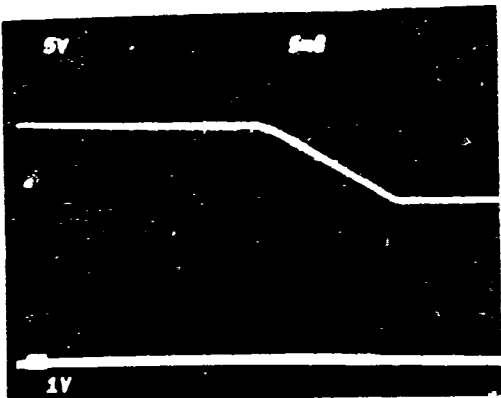
The reasons for the higher readings at low radiation levels, as discussed earlier, is due in part to the erroneous high amplifier contribution to the output signal because of the particular DC feedback signal which results when humidity introduces a resistive path to ground. At very high radiation levels this effect is overshadowed by the radiation signal itself. The reason for the abnormally low readings at very high input levels appears to be the result of a reduction in low amplifier output. The photographs shown in Figure 25 of the high and low range preamplifier outputs demonstrate both the erroneous high range amplifier signal at low radiation levels (Figure 25 D, E, F and G) and the reduced low range amplifier signal (Figure 25 H) at high radiation levels. (The oscillation present on the high range preamplifier output was caused by the test setup.)



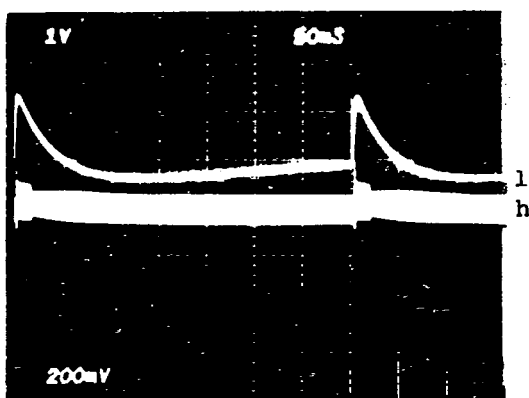
A. Dry, Source 1R/hr.
Meter .05R/hr.



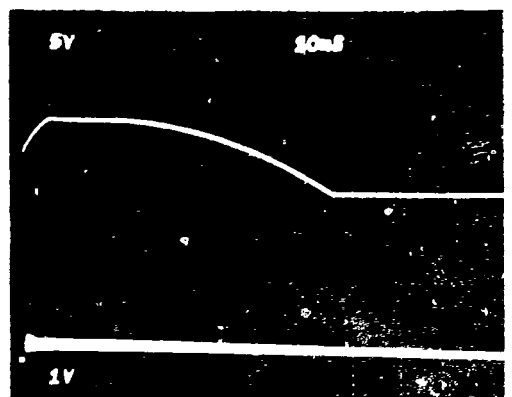
D. Wet, Source Background
Meter 2.5 R/hr.



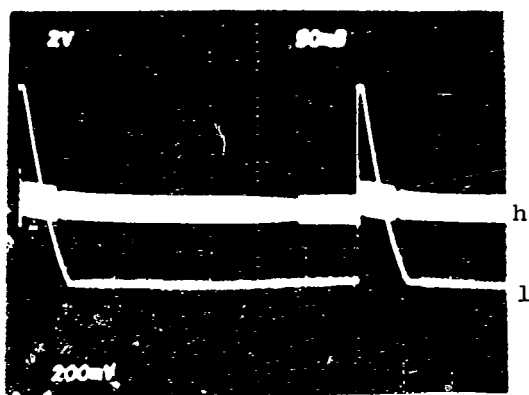
B. Dry, Source 10R/hr.
Meter 9R/hr.



E. Wet, Source 1R/hr.
Meter 5.5R/hr.

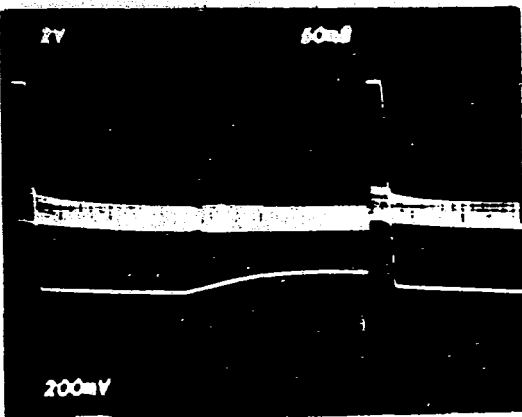


C. Dry Source 500R/hr.
Meter 500R/hr.

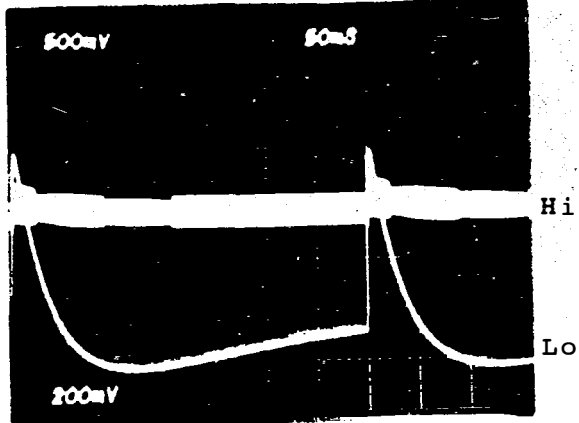


F. Wet, Source 10R/hr.
Meter 40R/hr.

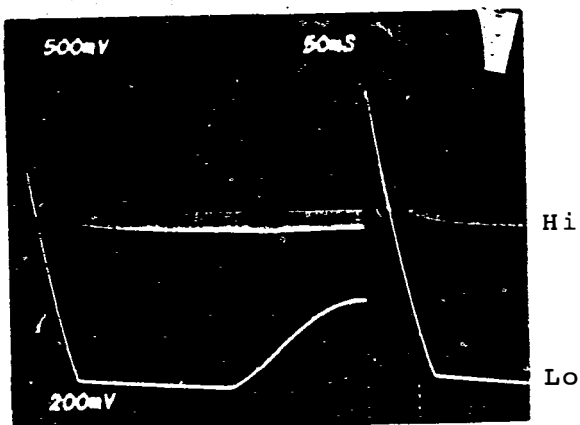
Figure 25. HP-R-214 Lo Amp and Hi Amp Outputs. The detector was exposed to radiation levels varying from background to 500 R/hr under both dry (low humidity) and wet (100% RH) conditions.



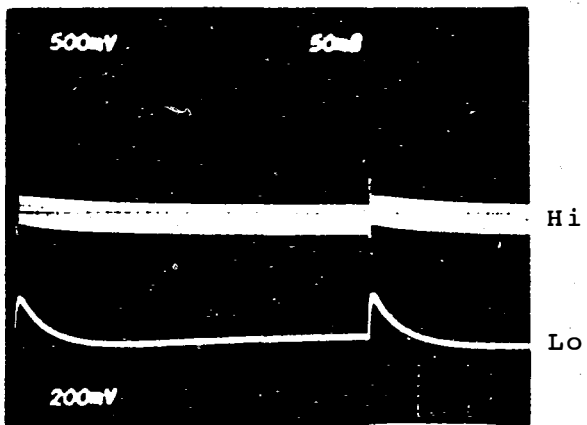
G. Wet, Source 50R/hr.
Meter 50R/hr.



I. Wet, Source Background #2
Meter 8R/hr.



H. Wet, Source 500R/hr.
Meter 55R/hr.



J. Wet, Source Background
#2 + 1 hr.
Meter 8mR/hr.

Figure 25 (Continued).

We have shown the inaccuracies observed when moisture is introduced into the detector. In addition to this, however, these inaccuracies are variable with time after exposure to radiation. This can be demonstrated by comparing Figure 25, Photographs D, I, and J. Photograph D is background before the unit was exposed to the source and it reads 2.5 R/hr. Photograph I is after going from 1 R/hr to 500 R/hr and then back to background, and it now reads 8 R/hr. After letting it stabilize at background for one hour, the reading has gone to 8 mR/hr as shown in Photograph J. These variations vs. time and humidity make it very difficult to make repeatable measurements. It is no wonder that the stripchart recording of the Dome Monitor during the accident is confusing.

V. RADIATION TOTAL DOSE

The total gamma radiation doses received by the detector electronics and the HP-R-214 power and signal cable, which is outside the ss vessel, are estimated in this section. Transistor gain degradation was used as the dose indicator for the detector, and elastomeric degradation properties were used for the cable. In addition, we have compiled doses estimated for other instruments inside containment which were similarly estimated. (See References 10, 11, 12). Table 1 summarizes these doses.

1. Detector Gamma Dose--It is possible to estimate the gamma dose received by the detector by comparing the gain degradation of similar transistors which have been exposed to known levels of radiation (Reference 10). In order to generate this calibration data, a number of transistors of each type was exposed in a Co 60 facility. Exposures were made in increments in order to characterize the transistors as dose was accumulated. These transistors had collector currents of 100 uA and were thus active during exposure.

Figure 26 shows an example of the data generated for ten 2N3565 Fairchild transistors. The upper curve is that measured on the particular transistor having the highest gain of the ten. The middle curve is the average of the ten, and the lower curve shows the minimum gain device. The transistor gain (HFE) for this particular set of data was measured at 100 uA of collector current. The average HFE of the HP-R-214 transistors was 115. From the curves this corresponds to a total dose of between 2.5 and 3.6×10^5 rads. Appendix G contains calibration data of this type on other transistor types. Table 4 summarizes our dose estimate findings for each of 4 transistor types. The average HFE of each type of transistor removed from HP-R-214 is given. Below each of these averages are the estimates we made using the procedure described above. To obtain the overall average dose estimates, we simply uniformly weighted each set of measurements. The average of this data shows that the detector received a dose of approximately 2.2×10^5 rads.

The accuracy of this method of arriving at dose estimates is uncertain for a variety of reasons. Manufacturer-to-manufacturer and lot-to-lot differences in transistors as well as processing differences all contribute to errors; however, we feel that by characterizing a number of devices we can obtain a reasonable dose estimate. Another modifier in this process is that of transistor gain annealing. Undoubtedly, annealing took place inside containment between the time of exposure and the time we were able to measure the gains of the device.

Table 4. Transistor Total Dose Estimates. FSC, GE, MOT refer to the manufacturers of the transistors which we characterized. The numbers immediately adjacent to the manufacturer are the numbers of transistors characterized. The numbers in the columns are the minimum, maximum, and average gamma dose estimates.

<u>Transistor Type</u>	<u>Estimated Dose (Rads)</u>		
	<u>Minimum</u>	<u>Average</u>	<u>Maximum</u>
2N3904 (HFE = 38)			
FSC (3)	1.9E5	2.1E5	2.2E5
GE (3)	4.4E5	4.8E5	7.5E5
MOT (4)	0.8E5	3.3E5	10.0E5
2N3643 (HFE = 18)			
FSC (10)	1.7E5	2.1E5	2.7E5
2N3565 (HFE = 115)			
FSC (10)	2.5E5	3.0E5	3.6E5
2N4249 (HFE = 163)			
FSC (10)	-	0.3E5	0.5E5
Overall Average			
Total Dose	2.1E5	2.2E5	3.3E5

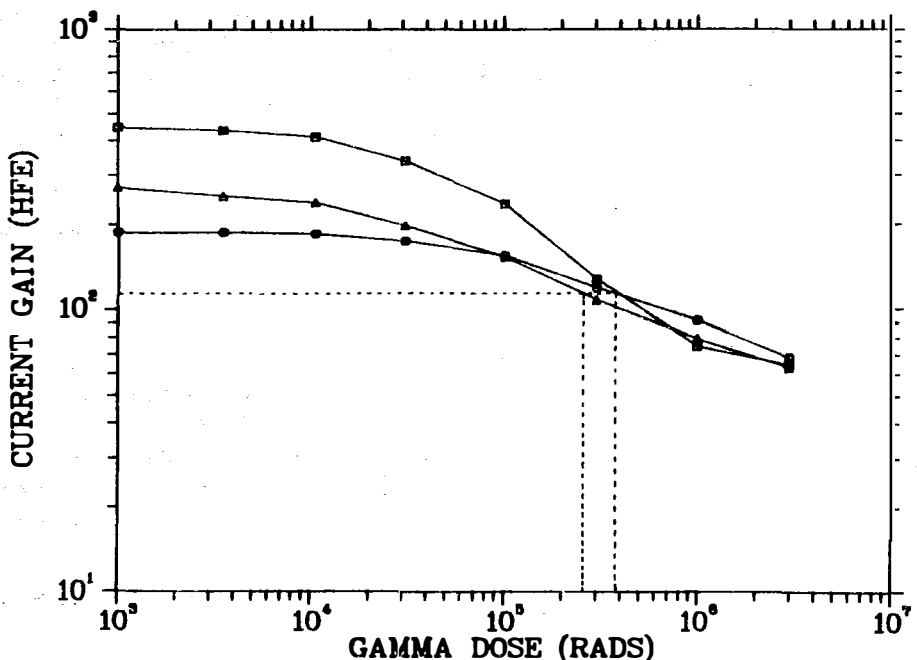


Figure 26. 2N3565 Fairchild NPN Transistor Gain Degradation.

Figure 27 shows data that we took to determine the effects of annealing. In these tests, transistors were biased at collector currents of 100 uA and were exposed to 5×10^5 rads. The gains were measured for three devices of each type as time passed after the exposure. We see from these curves that annealing did occur, but not to any great degree. Since the total dose estimates have fairly wide error bars associated with them, we have elected to ignore the effects of annealing. By doing this, our total dose estimates will be slightly lower than the doses the devices actually received.

2. Cable Gamma Dose--The HP-R-214 cable has 20-conductors of No. 16 wire; each conductor has a silicone insulation which is covered with glass braid. The bundle of 20 conductors are wrapped with 2 mil aluminum and mylar foil. The outer jacket is asbestos braid. A picture of the cable is shown in Figure 28. In order to estimate the radiation dose received by the cable, radiation degradation characteristics of the silicone insulation and mylar foil were measured.

The glass braid from the wires was removed and the wire was pulled out of the silicone covering. The covering was then tested on an Instron machine to determine percent elongation at break and its tensile break strength. As with the transistors, new cable samples were exposed to increasing levels of Co 60 radiation and calibration curves were plotted. These samples were from the same spool of cable at TMI-2 from which the HP-R-214 cable had come. These degradation characteristic curves as well as the HP-R-214 measured date are shown in Figure 29. Table 5 shows the percent elongations and break strengths measured for the HP-R-214 cable sample. The estimates of radiation dose are also shown. These data indicate that the cable was exposed to approximately 7.9×10^6 rads. Similar tests using light transmittance changes as the dose indicator of mylar wrap indicated dose levels of 2.0×10^6 rads (Appendix G). We have more confidence in the silicone measurement; therefore, we present our best estimate as 7.9×10^6 rads.

Since the cable, unlike the detector transistors, was exposed to both beta and gamma radiation, we were concerned that the doses measured might contain beta damage as well. Beta damage should be low in the silicone because the range of betas is quite limited and the asbestos and aluminum/mylar layers should shield the silicone insulation.

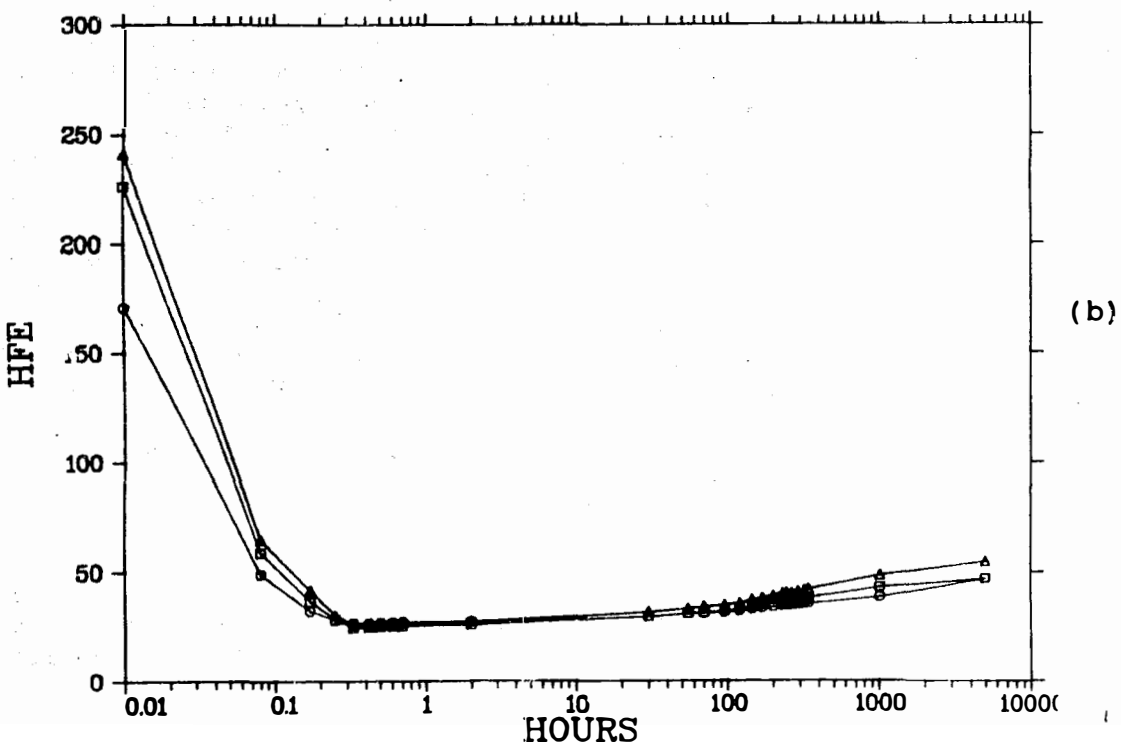
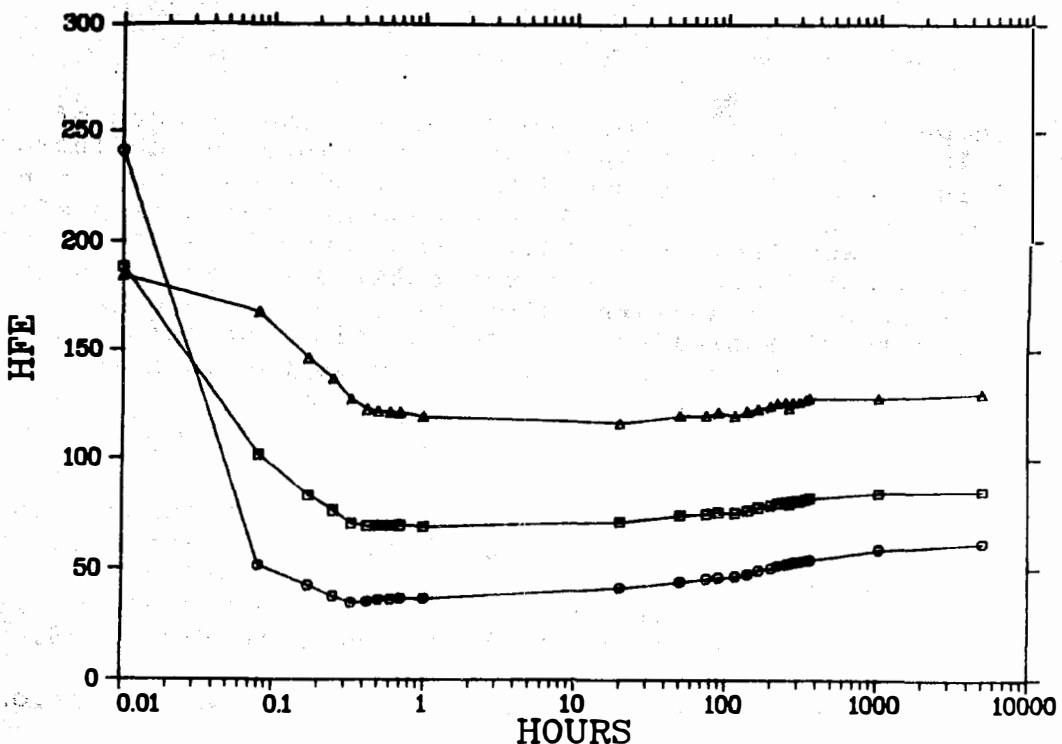


Figure 27. Transistor Annealing Characteristics. The top plot shows HFE annealing of three 2N3565 transistors which were exposed to an abrupt 5×10^5 rads. The lower plot shows a similar exposure of three 2N3904 transistors.

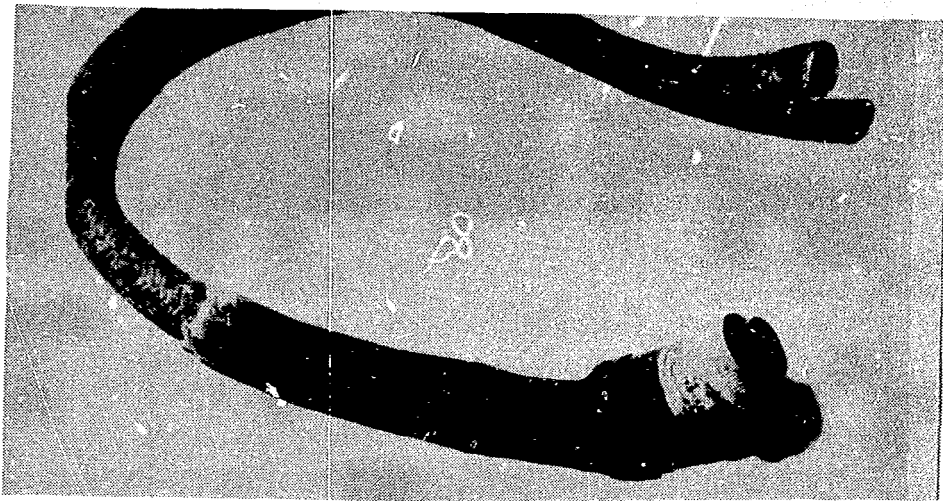


Figure 28. HP-R-214 cable. This photograph shows the cable end that mated to HP-R-214.

Table 5. HP-R-214 Cable Total Dose Estimates. The numbers in parenthesis are our dose estimates for that particular set of wires.

Wire Number	Elongation Percent	Average	Tensile Break Strength (Lbs)	Average
1	223		8.58	
2	250		10.36	
3	198		7.56	8.4
4	215	211.4	8.96	
5	201	(5.0x10E6 rads)	8.02	(1.0x10E7 rads)
6	192		7.78	
7	201		7.72	
8	176		7.12	
9	186		8.18	
10	200		8.18	
11	210		8.60	
12	218	206.8	9.18	8.5
13	218	(6.2x10E6 rads)	8.60	(1.0x10E7 rads)
14	236		9.42	
15	221		8.78	
16	193		7.76	
17	213		8.68	
18	233		10.00	
19	186		7.56	
20	198		8.36	

Average of Samples

1-20	208.4	(5.8x10E6 rads)	8.47	(1.0x10E7 rads)
------	-------	-----------------	------	-----------------

Average of Elongation and Tensile Break = 7.9×10^6 rads.

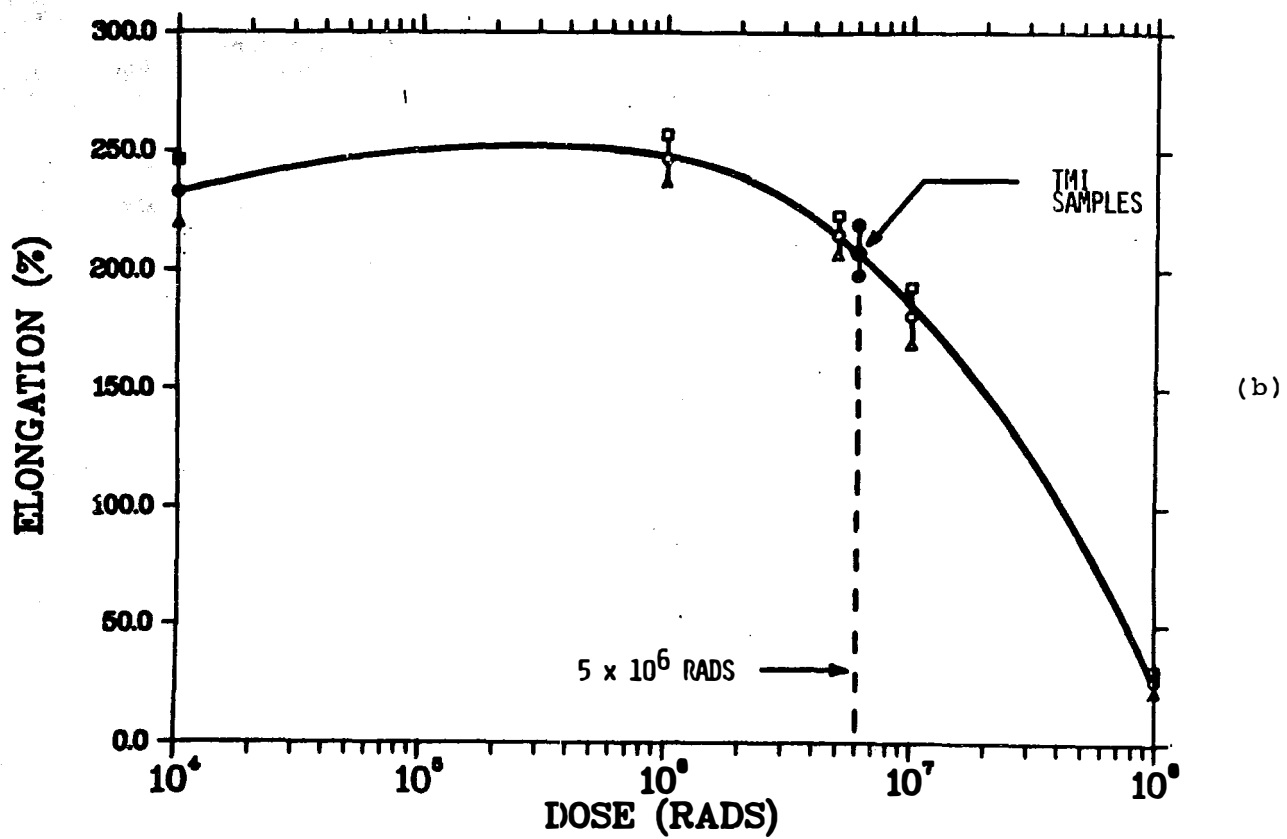
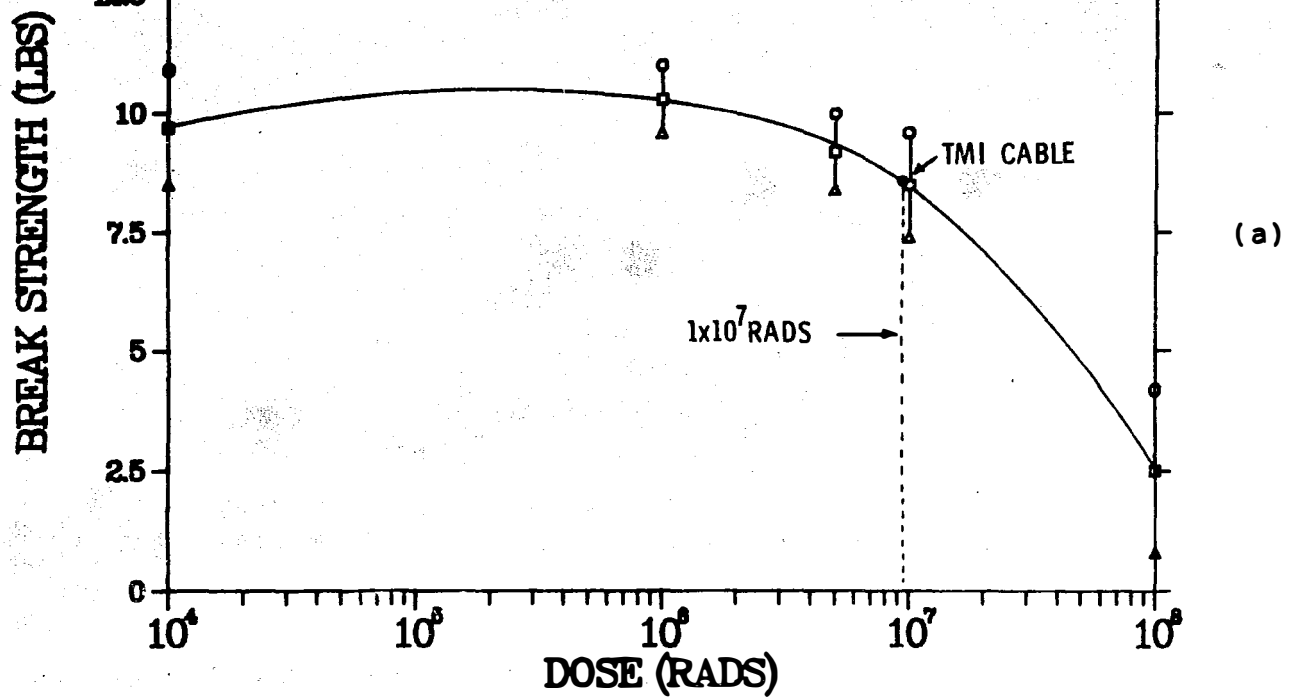


Figure 29. Cable Silicone Insulation Degradation
Characterization

VI. TMI-2 RADIATION TIME HISTORY

By far, the most difficult task of this analysis has been that of estimating the true radiation levels inside containment over the course of the accident. To do this, presumably, we can use the HP-R-214 failure modes, the radiation total dose information, the ss vessel attenuation characteristics, the radionuclide content estimates, and the events of the TMI-2 accident. This task is important because the information gained from such an analysis could be quite useful in validating LOCA release models and providing the industry with a true, small-scale, LOCA radiation profile. We cannot overemphasize the fact that the HP-R-214 was the only instrument inside containment that could be used for this purpose. What follows is a discussion about the salient features of the stripchart recording and radiation levels inside the ss vessel. From this, we present two hypotheses about the true radiation levels both inside and outside the vessel. Unfortunately, there is conflicting data associated with each hypothesis making it difficult to determine which is actually more likely to be true.

A. DOME MONITOR STRIPCHART CORRECTION

The Victoreen 846-1 Readout Module (SN1030) was delivered to Sandia in February 1982 after being removed from the cabinet in the TMI-2 Control Room. In the process of checking the calibration of the readout, we found that the stripchart recorder output circuit had been changed from that shown in the drawing schematic. Resistors R1 and R2 had been changed from $80.6\text{ K}\Omega$ and 402Ω to $62\text{ K}\Omega$ and $20\text{ K}\Omega$ respectively. This was presumably done to increase the readout output from 50 mV full scale to 0.8 V full scale. This change would seem to be appropriate except that the full scale reading with an input voltage of 8.0 V was only 0.75 V. Another problem with the change is that the output impedance to the stripchart recorder instead of being approximately 300Ω is now about $10\text{ K}\Omega$. This could cause scaling errors if the stripchart recorder input impedance was not fairly high. Appendix C shows our measured calibration curves for the recorder output and the readout meter. We found the meter output to be accurate within specifications. The calibration error, taken by itself, would cause the recorder to indicate levels lower than proper by a factor of exactly 2.

The HP-UR-1901 multichannel stripchart recorder was also found by Donald Nitti of Babcock and Wilcox to be improperly calibrated during the accident. Appendix D contains a letter written by Donald Nitti on June 27, 1979 on the subject "Containment Dome Radiation Monitor." In this letter, Nitti discusses the following two problems in interpreting the Dome Monitor readings:

1. "The recorder is a 5 decade log recorder, whereas the dome monitor is an 8 decade instrument which is linear within each decade. (Thus, the recorder was printing an 8 decade signal on 5 decade log paper)."
2. "There was a calibration error between the dome monitor indicator and the recorder such that the 8 decade signal was printed only over the first 3.78 decades of the 5 decade chart paper."

Nitti used this information to correct the stripchart. He then verified the accuracy of his work by comparing periodic meter readings recorded by Control Room operators.

We did not examine the HP-UR-1901 stripchart recorder, because following the accident it was used for various other recording functions and was most likely readjusted to record other signals. With this loss in calibration data, we must rely on Nitti's work. Therefore, even though the ratemeter recorder output was found to be uncalibrated, we must assume that the combination of ratemeter and recorder were set as outlined by Nitti. We believe that this is acceptable because of Nitti's comparisons of meter readings with his stripchart corrections. We have used Nitti's correction factors and have reread the stripchart and corrected the readings per the following equation:

$$\text{Corrected level} = \left(\frac{5}{3.78} \right) \left(\frac{8}{5} \right) [\log (\text{stripchart value} \times 10)] - 1$$

The result is the corrected stripchart shown in Figure 30. This agrees closely with Nitti's results. The actual data points are given in Appendix D. The detector quiescent readings both at TMI-2 (in situ) and at SNL are shown. The detector was behaving erratically during both of these readings.

B. TWO HYPOTHESES REGARDING RADIATION LEVELS

If we accept Figure 30 as an accurate representation of the Dome Monitor output, what can we say about the accuracy of the radiation measurements themselves? In this and the next section, we attempt to tie together the information we have on the Dome Monitor and the events taking place inside containment during the accident. We arrive at two estimates of what the true radiation levels were inside the ss vessel. From the inside estimates, we can also estimate levels outside the vessel using a fission release model. However, there is conflicting data. The data suggest two dramatically different radiation level hypotheses: Hypothesis 1 says that radiation levels as measured by HP-R-214

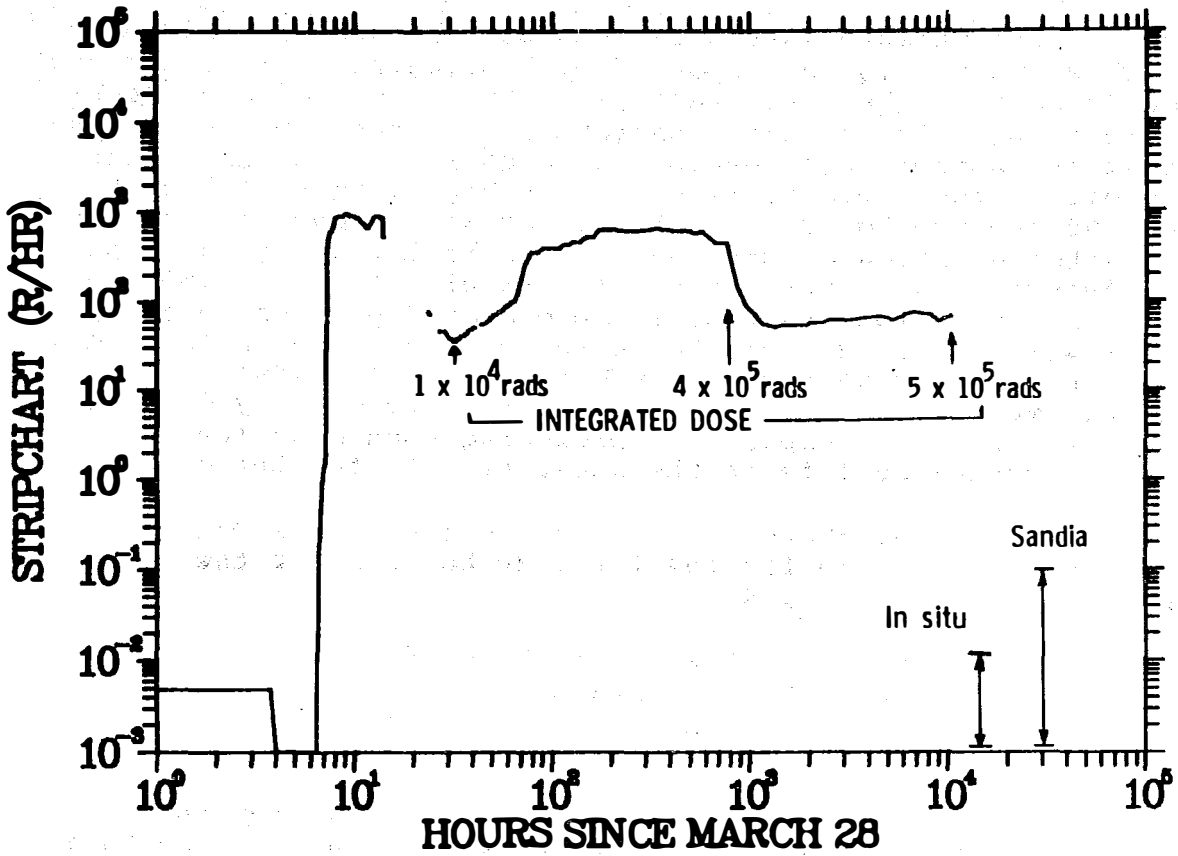


Figure 30. HP-R-214 Stripchart. The original stripchart has been corrected in this plot to account for the incorrect log paper and scaling. The "in situ" and "Sandia" notations refer to measurements made in place by TEC at TMI-2 and those made at Sandia. The vertical lines show the variability of level indications. This chart also shows the gamma integrated dose at three points in time. These doses were calculated by integrating the area under the stripchart curve.

were essentially correct during the first 800 hours of the accident; Hypothesis 2 surmises that the detector was never correct and that true levels were considerably higher than those measured. It might appear that one could reasonably postulate a number of other hypotheses because of the striking differences in these two; however, there is quite a lot of information which supports each hypothesis. No other reasonable theories were discovered.

Hypothesis 1. Detector measurements during the first 800 hours of the accident were essentially correct, even though moisture had at some time circumvented the ss vessel seal. After

800 hours, the measurements were incorrect because of this moisture. This hypothesis is supported by convincing indications that the early part of the stripchart is correct. Noble gas concentrations thought to be inside containment at the time could have produced the approximate levels indicated. The weakness of this hypothesis is the dramatic rise to very high levels of radiation between 60 and 800 hours. The total radiation dose received by the detector electronics was measured to be 2.2×10^5 and that in the detector cable outside the ss vessel was 7.9×10^6 rads. Most of the 2.2×10^5 rads would have been deposited in the detector electronics during the 60 to 800 hour time period. Only 1×10^4 rads would have been accumulated in the first 20 hours using this model. What we have been unable to clearly determine is a radiation source capable of producing such high levels inside the vessel so late in the accident. To further expand:

1. As we shall see, there is good evidence that the Dome Monitor was reasonably accurate for the first 30 hours after the beginning of March 28, 1979.
2. There is good evidence that from 30 to 60 hours radiation levels were below 100 R/hr. We cannot say with much certainty how low they were. The Dome Monitor may or may not have been accurate during this period.
3. There is conflicting evidence on the accuracy from 60 to approximately 800 hours. Nevertheless, a weak case can be made that the readings were reasonably accurate over this period also.
4. There is overwhelming evidence that from approximately 800 hours and later the Dome Monitor was totally inaccurate.

These conclusions are based in part on the following points.

1. Moisture may have entered the vessel and detector during the first 800 hours, but the effect was negligible except for the brief period from 30 to 60 hours. The effects of moisture are evident after 800 hours.
2. Radioactive gas in small quantities probably did enter the vessel. However, the effect on radiation readings was small when compared to radiation intensity from sources outside the vessel.
3. The 1.27 cm hole and breach of the outer ss vessel jacket had little effect on radiation readings.
4. The degraded MOS transistors, although bad from a design point of view, had little effect on accuracy.
5. Capacitor C17 failed sometime after 10,000 hours.

6. Throughout the accident, the Dome Monitor was measuring radiation from one or more of the following at any given time: radioactive gas, particles suspended or dissolved in the aerosol, plateout on surfaces, and direct shine from the steam generator "B" candy cane. As the discussion later will show, there is conflicting evidence regarding events happening inside containment and the actual source or sources of radiation.

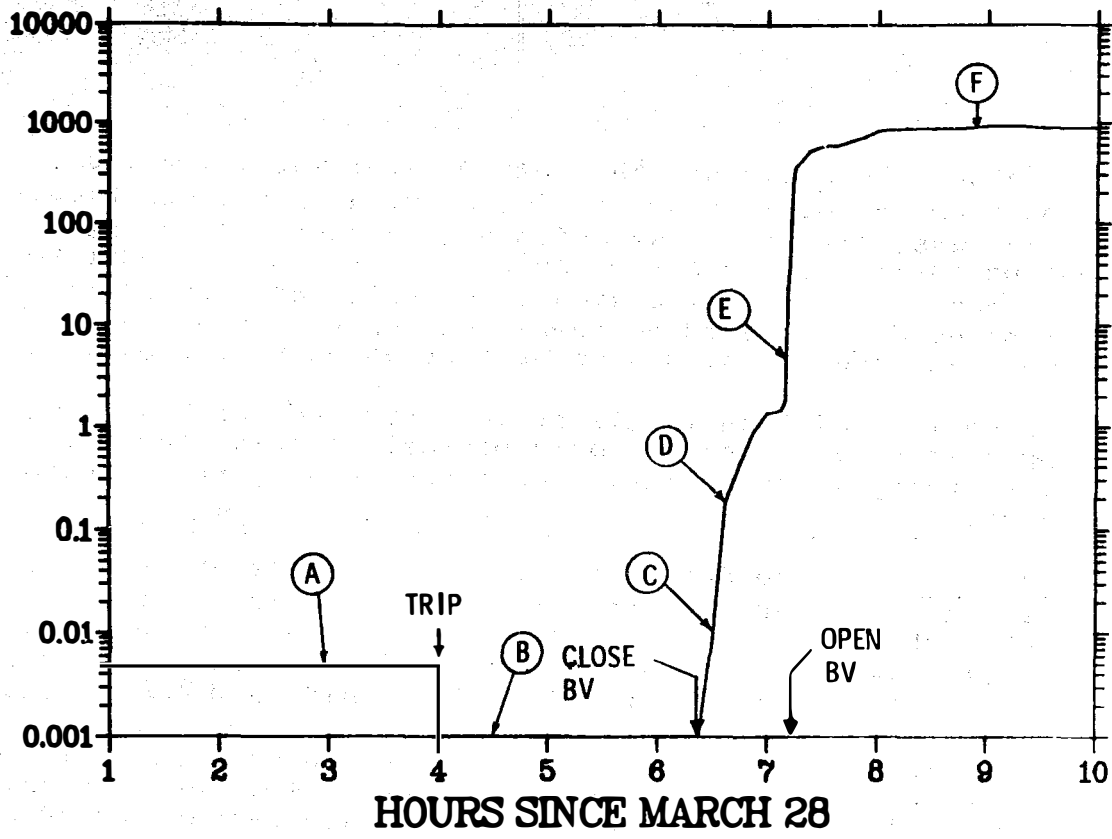
7. The rise in radiation levels at 60 hours and the high levels until approximately 800 hours could be real as evidenced by, among other things, the radiation dose received by the detector electronics.

Hypothesis 2. The detector was never correct and radiation levels (particularly during the first 20 hours) were possibly 25 times higher than the detector registered. If we assume a fission product release spectrum which is similar to that of noble gas, the correct dose of 7.9×10^6 rads outside and 2.2×10^5 rads inside the ss vessel could have accumulated in this way. This hypothesis is further supported by the unusual manner in which the detector responds in the presence of moisture. Also, these high levels are supported in part by measurements by HP-R-213. What is difficult to explain is how a sufficient quantity of moisture could have violated the seal so early in the accident. Moisture would have had to enter the detector sometime after 7:00 am. Since Containment Building pressure averaged only 2 psig during the first 14 hours, the forcing function was low. Using the ideal gas law $PV = NkT$ we see that the number of gas molecules inside can increase by only 20% for a change in pressure of 3 psig. If, however, liquid water was forced inside, the humidity inside the vessel could have risen considerably. As is the case with Hypothesis 1, the effects of radioactive gas in the vessel and of shine through the 1.27 cm hole were small. The degraded MOS transistor and capacitor failure were not significant early in the accident. The following discussion about stripchart features gives more detail regarding Hypothesis 1 and Hypothesis 2.

C. DISCUSSION OF STRIPCHART FEATURES

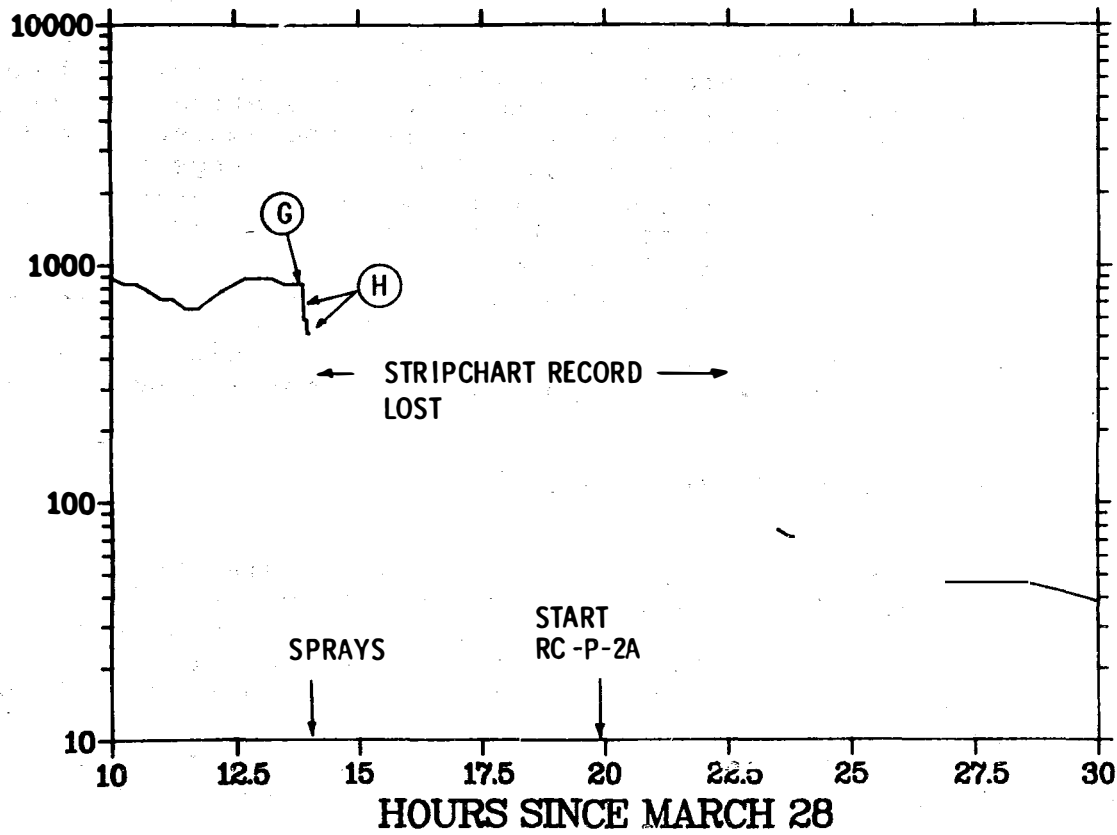
Let us now examine the stripchart in detail and discuss its salient features. The stripchart has been broken into four sections (Figures 31 and 32). Each section uses linear time scales in order to show finer detail. Circled letters indicate the various points to be covered in the discussion which follows. Please refer to Reference 15 for relevant containment events during the accident. It should be noted that the stripchart times may be in error by as much as 2 to 3 minutes.

STRIPCHART R/HR



(a)

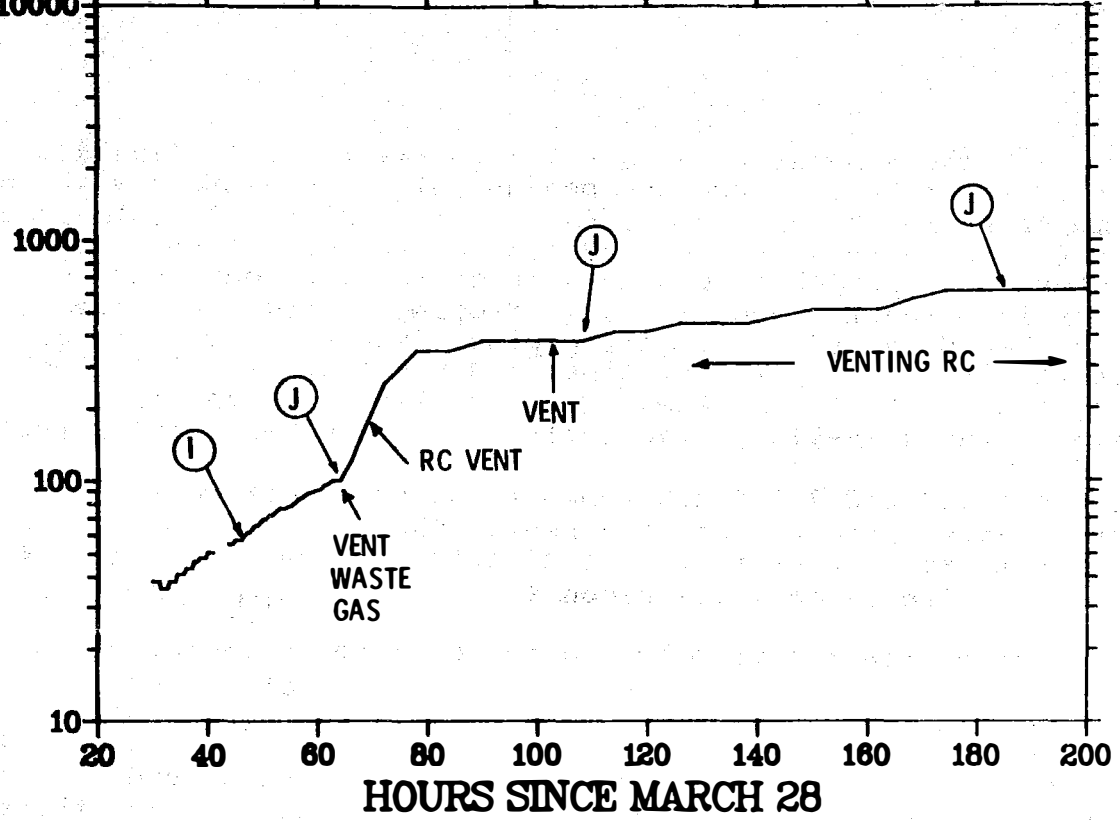
STRIPCHART R/HR



(b)

Figure 31. Expanded Scale Stripchart, 1 to 30 Hours.

STRIPCHART R/HR



STRIPCHART R/HR

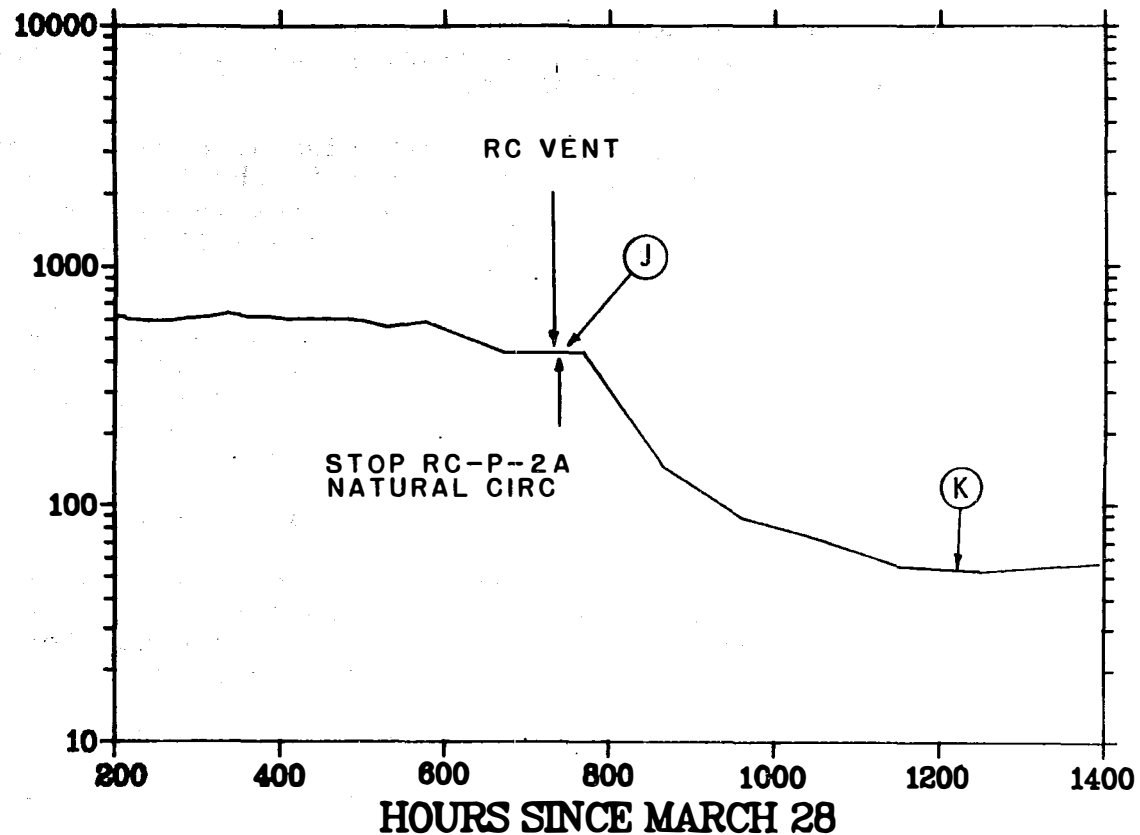


Figure 32. Expanded Scale Stripchart, 20 to 1400 Hours.

(A) The 5 mR/hr reading prior to reactor trip 4:00 a.m. on March 28 (four hours since the beginning) is consistent with the 100 mR/hr HP-R-213 readings (Reference 12). HP-R-213 is located near the incore tubes on the 347-foot containment level. Both detectors were probably reading N 16 gamma emissions from the primary loop reactor coolant water flowing through the steam generator, "candy cane" input-port piping. These candy canes are above the 347 foot operating floor and are separated from HP-R-213 by four feet of concrete. A direct line-of-sight is available for HP-R-214 particularly from Steam Generator B (see Appendix E).

N 16 has 6.129 and 7.115 MeV gamma emissions which would be only slightly attenuated by the ss vessel. The abrupt drop in detector outputs at reactor trip is indicative of the decay of N 16 whose half life is only 7.1 seconds.

(B) At reactor trip both detector outputs decreased to minimum scale and stayed there until both rose at around 6:30 a.m. This is clear evidence that a significant amount of moisture had not entered the ss vessel by this time. Up to this time, Reactor Building pressures were fluctuating around 2 psig. Since the pressure inside the ss vessel began at -1 psig, there was a function to force saturated atmosphere into the vessel. Humidity tests on the detector clearly show that had any significant amount of moisture entered the vessel, the detector reading would have been at least 100 mR/hr.

(C) The abrupt rise in radiation recorded at 6:27 a.m. by HP-R-213 and at 6:32 a.m. by the Dome Monitor is the first indication of failed fuel rods. The pressurizer block valve was closed at 6:22 a.m. The radiation as seen by HP-R-213 and HP-R-214 could have come from radioactive gas released through the block valve just prior to its closure, from shine from the uncovered core, or from shine from gas trapped in the steam generator candy canes. At least a small amount of radioactive gas was inside containment at that time since the Reactor Building air particulate sample monitor also reached its alarm setpoint. Probably, only slight cladding damage had occurred at this point and only a small amount of gas was released. It then took several minutes for the gas to be seen at the 347 foot level.

(D) At this time, HP-R-213 reached its upper limit of 10 R/hr. HP-R-214 was reading approximately 0.185 R/hr inside the vessel at a higher elevation. These two numbers are consistent indicating that HP-R-214 was probably correct to this point.

(E) At approximately 7:11 a.m. the Dome Monitor shows a marked increase in level. Two events happened near this time: Reactor Coolant Pump 2B was started at 6:45 a.m. and the block valve was opened at 7:13 a.m. Approximately 800 hours later,

the operation of coolant pumps seems to be tied to radiation level changes. However, in this case, the detectors are probably seeing gas released through the block valve. The time difference is probably a result of timing errors.

(F) Radiation levels appeared to be relatively constant at around 830 R/hr, for about seven hours. The block valve was repeatedly cycled from 7:40 a.m. until 5:08 p.m. when it was finally closed. The source range neutron detectors indicate that the core finally was covered at around 7:30 a.m. There was still no loop flow even when Reactor Coolant Pump 2B was running.

If we assume an exponential release of noble gas from the core into containment via the block valve using a time constant of two hours, and account for decay of noble gas radioisotopes, the radiation levels measured by the Dome Monitor would be relatively flat over this period. This is shown in the next section of this report which discusses fission product release and levels. These calculations suggest that from 20 to 40% of the core's noble gas inventory would have had to be released during this period in order to match the Dome Monitor stripchart (Hypothesis 1). This seems fairly reasonable since this amount of inventory could conceivably be in the zircalloy to fuel pellet gap and would thus be easily released. Of course, other volatile fission products would have been released also.

Radiation levels during this time could also have been much higher (Hypothesis 2). If we assume that moisture entered the detector in the 7:00 a.m. to 11:00 a.m. time frame, peak levels would have had to have been on the order of 20,000 R/hr inside the vessel to account for the radiation dose. Figure 24, which plots readout vs. Co 60 source strength, shows that a detector reading of 830 R/hr could either be a 900 R/hr source strength for a dry detector or a 5000 R/hr source strength for a 100% RH atmosphere. Unfortunately because of the variability of laboratory measurements of detector response to radiation in a moisture atmosphere and spatial calibration of our instruments, we believe that our measurements could easily be in error by a factor of 2. This applies to total dose estimates as well as Co 60 characterizations. These potential errors and others might make up the difference between 5000 and 20,000 R/hr.

(G) HP-R-214 measures approximately 837 R/hr at this point in time. Fortunately, we have another indicator of radiation level. We can use the multivalued behavior of HP-R-213. HP-R-213 was pegged at its upper limit of 10 R/hr (Appendix F) until at 11.75 hours its output began to decrease. At 14 hours, it read 1 R/hr. Our examination of HP-R-213, HP-R-211, and HP-R-212 showed that when transistors in these detectors are degraded by radiation, they can indicate low radiation levels when in fact they are quite high (References 10, 11, 12). This behavior is shown in Figure 33. The discussion which follows indicates that radiation levels at 14 hours were considerably higher than HP-R-214 would indicate.

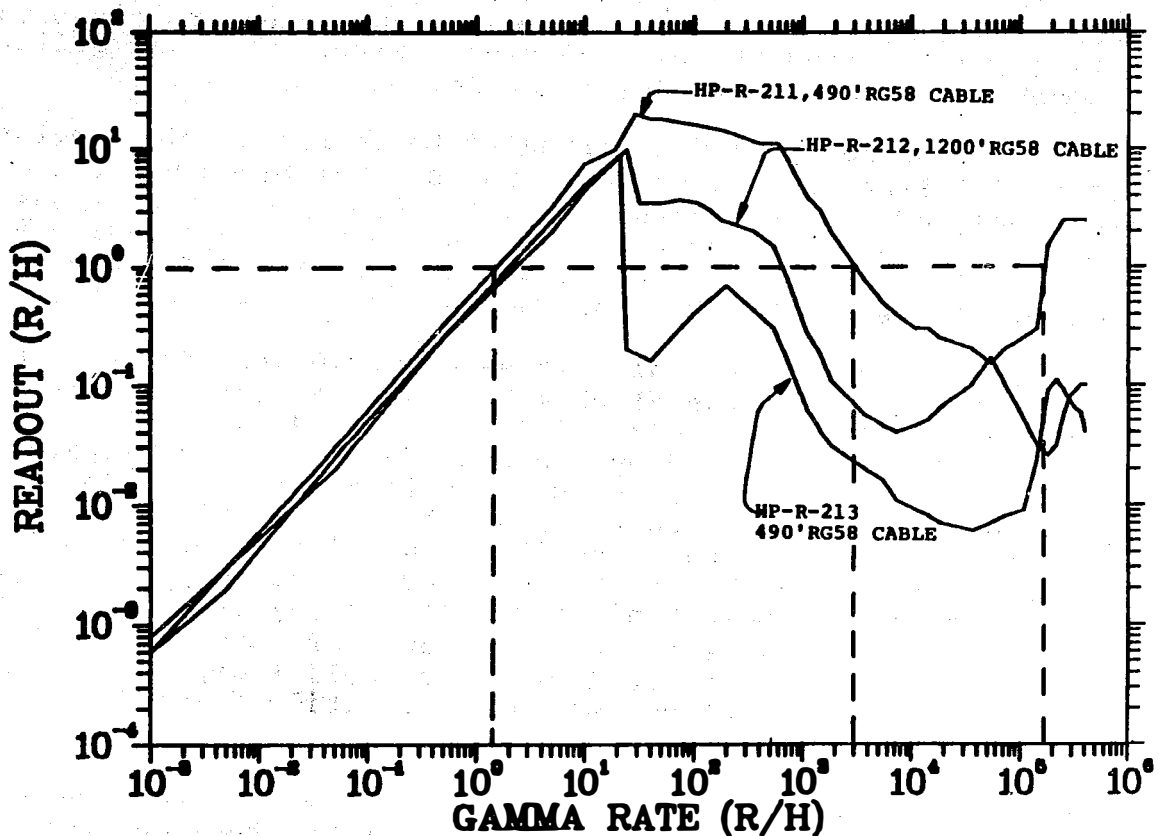


Figure 33. Multivalued Response. These curves demonstrate the multivalued response of HP-R-211, HP-R-212, and HP-R-213 when exposed to radiation levels far above 10R/hr which is the upper limit of these detectors.

If we first assume that Hypothesis 1 is the case, the total dose received by HP-R-213 at 14 hours would have been at most 4×10^{14} rads. (See next section for a 20% release of noble gas.) A dose of only 4×10^{14} rads is probably too low for the detector to exhibit a multivalued behavior. (For example, HP-R-211 received a dose of 2.5×10^{15} rads.)

If on the other hand, we assume that levels were 25 times higher as posited in Hypothesis 2, the dose received by HP-R-213 at 14 hours is at most 1×10^{15} rads. The difference in elevation and shielding, however, probably account for the factor of 7.9 difference between doses measured for HP-R-213 and the HP-R-214 cable. Thus, if we reduce the 1×10^{15} rads by this factor, the dose for HP-R-213 at 14 hours could have possibly been 1.4×10^{15} rads. If we extrapolate the multivalued behavior curves for this dose, we see that the gamma rate could have been as high as 200,000 R/hr. This is strong evidence that levels were very high at this point in time.

the hydrogen burn which occurred at 9:50 a.m. At that time, the stripchart recorder output, shown in Figure 34, clearly indicates that HP-R-213 was lost. We attribute the failure of HP-R-213 to the pressure-induced shock. At this time, the stripchart indicates an abrupt drop from 590 to 517 R/hr in the Dome Monitor level. This was probably caused by the shock since we found the detector to be quite shock sensitive. What is left of the stripchart before it printed in place is significant. After the abrupt drop, the Dome Monitor stripchart level continues to decrease at the same slow rate as before the shock, even though the building sprays are running. The sprays stay on for a total of 6 minutes, and approximately 5 minutes of stripchart are available before the stripchart stopped advancing and began printing over itself.

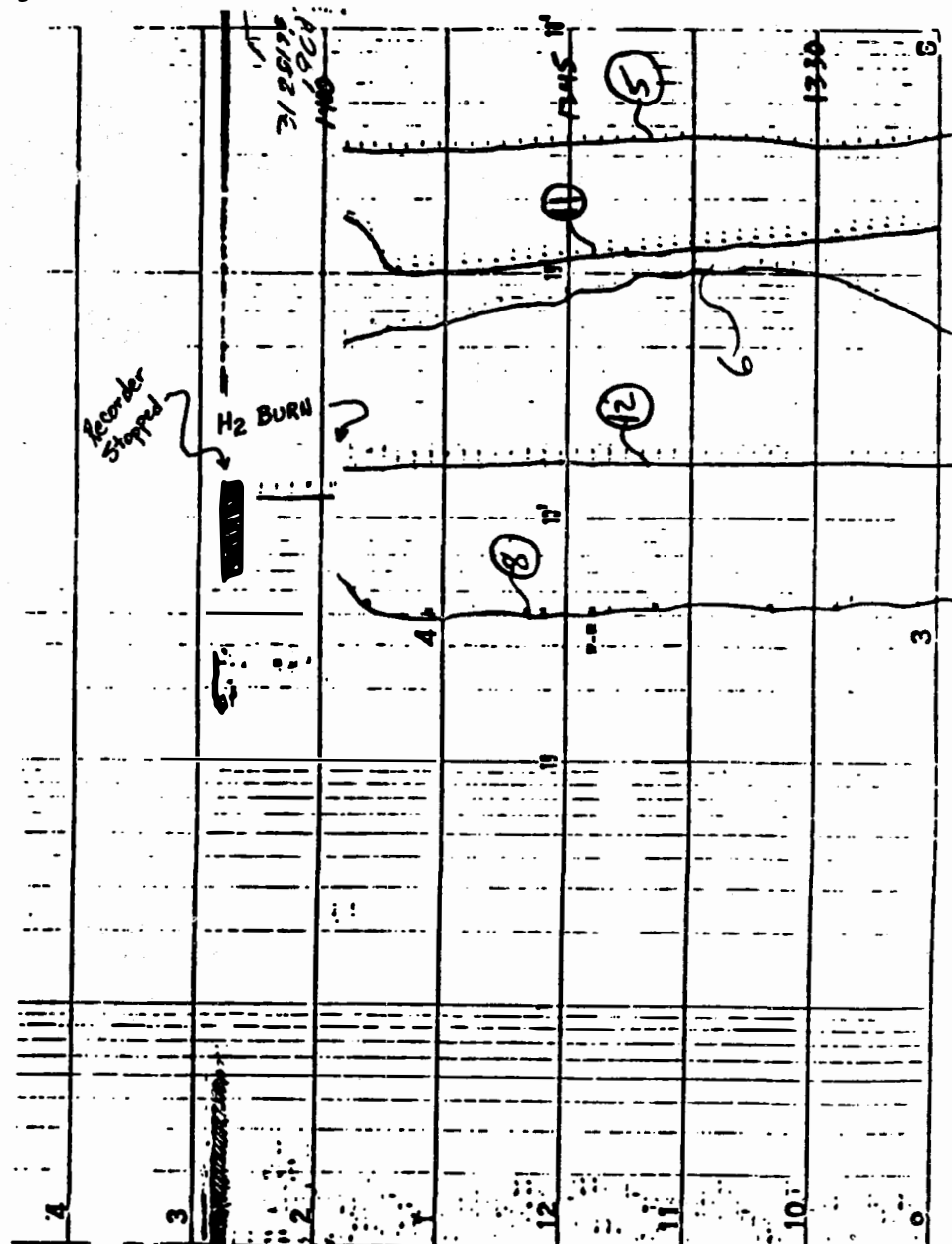


Figure 34. Actual HP-R-214 Stripchart Recording. The time axis is reversed and time increased toward the left. HP-R-214 is Channel 12 and HP-R-213 is Channel 11. The chart shows that HP-R-214 was functional after the hydrogen burn shock.

There is no marked decrease in radiation level during this time. This seems to indicate that the sprays were not removing significant aerosol radiation. This is reasonable only if noble gas was the prime radiation source. It does seem as though levels would decrease more than they did, however, since there certainly were some amounts of volatiles and it is possible that the sprays did not come on until after the record was lost. Even though the recorder printed over itself, the record of overprinting is more or less uniform in darkness, possibly indicating that levels decreased somewhat uniformly. Again, this is indicative of the decay of noble gas. Unfortunately, the record was lost for the next 10 hours. The evidence from this discussion is that the prime radiation source was noble gas and/or shine from the B loop candy cane.

(I) This rise is difficult to explain. The block valve was not opened again after 17 hours, and a review of the operator's log shows that no venting to containment occurred during this time. Unless some venting occurred, we conclude that finally the effects of moisture in the vessel and detector are being seen. If we look at the stripchart after 1000 hours, we see that the level there is between 50 and 70 R/hr just as it is during this period of between 30 and 60 hours. Our humidity tests on the detector as shown in Figure 24 show that for low radiation level inputs, the detector could register in the 50 R/hr range; this is particularly true if the unit were operating at an elevated temperature.

The effects of humidity will be discussed in more detail later in this report. It is important, however, to note that in all of our detector tests (even with moisture present) high radiation levels can be measured if they are high enough to swamp out the effects of moisture. This is true, simply because of the way the detector circuit operates. During this time period, we can say with confidence that radiation levels were either high enough to produce the levels shown on the stripchart, or else they were lower than indicated, i.e., radiation levels were not higher than this.

(J) This rapid rise and the subsequent high level readings up to approximately 800 hours will now be discussed. This portion of the stripchart has been the most difficult to explain because it does not seem reasonable that levels, days or even weeks after the accident began, could be almost as high as those at the beginning simply because of the radioactive decay process. To understand this portion of the stripchart, we must look at radiation release into containment via waste gas or primary venting, HP-R-214 circuit operation, reactor coolant flow and possible shine from it, and the radiation dose received by HP-R-214.

1. Venting--The rise in radiation levels at 64 hours is practically coincident with venting of waste gas from the waste gas decay tanks into containment at 62.5 hours. At this time and subsequently for hundreds of hours, operators either vented gas from the decay tanks via Valve WDG-V-30B or directly from the primary via RC-V-137. Venting of waste gas was necessary because the two tanks were being filled with gas from the letdown and purification system and were in danger of being overpressurized. The letdown system produced large quantities of gas because of the large reduction in pressure. This gas was also quite "dirty" since the purification filters rapidly became ineffectual as they were clogged with fuel debris. Venting from the primary was done to attempt to rid the primary of its hydrogen "bubble".

This venting probably released both aerosol-suspended particles as well as the rest of the core's remaining inventory of noble gas. The ventings are shown on the expanded scale figure. It is important to note that the venting which occurs at 62.5 hours is the only venting which occurred since the block valve was closed at 17 hours. The rises in stripchart radiation level generally coincide rather closely with the vents. The last venting we were able to find occurred at 726 hours.

The problem with the supposition that venting caused such high radiation levels during this time period is that, in addition to radioactive decay reduction by this point in time, just not that much gas was actually vented into containment. The containment volume is quite large and the waste gas decay tanks are tiny by comparison. One would expect only a minor rise in levels.

2. HP-R-214--Our analysis of the circuit operation shows that, even in the presence of moisture, radiation can be detected if the radiation generated signal is large enough to overshadow the moisture generated signal. The detector undoubtedly saw the waste gas tank release at 64 hours, meaning that it could detect radiation at that point in time. Another point is that we were unable to find a reasonable failure mechanism which would cause the detector output to peg at a certain level and stay there if the radiation were removed; the waste gas release would not have caused the detector to go high and stay there even after the gas had decayed. The question is why did the indicated level rise to over 500 R/hr and stay there?

Before proceeding, we will review the operation of the detector. Figure 35 shows a block diagram of the detector amplifier circuits. Signals originating in either the low or high range chambers are treated in the same way. The ion chamber signal is

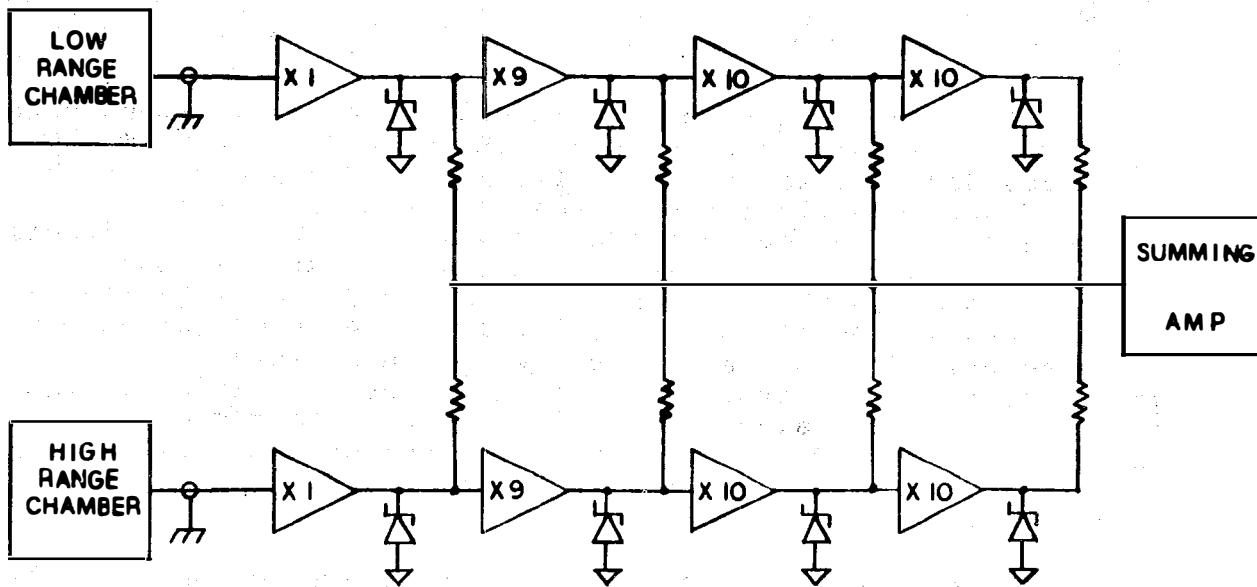


Figure 35. HP-R-214 Detector Block Diagram.

multiplied by 1, 9, 10, and finally 10, and the output of each amplifier is summed and contributes to the total. However, each section can contribute only up to 9.5 volts (which is later scaled to one volt for each). For example, if the low range chamber output signal were 20 mV, 9 volts rather than 18 volts would be contributed by the last times 10 amplifier, 1.8 volts would be contributed by the next-to-last amplifier in the chain, 0.18 volts from the X9 amplifier, and finally 0.02 volts from the X1 amplifier. The last times 10 amplifier, after scaling and summing could itself produce a 0.9-volt signal to go to the detector readout meter and could cause the needle to indicate nearly a one-decade radiation change.

Two distinct possibilities exist to explain the increase at 64 hours and the high levels until 800 hours. 1) One is that the detector low range circuit was responding properly by putting out 4 volts and that the radiation levels were high enough to overshadow the moisture-induced signal in the high range circuit. If this were the case, the measured levels are correct. 2) If, on the other hand, the true radiation levels in the vessel were below 1 R/hr the low range circuit would be able to respond to slight radiation increases and the rise at 64 hours would have to be produced by the low range amplifier signal. In this case, the high range would have to produce 3 decades (3 volts) of moisture-induced signal. Although we did not see this magnitude of offset caused by moisture in any of our tests, there is good evidence that this did happen. First, in our tests, we found moisture to cause highly variable levels, i.e. moisture interaction with the circuit is variable. Secondly, we are reasonably certain that the 60 R/hr Dome Monitor indication after 1000 hours is moisture

induced. If this is the case, with moisture in the detector and no radiation, the detector output would be 5.6 volts. It is quite likely that the high range circuit could produce a 3-volt contribution.

Based on a 1 R/hr reading from HP-R-212 at 2300 hours, it seems reasonable that in the 60 to 100 hour time frame the levels inside containment could have been as high as 100 R/hr. If we assume a vessel attenuation factor of 50 for radiation levels inside the vessel, the inside level would have been 2 R/hr or large enough to peg the low range circuit. Conversely, if the attenuation factor were 300 because of a softened spectrum (sure to be true for noble gasses), the level inside would be 300 mR/hr and the low range circuit could respond as described. One must find a radiation source other than noble gas to explain the rise. We conclude that the circuit operational aspects could support either hypothesis, depending on what the radiation source was.

3. Shine From Candy Canes--As shown in Appendix E, a direct line of sight path seems to exist between Steam Generator B candy cane and the HP-R-214. We can postulate that radiation of highly contaminated liquid (which could be inside the primary piping where it enters the top of the steam generators) could be detected by the Dome Monitor and that a good part of the radiation level seen during the 60 to 800-hour time frame is from this shine.

This radiation source is posed as a possibility because the decay and spectrum softening of noble gas constituents simply eliminate the constituents as significant radiation contributors in the time frame of several hundreds of hours. We must, thus, assume a different radiation source. Two bits of information support the postulate of shine from the candy canes.

At 2:08 p.m. on April 27, the reactor coolant pump, 2A, was powered down and the system went on natural circulation cooling. Curiously, this coincides approximately with the slow tailing off of radiation levels as measured by HP-R-214 beginning at about 700 hours. Also, early in the accident, the reactor coolant pump 2B, was started at 6:54 a.m. on March 28 and ran for approximately 20 minutes in an effort at that time to establish coolant flow; however, good flow was never achieved. No other pumps were run for any appreciable time until pump 1A was successfully started at approximately 20 hours. The slow rise in radiation level beginning at 30 hours could be the result of reverse flow of contaminated coolant in the nearer (to HP-R-214) steam generator B leg.

The ventings of the primary system described earlier were done to flush out the hydrogen gas which was present in the upper part of the reactor vessel and candy canes. This was done to allow coolant flow through the vessel and candy canes. Over the period of ventings, it is not clear how much coolant flow through the candy canes was actually taking place. Later, after the

ventings, we assume that a reasonable flow had been established, thus presumably accounting for the more or less constant detector reading in the 60 to 800 hour time period.

The forcing of water through the core debris undoubtedly distributed particulates throughout the system in a rather uniform fashion. When natural circulation was accomplished, these particulates would tend to settle out. This explanation sounds reasonable; however, we have calculated that if the activity in the upper part of the candy cane were 1 Ci/l and had a 1.2 MeV emission spectrum, the radiation level on the outside of the ss vessel would be only 675 R/hr. Therefore, it does not look as though the 600 R/hr readings inside the vessel were due to shine from the candy canes. Obviously, low levels of radiation from shine could be present inside the vessel, and in fact if the detector high range circuit had malfunctioned due to moisture, the 600 R/hr reading could be the result of shine.

4. Radiation Dose--We could present fairly convincing evidence that, because of the circuit operation of HP-R-214 in a humid environment, the high level rise at 60 hours is essentially not real. Two very hard pieces of data prevent us from doing this: the radiation doses received by the detector transistors and the cable sample. If we calculate the dose inside the vessel assuming that only the first 20 hours of the stripchart are correct, the dose received by the transistors would only be $1 \times 10E4$ rads. Also, assuming a 20% exponential release of noble gas, the dose to the cable after 300 hours is only $2.5 \times 10E5$ rads as shown in the next section. Both these numbers are low by a factor of about 30 from the $2.2 \times 10E5$ rads and $7.9 \times 10E6$ rads measured for the transistors and cable.

If we assume the stripchart is essentially correct up to 800 hours (Hypothesis 1), the dose received by the detector would have been approximately $4 \times 10E5$ rads, or very near the $2.2 \times 10E5$ rads measured. Thus, from this standpoint, the stripchart could be correct up to 800 hours.

(K) Radiation indications here are undoubtedly incorrect because at 2300 hours, HP-R-212 was activated at the 305-foot elevation and measured 1 R/hr (Appendix F). Even if levels were an order to magnitude or two higher at the 372-foot elevation, the lead shielding would attenuate the source too much to produce the 60 R/hr measured here. Our humidity tests are fairly conclusive when they show that humidity, in the presence of low radiation levels, caused the detector to read erroneously; the detector continued to read erroneously until it was taken out of service.

D. RADIATION LEVELS OUTSIDE THE VESSEL, HYPOTHESIS 1

The releases into containment probably were largely confined to noble gasses and volatile elements. Initially in the accident, these fission products would have come from the gap between the

zircalloy cladding and the fuel pellets. In this section, we calculate radiation levels at the 372-foot elevation assuming only noble gas as a radiation source. To do this, we assume a volumetric spherical source containing various percentages of the core's total inventory of noble gas and calculate the radiation levels at one edge of the sphere.

Gamma transport calculations using buildup factors were then made to transport the photons through the ss and lead layers to the detector inside. This process is an iterative one and is continued until the calculated levels inside match the early portion of the Dome Monitor measurements. When this match is made, the levels outside are known. Monte Carlo computer transport codes were initially considered to make the transport calculations; however, these were not used. In order to have used these codes, we would have had to first develop a geometrical model of the shield and then the detector. This would have been a complex task for this geometry and the accuracy was not felt to be significantly better than using buildup factors and exponential attenuation. For our transport calculations, the following methods and assumptions apply:

1. The noble gas released was uniformly mixed in the upper part of the dome from the 347 foot elevation to the 473 foot elevation. No volatiles were assumed.
2. Noble gas concentrations as a function of time were supplied by W. C. Hopkins of Bechtel (Reference 13). This mixture of noble gasses accounts for the operating time of TMI-2 when the accident occurred.
3. The containment upper level volume was assumed to be 33189 m^3 . This was transformed into a sphere of radius 19.93 m.
4. We accounted for attenuation by air.
5. The following equation for radiation rate outside the ss vessel was used for the calculations. This expression was derived by W. C. Hopkins and was verified by Sandia. An explanation of terms is given in Appendix H.

$$\dot{D}_o = D_K \mu_{ME}(\text{AIR}) \frac{S_v E_p}{2\mu} \left[1 - \frac{1}{2\mu R} (1 - e^{-2\mu R}) \right]$$

6. The following expression was used to calculate levels inside the ss vessel:

$$\dot{D}_i = \dot{D}_o B [\mu(Pb), d(Pb+Fe), E_p] e^{-\mu(Pb)d(Pb)} e^{-\mu(Fe)d(Fe)}$$

7. The radiation was released exponentially as follows:

$$S_v E_p(t) = S_v E_p(t_0) [1 - e^{-t/t_0}]$$

8. The effects of the hole in the vessel were not considered.

9. Any effects of radioactive gas inside the vessel were not considered.

Appendix H contains more information pertaining to these and other transport calculations. The result of these calculations is shown in Figure 36. The gamma rate outside the ss vessel (labeled ss pig) peaks at about 8000 R/hr and decays by two orders of magnitude by 500 hours. The calculated rate inside the vessel is shown overlaid with the Dome Monitor corrected stripchart. Notice that the calculated level drops off quite sharply in the 20 to 30-hour time frame. This is caused by the softening of the noble gas spectrum as time progresses. We have matched the early part of the stripchart recording very well. However, this model does not predict or explain the rise in measured levels at 60 hours and later. One can pose explanations for the rise 60 hours and later. Some of these explanations are addressed below.

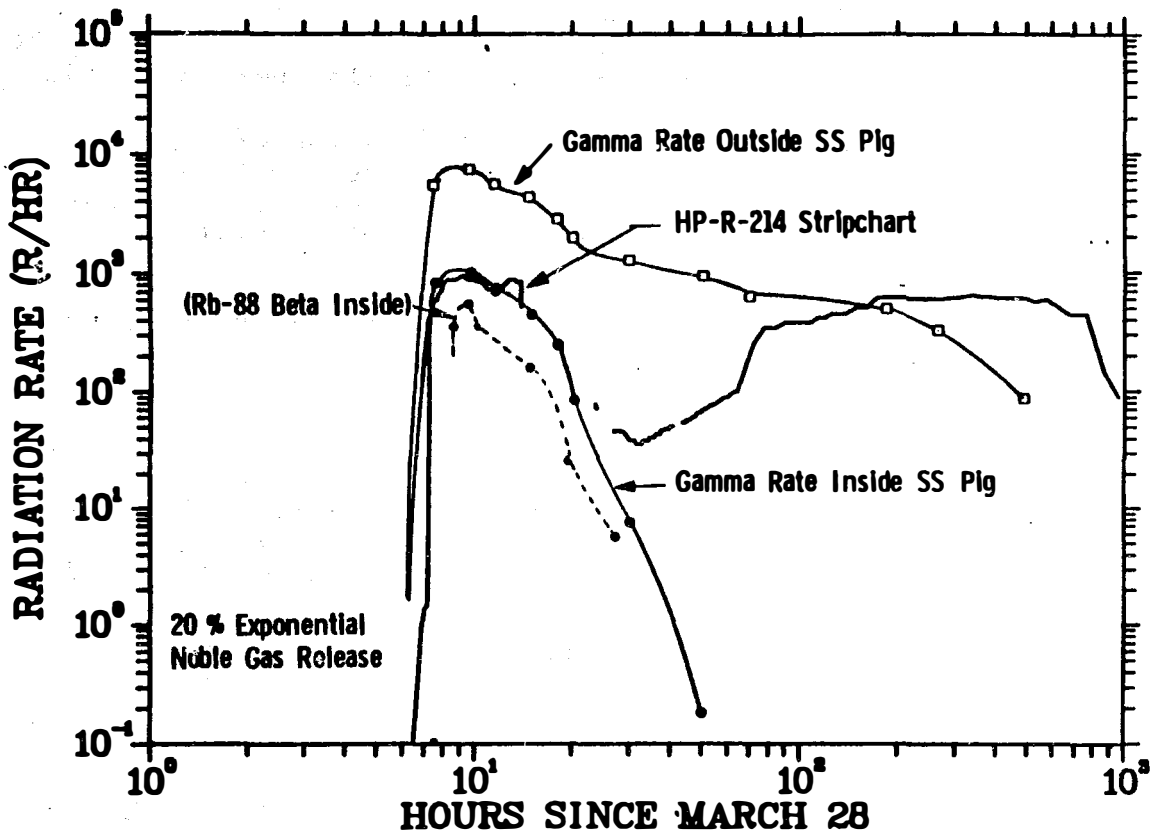


Figure 36. TMI-2 Gamma Rate History, Hypothesis 1. The first 20 hours of the stripchart recording is matched by assuming a 20% exponential noble gas release. This figure also shows what the level outside the vessel needed to be to produce the assumed level inside the vessel. If radioactive gas were present inside the vessel, Rb 88 high energy betas would have produced the response shown.

1. Effect of Gas Inside the Vessel. It has been postulated that the Dome Monitor readings were in error because radioactive gas had leaked inside the ss vessel and thus circumvented the shield causing the monitor to read exceptionally high. The effect of gas inside the vessel is shown in Figure 37. Here, the vessel was assumed to be completely full of radioactive gas of the same concentrations and activity as that outside the vessel. A 60% instantaneous release was assumed to occur at 6:30 a.m.

The contribution by gas inside the vessel is almost one order of magnitude less than that due to gas outside the vessel early after the release because the volume of gas inside is quite small. Later, after 20 hours, the gas inside the vessel dominates because the spectrum softening is not nearly so much a factor. The effect of the 5.34 MeV beta emission of Rb 88 is shown in Figure 36 for the case of a 20% instantaneous release and immediate entry into the vessel. The effect, in this unlikely event, is still below that calculated for gas outside the vessel.

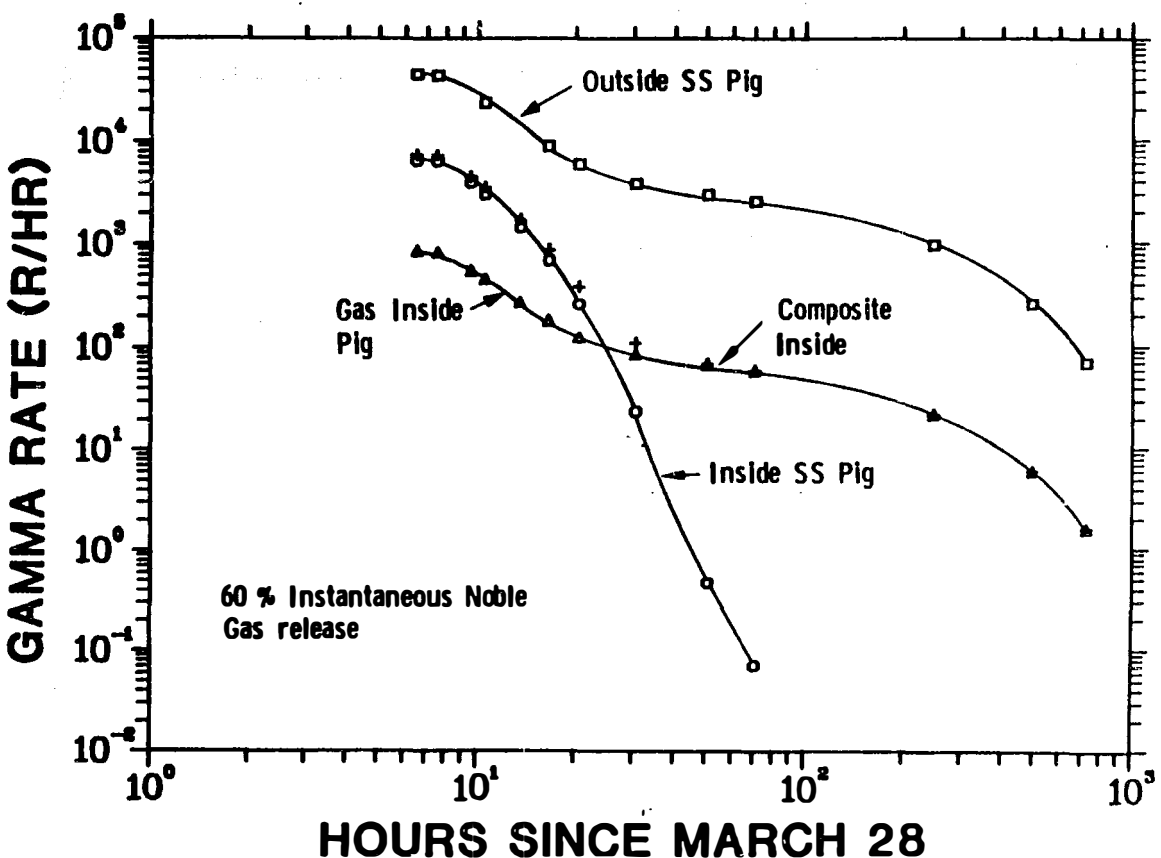


Figure 37. Effects of Radioactive Gas Inside the SS Vessel. If we assume that a 60% release of the core's inventory of noble gas occurred and that the containment atmosphere could somehow be present inside the ss vessel, radiation levels inside the vessel would be the "composite" curve. This curve and the contributions of gas inside the vessel and that due to the outer volume of containment atmosphere are shown in this figure.

From these calculations, we find that, even if radioactive gas of equal makeup and concentration as that outside the vessel were present inside, the contribution to the overall response early in the accident would have been small. We conclude, therefore, that the effects of radioactive gas inside the vessel were negligible.

2. Effect of the 1.27 Cm Hole. We conclude that radiation levels inside the ss vessel were increased by a negligible amount because of the 1.2 cm diameter hole through the ss vessel lead shield. This conclusion is based on the fact that the hole subtends a small solid angle and, therefore, the volume of gas actually "shining" through the hole is some 30 times smaller than that incident on the total vessel surface. In addition, only a small volume of the detector chambers are illuminated. This conclusion is in part substantiated by the fact that the radiation dose received by the detector electronics could not have been delivered through the hole due to its vertical placement.

3. Moisture Correction. Figure 38 shows the effect of moisture inside the detector. For this case, the stripchart has been

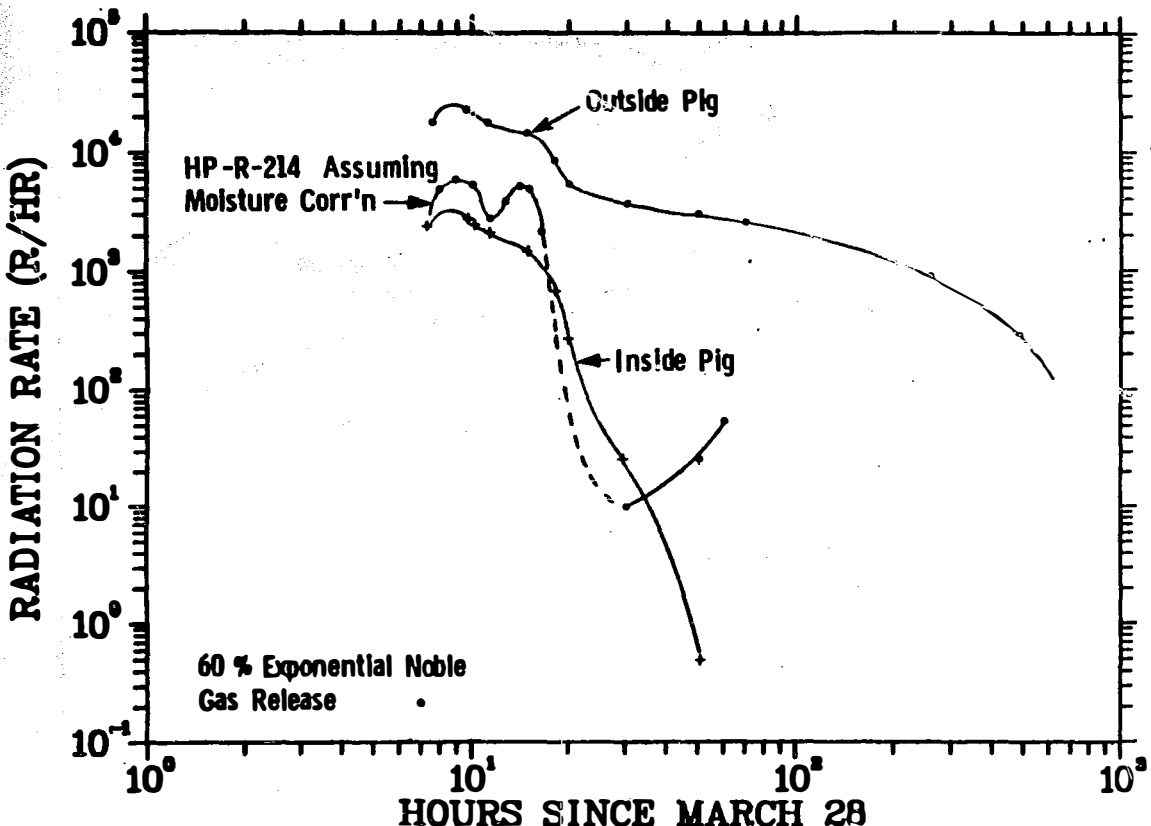


Figure 38. Moisture Correction. This set of curves shows the calculated rates inside and outside the ss vessel assuming a 60% noble gas release which is released exponentially with a two hour time constant. The additional curve shows what the detector would indicate if moisture were inside the vessel. This curve was derived by using Figure 24. Notice that the "Inside Pig" curves are both substantially higher than the actual stripchart recording, indicating that a 60% release is too high.

adjusted to indicate actual levels if moisture were present inside the vessel at the time of radiation release. Calculated levels assuming a 60% exponential release of noble gas are shown. The curve fit is not very good.

E. RADIATION LEVELS OUTSIDE THE VESSEL, HYPOTHESIS 2

If we assume that the fission product release into containment had, in addition to noble gas, a considerable quantity of volatile elements and that they are suspended in the aerosol, radiation levels inside containment could have been considerably higher than those found for a 20% release of noble gas. We now use the information we have on the radiation total doses received by the cable and detector to adjust radiation rates. To do this, we calculate levels inside and outside the vessel just as we did for Hypothesis 1, except that we just increase the level of release until the total integrated doses are approximately correct. The error here, of course, is that we are using the noble gas spectrum and decay characteristics to approximate that of both noble gas and volatiles.

Reference 14 shows that the spectrum and decay characteristics for a source term containing both noble gas and volatiles is quite similar to that of noble gas alone. Also, if the volatiles are indeed suspended in the aerosol, our volumetric gas model is also reasonable. Even if considerable plateout has occurred, the model is not unreasonable since we would now have a source distributed on the inner surface of a sphere. For the hotter spectrum early on, the attenuation by air is a small factor, and the difference between a volumetric and a surface source becomes less significant.

The results of these calculations is shown in Figure 2. Gamma rates outside the ss vessel peak at 200,000 R/hr. Those inside peak at 30,000 R/hr. Notice that both the inside and outside integrated doses are very close to those actually measured.

F. CONCLUSIONS REGARDING HYPOTHESES 1 AND 2

As stated in the Summary of this report, we believe Hypothesis 2 to be the more likely explanation. In this case, the ss vessel seal would have had to be circumvented by moisture quite early in the accident. If this did happen, both the low stripchart reading in the 10 hour timeframe and the rise and plateau level in the 60 to 800 hour timeframe are explainable at least qualitatively by the way in which the detector responds in the presence of moisture. Unfortunately, we will never be able to say with absolute certainty what the radiation rates really were. This is disturbing since this instrument should have provided us with this information in such a way as to leave no doubt regarding its accuracy.

ABBREVIATIONS AND ACRONYMS

Ci - Curie (Unit of radiation source strength)

CO 60 Source - Cobalt 60 Gamma Source

Contaminant Building - The large, steel reinforced concrete building at TMI-2 which houses the reactor, steam generators, and other primary coolant piping and equipment.

CPM - Counts Per Minute

DECON - decontamination

DOE - Department of Energy

EDS - Energy Dispersive Spectroscopy

EG&G - EG&G, Inc.

EMP - Electromagnetic Pulse

FSC - Fairchild, Inc.

GE - General Electric, Inc.

GIF - Gamma Irradiation Facility at SNL

GPU - General Public Utilities

HFE - Transistor current gain

HIACA - High Intensity Adjustable Cobalt Array at SNL

HP-R-214 - Equipment tag number at TMI-2 for the Dome Radiation Monitor

ICBD, ICED, IEBO - Transistor Leakage Currents

KeV - Thousand Electron Volts

LOCA - Loss-of-Cooling Accident

MeV - Million Electron Volts

MOS Transistor - Metal Oxide Semiconductor Transistor

MOT - Motorola, Inc.

mR - milliroentgen (unit of radiation exposure)

mR/H - milliroentgen per hour

Multivalued Characteristic - Dual Valued Response to Radiation

NAT - National, Inc.

NBS - National Bureau of Standards

NRC - Nuclear Regulatory Commission

psig - Pounds Per Square Inch Guage Pressure

R - Roentgen

R/hr - Roentgen Per Hour

RAD - Radiation absorbed dose, now rd.

Rd - Unit of absorbed radiation. One Rd is equal to 100 ergs of energy per gram of material; originally written as an acronym:

RAD

RH - Relative Humidity

SEM - Scanning Electronic Micsroscopy

SiO₂ - Silicon Dioxide

SNL - Sandia National Laboratories

SS - Stainless Steel

TEC - Technology for Energy, Inc.

TI - Texas Instruments, Inc.

TIO - Technical Integration Office at Three Mile Island

TLD - Thermoluminescent Dosimeter

TMI - Three Mile Island

TMI-2 - Three Mile Island, Unit 2

VBES - Transistor base to emitter saturation voltage

VCES - Transistor collector to emitter saturation voltage

VR - SNL Vertical Range Gamma Facility

REFERENCES

1. Technical Specifications, Three Mile Island, Unit 2, Nuclear Power Generating Station.
2. U. S. Nuclear Regulatory Commission, Regulatory Guide, 1.97, "Instrumentation for Light-Water-Cooled Nuclear Power Plants to Assess Plant Environ Conditions During and Following an Accident," December 1980, Revision 2.
3. U. S. Nuclear Regulatory Commission Investigative Report, No. 50-320/79-10, "Investigation into the March 28, 1979 Three Mile Island Accident by the Office of Inspection and Enforcement."
4. Victoreen Inc. Manual, "Instruction Manual for Area Monitor 845," April 1980.
5. Sandia Engineering Notebook, ENG-F-896, 9-1-82, William C. Jernigan, III.
6. Sandia Engineering Notebook, ENG-F-874, 2-4-82, William C. Jernigan, III.
7. Sandia Engineering Notebook, ENG-F-815, 5-29-81, Geoffrey M. Mueller
8. GEND-INF-017, "Field Measurements and Interpretation of TMI-2 Instrumentation: HP-R-214," J. E. Jones, J. T. Smith, M. V. Mathis, April 1982.
9. "Analysis of Three Mile Island, Unit 2 Accident," NSAC-1, October 1979.
10. "Examination Results of the Three Mile Island Radiation Detector HP-R-211," Sandia Laboratories Report, SAND81-0725, Michael B. Murphy, Geoffrey M. Mueller, Frank V. Thome, September 1981.
11. Sandia Laboratories Report, SAND83-1930, Geoffrey M. Mueller, "Examination Results of the Three Mile Island Radiation Detector, HP-R-212," December 1983.
12. Sandia Laboratories Report, SAND82-1173, Geoffrey M. Mueller, "Examination Results of the Three Mile Island Radiation Detector, HP-R-213", August 1982.
13. Bechtel Inc., Informal Report, W. C. Hopkins, "TMI-2 Containment Post Accident D and D for Each Elevation," Volumes 1 and 2, 1982.
14. Sandia Laboratories Report, SAND81-7159, D. D. Thayer, D. H. Houston, N. A. Lurie, "Updated Best-Estimate LOCA Radiation Signature," August 1981.

We found that silicone toward the center of the cable received slightly less dose than those samples on the outside. This might indicate some beta damage in the outer silicone. However, the difference in doses is small. To try and determine whether beta dose had accumulated, we acquired a cable sample from inside the conduit going to the detector. This sample was probably 0.3 m from the cable sample just described, but it was inside the conduit. The conduit would be a very effective shield against beta radiation from the containment volume of gas. Our test results were approximately the same as those with the cable outside the conduit. This indicates our measurements probably are, in fact, revealing gamma and not beta damage. Note that it is probable that radioactive gas did enter the conduit; however, presumably the volume would be low and thus severely limit any beta contributions.

15. TMI-2 Control Room Operators Log, March 28, 1979-July 25, 1979.
16. Glasstone and Sesonske, "Nuclear Reactor Engineering," Van Nostrand Reinhold Company, 1967.
17. W. H Tait, "Radiation Detection," Butterworths Co., 1980.
18. Harold Etherington, Editor, "Nuclear Engineering Handbook," McGraw Hill Book Co., 1958.

APPENDIX A

Radiation Detector Operation

FUNCTIONAL DESCRIPTION

Detector 847-1 comprises the following sub-assemblies:

Ion Chamber Assembly 847-1-50
High Amplifier Circuit Board Assembly 847-1-15
Low Amplifier Circuit Board Assembly 847-1-20
Auxiliary Circuit Board Assembly 847-1-25
Power Supply Circuit Board Assembly 847-1-30

Ion Chamber Assembly - Detector 847-1 uses a dual coaxial ion chamber with a high and a low-range ion current output as shown in Figure A1. Each range covers four decades of radioactivity. The chambers operate synchronously with each output measured the same way.

The collector for the high-range chamber is a conventional axially-located electrode mounted in the usual way with a ceramic insulator and a guard. The guard is connected to the low-level or signal ground. The low-range collector is a cylindrical electrode surrounding the high-range chamber wall. The low-range chamber wall surrounds the low range collector. Although not shown in Figure A1, the low-range collector is supported, like the high-range collector, by a ceramic insulator, and protected by a guard that is connected to the low-level or signal ground. A collecting voltage of -150 V dc is applied to both the high-range and the low-range chamber walls. Surrounding the low-range chamber wall is a protective cover that is grounded to the instrument chassis.

High-Range Amplifier Circuit - Figure A2 is a schematic representation of the high-range amplifier. S1 is a reed switch, normally open, that is closed by action of coil T1. T1 is triggered through Q 14 by a timing circuit on the auxiliary circuit board. The switch is closed for four milliseconds, and open for 329 milliseconds, for a total cycle time of 333 milliseconds, or about 1/3 second.

While the reed switch is open, the chamber capacitance is charged by the ionization current. When the switch is closed, this charge is transferred to Capacitor C 21. During the rest of the cycle this charge decays toward zero through R 44. This charge and decay cycle causes a preamplifier output signal of the shape shown in Figure A3. The original height (amplitude) of the signal will depend on the level of ambient radioactivity.

Figure A2 shows three similar amplifier stages following the preamplifier. The first stage, which is typical of the three, is composed of Q1, Q2, Q3, and Q4 along with their related circuitry. Q2 is a unity-gain inverter and gate. It is triggered by Q1. The gate passes a 100-microsecond sample of the preamplifier output (measured from 9 milliseconds after the start of the cycle). This measurement is controlled by the

gate signal of 2F that comes from the timing circuit on the auxiliary circuit board, and by Capacitor C3. Q3 is a gain-of-nine inverting amplifier and Q4 is an output follower. In the next two stages, the amplifiers corresponding to Q3 are Q7 and Q11. They each have a gain of ten. The gain of the amplifier is approximately equal to the ratio of the two resistors on the base of the transistors (in the case of Q3, $R10/R8 = 82.5/9.09 = 9$). The waveforms of the three amplifier stage outputs are shown in Figure A4.

Low-Range Amplifier Circuit - Figure A5 is a schematic representation of the low-range amplifier circuit. With some minor modifications, the circuit operates in the same manner as the high-range circuit.

Auxiliary Circuit Board - The Auxiliary Circuit Board, Figure A6, contains the timing circuit that triggers the reed switches on the High-Range and Low-Range Amplifier Circuit Boards, and controls the timing of the 100 us sample used by the three cascaded amplifiers; an oscillator circuit that provides collecting and bias voltage; a summing amplifier that adds signals from the Low-Range Amplifier and the High-Range Amplifier; and a fail circuit.

Timing Circuit - The basic timing generator consists of the UJT Oscillator Q1 and pulse shaper Q2. Most of the time Q2 is ON, however, when the emitter of Q1 discharges C2 suddenly, Q2 cuts off. The time required for Q2 to turn back on is determined by the RC time constant of R5 and C3.

This circuit is shown on the left in Figure A6, and next to it are the 9-millisecond cascade one-shot multivibrator composed of Q3 and Q4, and the 100-microsecond one-shot multivibrator composed of Q5 and Q6. These latter circuits control the timing and duration of the 100-microsecond samples amplified by the cascaded amplifiers of the High-Range and Low-Range Amplifier Circuit Boards.

Oscillator Circuit - The oscillator (consisting of Q16 and T1) is a basic blocking type oscillator which operates at about 25 kHz. The secondaries of T1 provide for the collecting and bias supplies. Both supplies are zener regulated.

Summing Amplifier - The summing amplifier is broken into two stages. The first stage Q7 and Q8 inverts and sums the current signals from the eight amplifier outputs of the complete system.

The negative pulse output from Q8 is coupled into a unity gain inverter consisting of Q9, Q10 and Q11. This stage provides a positive pulse with a very low output impedance at the peak-reading voltmeter. Gain adjustment for the summing amplifier is done by means of R26. The gain of the summing amplifier is a small fraction reducing a signal potentially about 73 volts maximum to a maximum of 8.11 volts.

The peak-reading voltmeter comprises the diode CR7, capacitor C13 and source follower stage consisting of Q12 and the constant-current stage Q13. The positive pulse output of the summing amplifier charges C13 through the diode. Since the source follower has a high input impedance and CR7 has a low reverse leakage, a very small amount of charge will bleed off C13 between signal pulses. To speed up the decay time constant of the system, C13 is discharged for 9-milliseconds preceding every signal pulse. This is done by Q19 and R49. Q19 is biased and switched from the charge pump consisting of C22, CR13, Q18, and Q17.

When the trigger input is zero volts, Q17 is off and Q18 is on. C22 charges very fast through the saturated transistor Q18 and CR13. During this process the gate of Q19 is held near zero volts and Q19 maintains a low drain to source on resistance. When the trigger is returned + 12 volts, Q17 turns on and Q18 is driven off. The gate of Q19, therefore, sees the negative 12 volt charge on C13, causing the drain to source resistance of Q19 to become very large.

The dc output driver consists of a pnp-npn complementary emitter follower, Q14 and Q15. A capacitor is placed at the base of Q14 to smooth out the signal from the peak reading voltmeter. This capacitor determines the upscale response and can be reduced if faster response is desired.

Fail Circuit - The fail circuit monitors the collecting supply through Q20 and monitors the bias supply through Q21. The outputs of Q20 and Q21 are fed through an and gate to the fail indicator drive in the readout module. A fail circuit signal indicates a functioning system. Absence of a signal indicates a failure.

Power Supply Circuit Board - The Power Supply Circuit Board is a Mother board containing connections for the other circuit boards and routing wiring between the three boards and the P1 connector. The check source movement is mounted on this board. Figure A7 is a schematic circuit diagram of the Power Supply Circuit Board.

Readout Module - The circuit diagram of the readout module is shown in Figure A8. Four different functions are performed by the readout module:

- Give a meter indication of the measured radioactivity
- Actuate warning devices when the radiation reaches a certain level of intensity
- Give a warning of failure when any part of the system does not operate properly
- Provide low-voltage dc power for system use

Meter Indication - The signal from the detector enters the module through J2-B. The readout is a 50 uA D'Arsonval meter with appropriate multipliers to make a voltmeter. The series meter dropping resistor is in two parts, R4 and R10. In the eight-decade ALL mode of operation, R4 and R10 are both in series with the meter. For the various 3-decade modes of operation, R10 is replaced by a bias of zero to five volts opposing the input signal. The bias comes from zener diode CR1, and is adjusted by R9. The five volts should occur between R9 and R11. The series string R11, R12, R13, R14, R15 determines the level of the bias voltage seen by the meter. Computer and 10 mV recorder outputs are provided from the 50 mV divider string R1, R2, and R3.

Warning Actuation - The readout module has two alarm lights on its front panel: An amber ALERT alarm, and a red HIGH alarm. In addition, it has outputs for remote alarms. As shown in Figure A8, there are two similar alarm circuits, one for the ALERT alarm, and one for the HIGH alarm.

In the HIGH alarm circuit, Q1 is a comparator that compares the input at its base with the set level at its emitter (This level is set by adjustment of R20). When the input exceeds the set level by a certain amount, Q1, Q2, and Q3 start conducting. The red light goes on. If a remote alarm is connected, it actuates, and Relay K1 is actuated. If Jumper J1 is in place, the alarm will continue until it is reset manually. For automatic reset J1 must be removed. Once J1 is removed, it is difficult to replace. One segment of the Function Switch is connected in series with the reset button, and in CS position, opens the circuit thus defeating the alarm while the Check Source is in position.

The check source actuating circuit is a "dead man" circuit. That is to say, the normal at-rest position of the check source is in test position where it irradiates the ion chamber. It takes applied power to keep the check source retracted. Therefore, element S4C shows power applied to the check source except in the CS position where the check source line is grounded.

The ALERT alarm circuit operates in a manner analogous to the operation of the HIGH alarm circuit. There is no provision for a remote alarm with the ALERT circuit, other than from Relay K2.

Fail Warning Circuit - As long as the green FAIL light is on, the system is operating properly. A failure in the system is indicated by the light going out. Q9 is an electronic switch that switches off the light circuit on loss of a so-called fail signal from the detector.

Power Supplies - Line voltage is applied to the primary of T1 and the secondary provides 22-volt power which is rectified to provide operating power for lights and relays as well as power for the meter movement that operates the check source.

A regulated bias voltage of 14V is provided through Q11 driven by Q10. The differential amplifier, Q12 and Q13 supplies Q10. Q14 supplies constant current for Q13. CR14 supplies voltage regulation, and is temperature compensated by CR12 and CR13.

An 18-volt standby battery can be connected at J3-K and J3-L to support the channel operation during power failure.

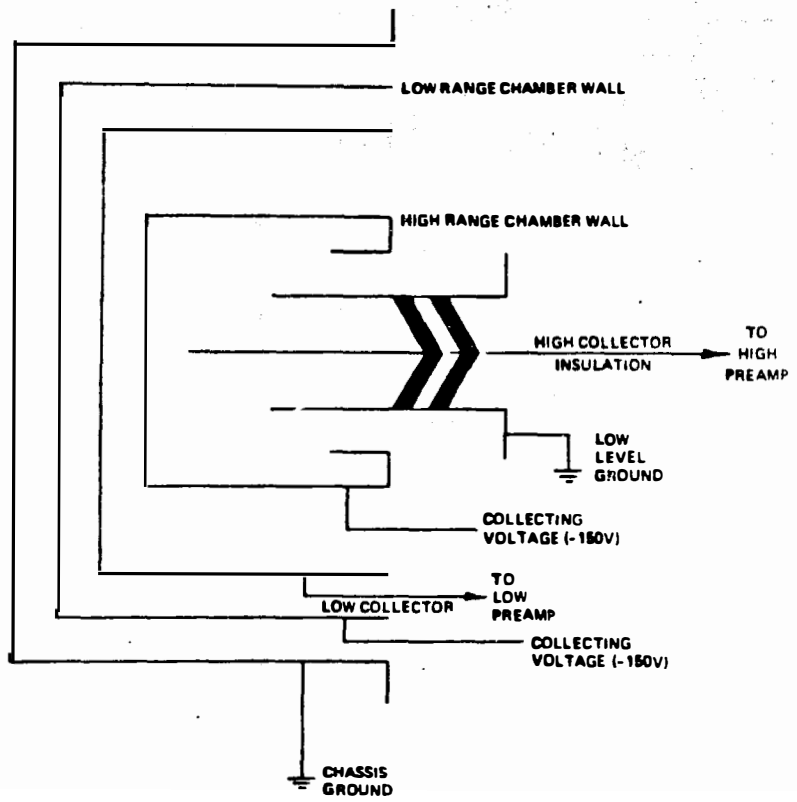


FIGURE A1. Dual Coaxial Ion Chamber

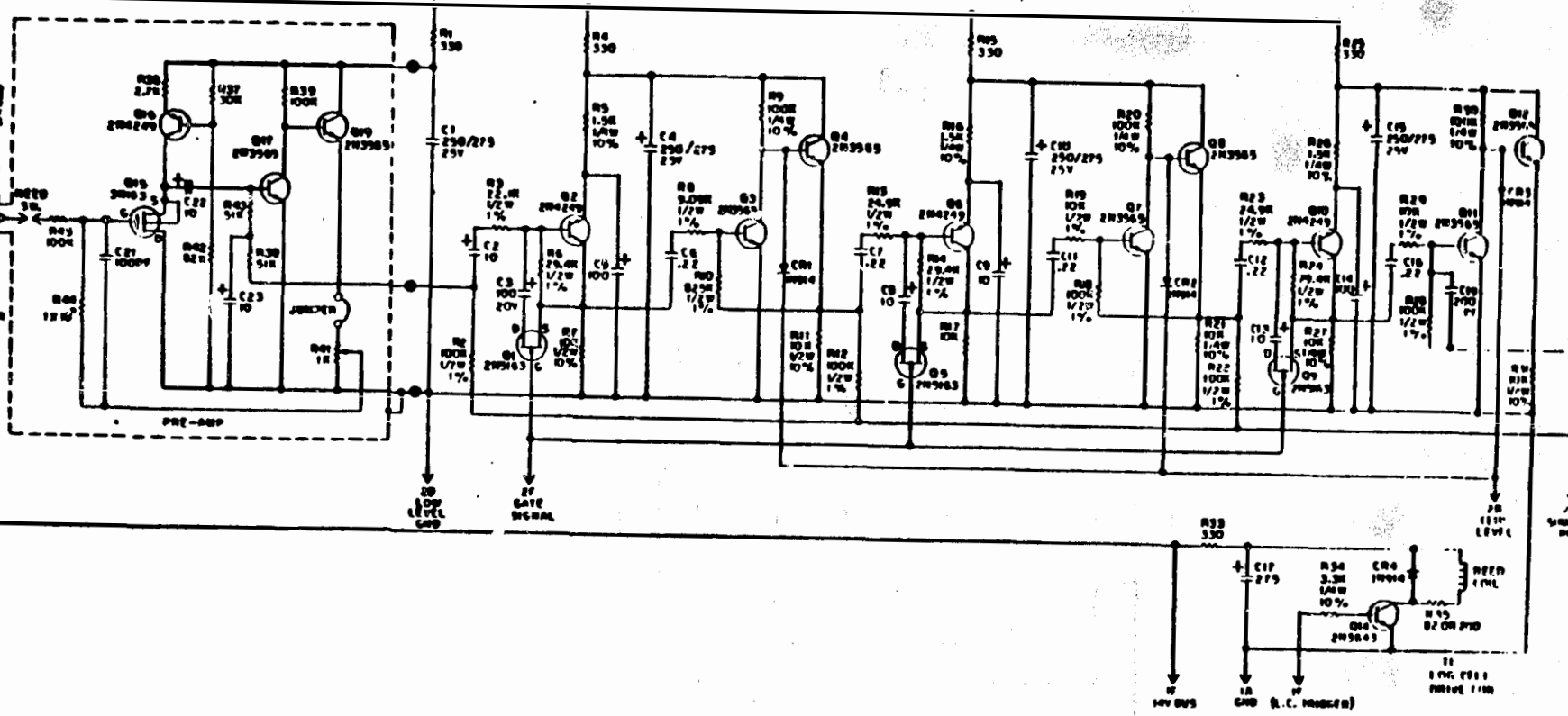


FIGURE A2. Schematic Diagram of High-Range Amplifier.

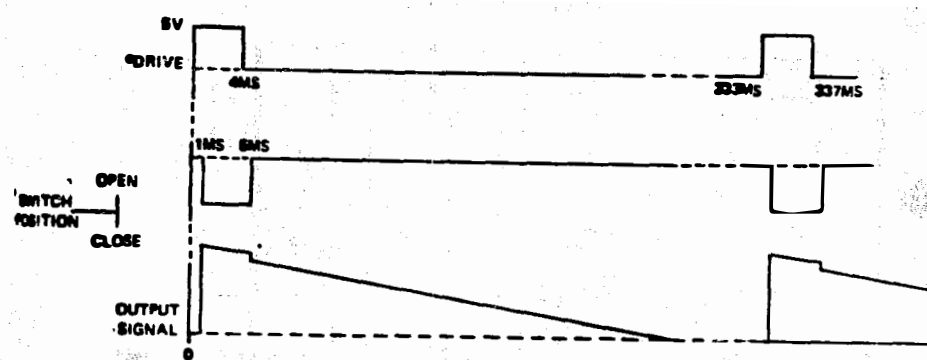


FIGURE A3. Preamplifier Waveforms.

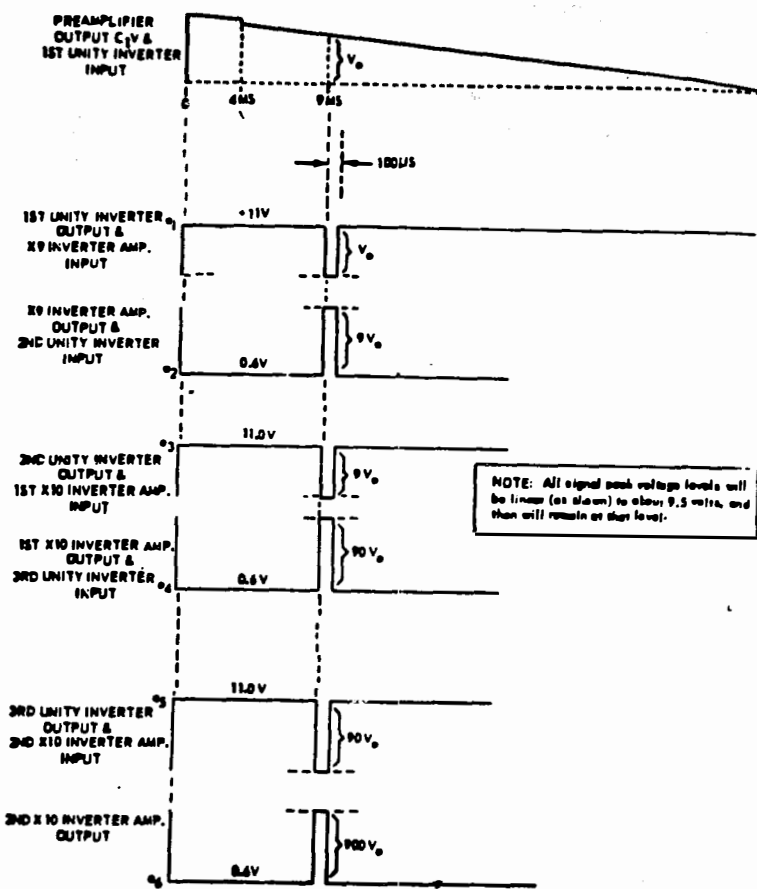


FIGURE A4. Decade Amplifier Output Signal Waveforms.

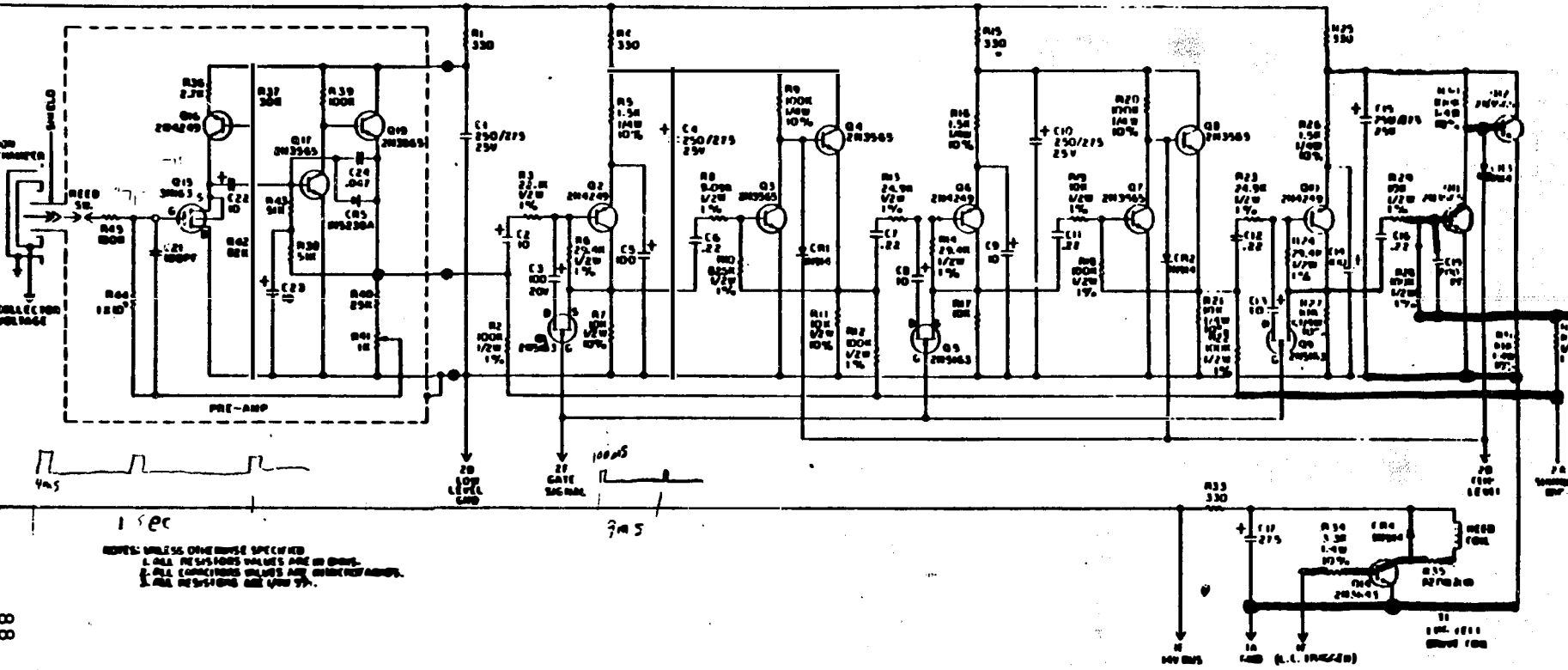


FIGURE A5. Schematic Diagram of Low-Range Amplifier.

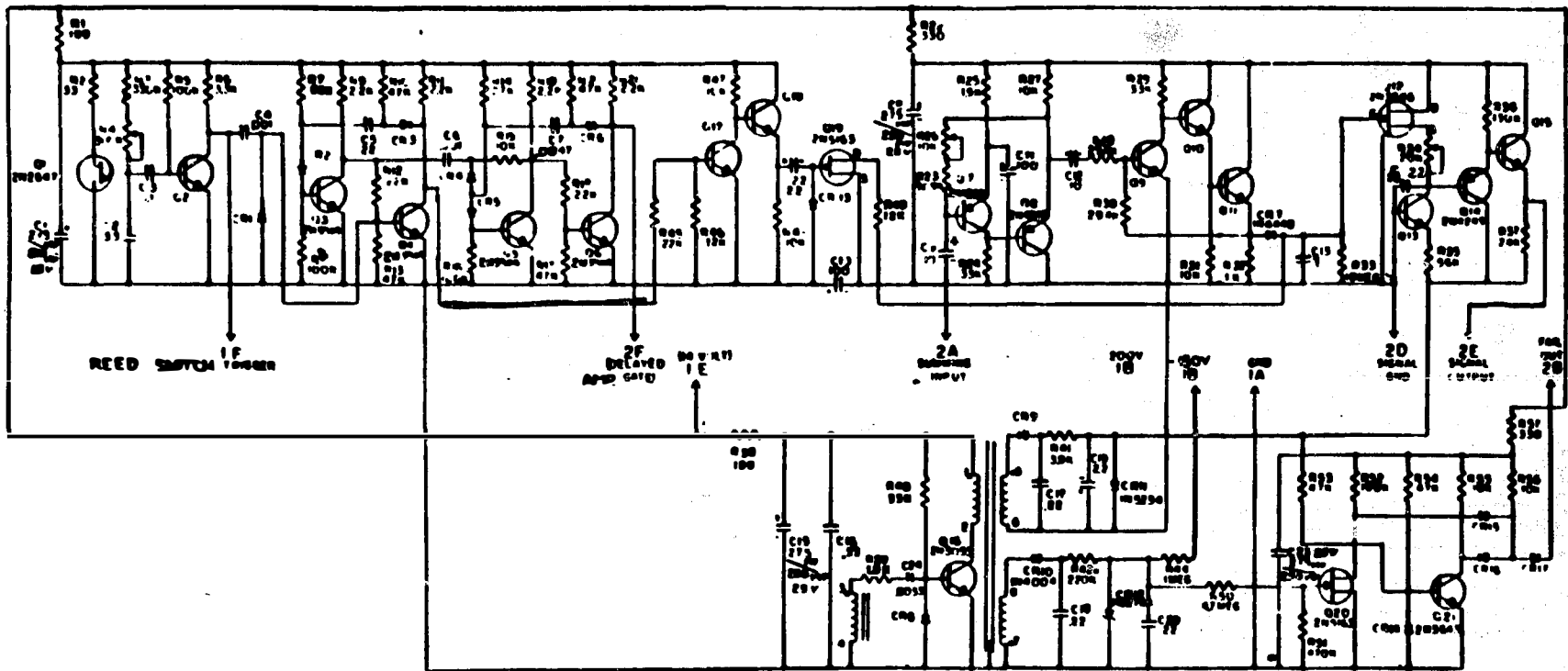


FIGURE A6. Schematic Diagram of the Auxiliary Circuit.

MODULE CHASSIS

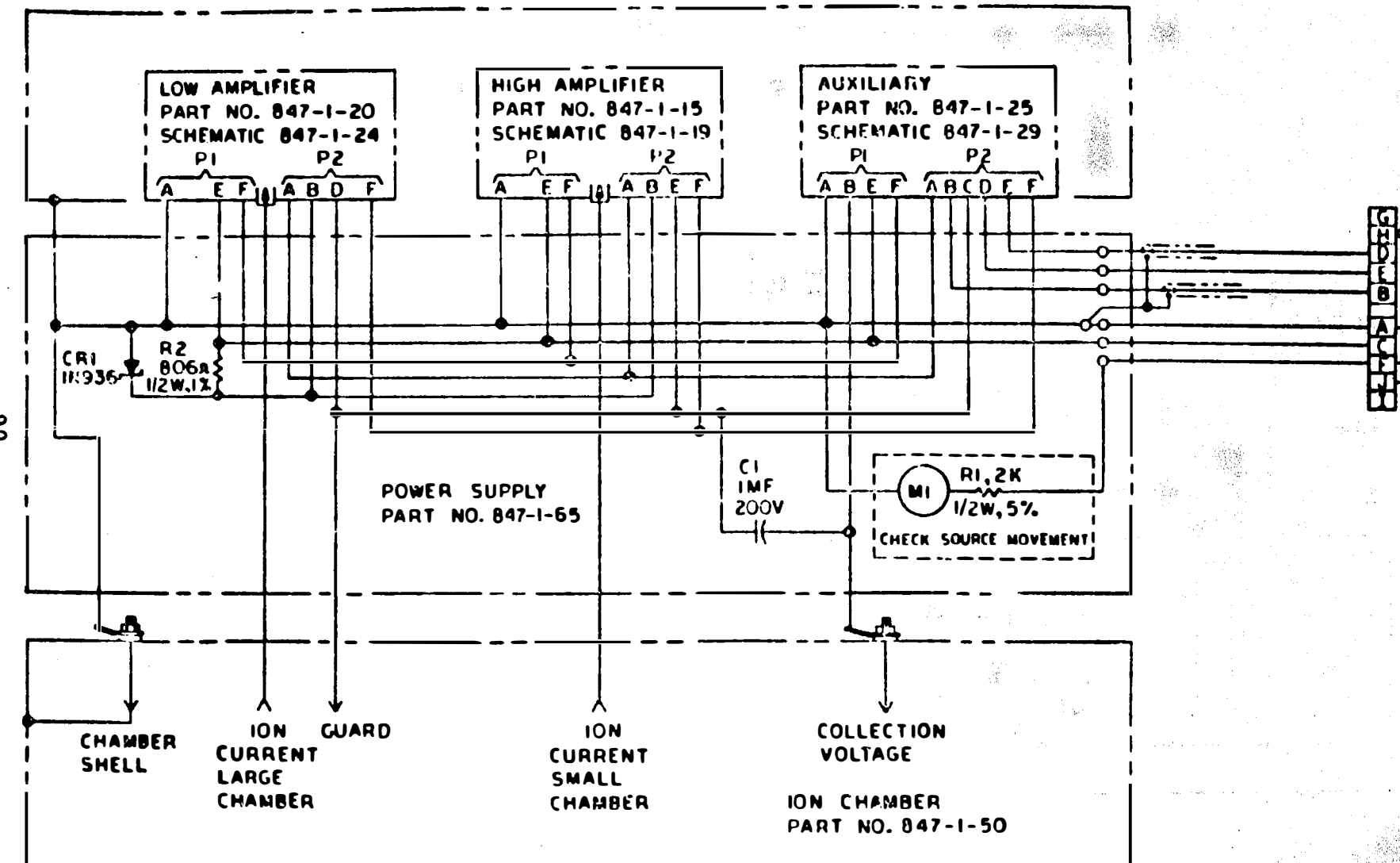


Figure A7. Schematic Diagram of the Power Supply Circuit Board.

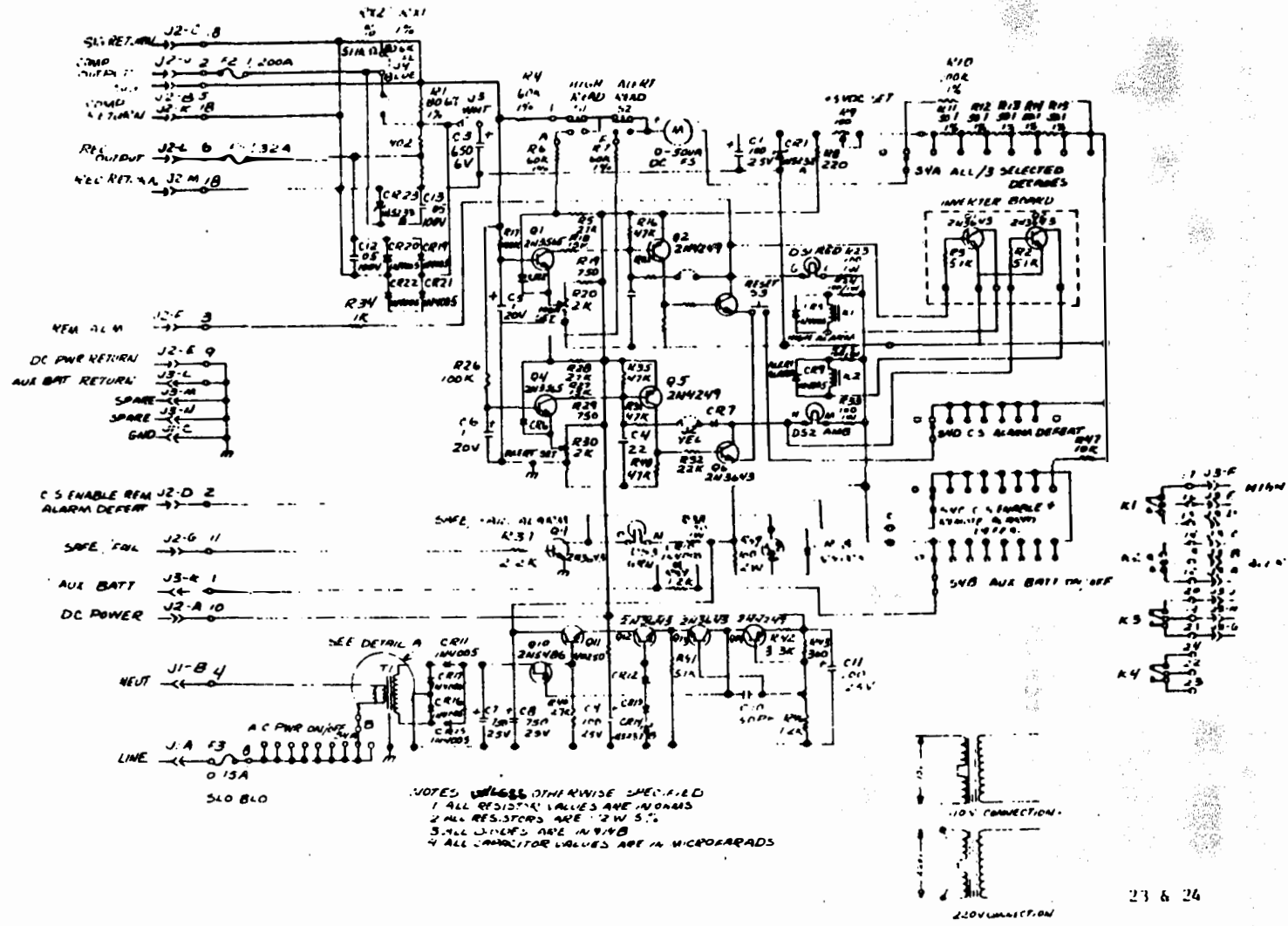


Figure A8. Readout Module Schematic.

Stainless Steel Vessel Contaminant Levels

and Chemical Analyses

This appendix contains the raw data collected on the contaminant levels inside the SS Vessel as well as those in the fiberglass insulation. The results of tests looking for boron are also included.

SWIPE SAMPLES

- Chart B1 - Swipe locations
- Chart B2 - Number of counts in 1 minute
- Chart B3-B10 - Activity Concentration in μCi of swipe Nos. 1, 2, 7, 9

FIBERGLASS SAMPLES

- Chart B11 - Fiberglass sample locations
- Chart B12 - B18 - Gamma Spectrum Analysis of 7 samples

CHEMICAL ANALYSIS OF VESSEL LID UNDERSIDE

Memo on Particulates

BORON ANALYSIS

- Chart B19 - Sample locations
- Chart B20 - Boron concentrations

CHART B1

Swipe Sample Locations

<u>Sample #</u>	<u>Location</u>
1	Oily Substance on Underside of Vessel Lid
2	Clean Area Under Lid Gasket
3	Detector Cable Near Detector
4	Area Under Lid Gasket, Inner Diameter
5	Bottom Side of Lid Approaching Gasket Seal
6	Top of Detector
7	Bottom of Vessel
8	Detector Cable Near Vessel Tube
9	Vessel Side Halfway Down

CHART B2

RESULT SUMMARY

9 SAMPLES COUNTED ON INSTRUMENT B FOR 1.0 MINUTES EACH
 DATE COUNTED 30-AUG-1982 FROM 10:43 FOR 13 TOTAL MINUTES

ALPHA EFFICIENCY = 19% |--| BETA EFFICIENCY = 40%
 ALPHA BACKGROUND = 0.00 CPM |--| BETA BACKGROUND = 3.00 CPM
 ALPHA MDA = 0.000 DPM |--| BETA MDA = 12.990 DPM

RESULTS ARE SHOWN \pm 2.0 SIGMA

<-- LOG NUMBER

SAMPLE #	ALPHA RESULTS - DPM	BETA RESULTS - DPM
1	184.211 \pm 62.275	31477.500 \pm 561.182
2	131.579 \pm 52.632	19075.000 \pm 436.921
3	LESS THAN BACKGROUND LEVEL	1067.500 \pm 104.043
4	321.053 \pm 82.213	55157.500 \pm 742.732
5	110.526 \pm 48.238	19482.500 \pm 441.560
6	5.263 \pm 10.526	647.500 \pm 81.394
7	184.211 \pm 62.275	24047.500 \pm 490.535
8	10.526 \pm 14.886	4102.500 \pm 202.916
9	21.053 \pm 21.053	2225.000 \pm 149.666

STANDARD NUMBERS = 821200. 10. 14485. 3683.

GAMMA SPECTRUM ANALYSIS

CANBERRA SPECTRAN-F V2.06 SOFTWARE

RADIATION COUNTING LABORATORY (3313)

18-OCT-82 12:16:12

ANALYSIS PARAMETERS

MCA UNIT NUMBER: 3 / ADC UNIT NUMBER: 1.0
DETECTOR NUMBER: 1 / GEOMETRY NUMBER: 7
SPECTRUM SIZE: 4096 CHANNELS
ORDER OF SMOOTHING FUNCTION: 5
NUMBER OF BACKGROUND CHANNELS: 4 ON EACH SIDE OF PEAK
PEAK CONFIDENCE FACTOR: 80.0%
IDENTIFICATION ENERGY WINDOW: +/- 1.00 KEV
ERROR QUOTATION: 1.00 SIGMA UNCERTAINTY

MULTIPLET ANALYSIS PERFORMED

SPECTRAL DATA READ DIRECTLY FROM MULTICHANNEL ANALYZER AND:
ANALYZED BY: ONEAL

SAMPLE DESCRIPTION: SWIPE TMI TOP #1
GEOMETRY DESCRIPTION: AIR FILTER (2.75)
SAMPLE SIZE: 1.0000E+00 EA / CONVERSION FACTOR: 1.0000E+00
STANDARD SIZE: 1.0000E+00 EA
ANALYSIS LIBRARY FILE: ANL000

COLLECT STARTED ON 18-OCT-82 AT 10:20:00

COLLECT LIVE TIME: 6000. SECONDS
REAL TIME: 6000. SECONDS
DEAD TIME: 00.00 %

DECAYED TO 0. DAYS, 0.0000 HOURS BEFORE THE START OF COLLECT

ENERGY CALIBRATION PERFORMED 8-AUG-82

EFFICIENCY CALIBRATION PERFORMED 18-OCT-82

RADIATION COUNTING LABORATORY (3313)

18-OCT-82 12:16:12

CHART B3

PK CHANNEL	CENTROID KEY	ENERGY KEV	FWHM KEV	BACKGND COUNTS	NET AREA COUNTS	ERROR %	NUCLIDES
1	703.13	351.89	1.2	91.	32.	52.5	PB-214
2	1323.00	661.64	1.9	36.	414.	5.5	CS-137

ERROR QUOTATION AT 1.00 SIGMA
 PEAK CONFIDENCE LEVEL AT 80.0%

RADIATION COUNTING LABORATORY (3313)

18-OCT-82 12:16:12

SAMPLE: SWIPE TMI, TOP #1

DATA COLLECTED ON 18-OCT-82 AT 10:20:00

DECAYED TO 0. DAYS, 0.0000 HOURS BEFORE THE START OF COLLECT.

RADIIONUCLIDE ANALYSIS REPORT

NUCLIDE ACTIVITY CONCENTRATION IN uCi/EA
 DECAY

	MEASURED	ERROR	CORRECTED	ERROR
--	----------	-------	-----------	-------

CS-137	9.60E-05	+7.64E-06	9.60E-05	+7.64E-06
--------	----------	-----------	----------	-----------

TOTAL	9.60E-05	+7.64E-06	9.60E-05	+7.64E-06
-------	----------	-----------	----------	-----------

ERROR QUOTATION AT 1.00 SIGMA

PEAKS NOT USED IN ANALYSIS

CENTROID CHANNEL	ENERGY KEY	NET AREA COUNTS	ERROR %	GAMMAS/SEC
---------------------	---------------	--------------------	------------	------------

703.13	351.89	32.	52.5	1.14E-01
--------	--------	-----	------	----------

ANL>

CHART B4

GAMMA SPECTRUM ANALYSIS

CANBERRA SPECTRAN-F V2.06 SOFTWARE

RADIATION COUNTING LAB. (3313)

18-OCT-82 14:41:24

A N A L Y S I S P A R A M E T E R S

MCA UNIT NUMBER: 3 / ADC UNIT NUMBER: 1.0
DETECTOR NUMBER: 1 / GEOMETRY NUMBER: 7
SPECTRUM SIZE: 4096 CHANNELS
ORDER OF SMOOTHING FUNCTION: 5
NUMBER OF BACKGROUND CHANNELS: 4 ON EACH SIDE OF PEAK
PEAK CONFIDENCE FACTOR: 80.0%
IDENTIFICATION ENERGY WINDOW: +- 1.00 KEV
ERROR QUOTATION: 1.00 SIGMA UNCERTAINTY

MULTIPLET ANALYSIS PERFORMED

SPECTRAL DATA READ DIRECTLY FROM MULTICHANNEL ANALYZER AND:
ANALYZED BY: ONEAL

SAMPLE DESCRIPTION: SWIPE TMI TOP #2
GEOMETRY DESCRIPTION: AIR FILTER 2.75 IN.
SAMPLE SIZE: 1.0000E+00 EA CONVERSION FACTOR: 1.0000E+00
STANDARD SIZE: 1.0000E+00 EA
ANALYSIS LIBRARY FILE: AML000

COLLECT STARTED ON 18-OCT-82 AT 13:47:11

COLLECT LIVE TIME: 3000. SECONDS
REAL TIME: 3003. SECONDS
DEAD TIME: 0.10 %

DECAYED TO 0. DAYS, 0.0000 HOURS BEFORE THE START OF COLLECT

ENERGY CALIBRATION PERFORMED 13-OCT-82

EFFICIENCY CALIBRATION PERFORMED 18-OCT-82

RADIATION COUNTING LAB. (3313)

18-OCT-82 14:41:24

CHART B5

PK	CENTROID CHANNEL	ENERGY KEY	FWHM KEY	BACKGND COUNTS	NET AREA COUNTS	ERROR %	NUCLIDES
1C	1126.34	562.90	1.6	516.	271.	13.6	CS-134
2C	1138.28	568.87	1.6	548.	416.	12.0	CS-134, BI-207
3	1209.19	604.31	1.7	561.	3125.	2.2	CS-134
4	1323.01	661.21	1.7	444.	34995.	0.5	CS-137
5C	1591.38	795.39	1.8	72.	2059.	2.4	CS-134
6C	1603.54	801.47	1.8	51.	179.	7.9	CS-134
7	2729.19	1364.66	2.5	15.	53.	18.8	CS-134
8	2799.48	1399.85	2.0	9.	72.	13.8	

ERROR QUOTATION AT 1.00 SIGMA
 PEAK CONFIDENCE LEVEL AT 80.0%

C - MULTIPLET ANALYSIS CONVERGED NORMALLY
 RADIATION COUNTING LAB. (3313)

18-OCT-82 14:41:24

SAMPLE: SWIPE TMI TOP #2

DATA COLLECTED ON 18-OCT-82 AT 13:47:11

DECAYED TO 0. DAYS, 0.0000 HOURS BEFORE THE START OF COLLECT.

R A D I O N U C L I D E A N A L Y S I S R E P O R T

N U C L I D E A C T I V I T Y C O N C E N T R A T I O N I N U C I / E A

D E C A Y

	MEASURED	ERROR	CORRECTED	ERROR
CS-134	1.37E-03	+-8.79E-05	1.37E-03	+-8.79E-05
CS-137	1.93E-02	+-1.12E-03	1.93E-02	+-1.12E-03
TOTAL	2.06E-02	+-1.12E-03	2.06E-02	+-1.12E-03

ERROR QUOTATION AT 1.00 SIGMA

P E A K S N O T U S E D I N A N A L Y S I S

CENTROID CHANNEL	ENERGY KEY	NET AREA COUNTS	ERROR %	GAMMAS/SEC
1126.34	562.90	271.	13.6	4.02E+00
1138.28	568.87	416.	12.0	6.23E+00
1603.54	801.47	179.	7.9	3.72E+00
2729.19	1364.66	53.	18.8	1.92E+00
2799.48	1399.85	72.	13.8	2.67E+00

ANL>

CHART B6

GAMMA SPECTRUM ANALYSIS

CANBERRA SPECTRAN-F V2.06 SOFTWARE

RADIATION COUNTING LAB. (3313)

19-OCT-82 11:23:12

ANALYSIS PARAMETERS

MCA UNIT NUMBER: 3 / ADC UNIT NUMBER: 1.0
DETECTOR NUMBER: 1 / GEOMETRY NUMBER: 7
SPECTRUM SIZE: 4096 CHANNELS
ORDER OF SMOOTHING FUNCTION: 5
NUMBER OF BACKGROUND CHANNELS: 4 ON EACH SIDE OF PEAK
PEAK CONFIDENCE FACTOR: 80.0%
IDENTIFICATION ENERGY WINDOW: +- 1.00 KEV
ERROR QUOTATION: 1.00 SIGMA UNCERTAINTY

MULTIPLET ANALYSIS PERFORMED

SPECTRAL DATA READ DIRECTLY FROM MULTICHANNEL ANALYZER AND:
ANALYZED BY: ONEAL

SAMPLE DESCRIPTION: SWIPE TMI #7 CASK B0
GEOMETRY DESCRIPTION: AIR FILTER 2.75 IN)
SAMPLE SIZE: 1.0000E+00 EA / CONVERSION FACTOR: 1.0000E+00
STANDARD SIZE: 1.0000E+00 EA
ANALYSIS LIBRARY FILE: ANL000

COLLECT STARTED ON 19-OCT-82 AT 10:30:00

COLLECT LIVE TIME: 3000. SECONDS
REAL TIME: 3024. SECONDS
DEAD TIME: 0.79 %

DECAYED TO 0. DAYS, 0.0000 HOURS BEFORE THE START OF COLLECT

ENERGY CALIBRATION PERFORMED 13-OCT-82
EFFICIENCY CALIBRATION PERFORMED 18-OCT-82

RADIATION COUNTING LAB. (3313)

19-OCT-82 11:23:12

CHART B7

PK	CENTROID CHANNEL	ENERGY KEY	FWHM KEY	BACKGND COUNTS	NET AREA COUNTS	ERROR %	NUCLIDES
10	1126.07	562.76	1.7	3621.	1935.	4.4	CS-134
20	1138.24	568.84	1.7	3368.	3366.	3.9	CS-134, BI-207
3	1209.03	604.23	1.7	3536.	21148.	0.8	CS-134
4	1322.92	661.16	1.7	2967.	240339.	0.2	CS-137
50	1591.29	795.34	1.8	371.	13920.	0.9	CS-134
60	1603.50	801.45	1.8	297.	1253.	2.9	CS-134
7	2076.68	1038.12	1.9	180.	158.	16.4	CD-56, I-135
80	2334.95	1167.34	2.3	165.	244.	13.0	
90	2346.74	1173.24	2.3	175.	98.	15.4	CD-60
10	2729.16	1364.64	2.2	32.	423.	5.4	CS-134
11	2799.26	1399.74	2.6	49.	444.	5.5	
12	3935.82	1969.02	1.0	5.	18.	34.2	

ERROR QUOTATION AT 1.00 SIGMA
 PEAK CONFIDENCE LEVEL AT 80.0%

C - MULTIPLET ANALYSIS CONVERGED NORMALLY
 RADIATION COUNTING LAB. (3313)

19-OCT-82 11:23:12

SAMPLE: SWIPE TMI #7 CASK BD
 DATA COLLECTED ON 19-OCT-82 AT 10:30:00
 DECAYED TO 0. DAYS, 0.0000 HOURS BEFORE THE START OF COLLECT.

R A D I O N U C L I D E A N A L Y S I S R E P O R T

NUCLIDE	ACTIVITY CONCENTRATION IN UC/EA			
	MEASURED	ERROR	CORRECTED	ERROR
CS-134	9.24E-03	+5.65E-04	9.24E-03	+5.65E-04
CS-137	1.32E-01	+7.63E-03	1.32E-01	+7.63E-03
TOTAL	1.41E-01	+7.65E-03	1.41E-01	+7.65E-03

ERROR QUOTATION AT 1.00 SIGMA

PEAKS NOT USED IN ANALYSIS

CENTROID CHANNEL	ENERGY KEY	NET AREA COUNTS	ERROR %	GAMMAS/SEC
1126.07	562.76	1935.	4.4	2.87E+01
1138.24	568.84	3366.	3.9	5.04E+01
1603.50	801.45	1253.	2.9	2.61E+01
2076.68	1038.12	158.	16.4	4.27E+00
2334.95	1167.34	244.	13.0	7.46E+00
2346.74	1173.24	98.	15.4	3.00E+00
2729.16	1364.64	423.	5.4	1.53E+01
2799.26	1399.74	444.	5.5	1.66E+01
3935.82	1969.02	18.	34.2	9.99E-01

• GAMMA SPECTRUM ANALYSIS

CANBERRA SPECTRAN-F V2.06 SOFTWARE

RADIATION COUNTING LAB. (3313)

19-OCT-82 14:17:31

ANALYSIS PARAMETERS

MCA UNIT NUMBER: 3 / ADC UNIT NUMBER: 1.0
DETECTOR NUMBER: 1 / GEOMETRY NUMBER: 7
SPECTRUM SIZE: 4096 CHANNELS
ORDER OF SMOOTHING FUNCTION: 5
NUMBER OF BACKGROUND CHANNELS: 4 ON EACH SIDE OF PEAK
PEAK CONFIDENCE FACTOR: 80.0%
IDENTIFICATION ENERGY WINDOW: +- 1.00 KEV
ERROR QUOTATION: 1.00 SIGMA UNCERTAINTY

MULTIPLET ANALYSIS PERFORMED

SPECTRAL DATA READ DIRECTLY FROM MULTICHANNEL ANALYZER AND:
ANALYZED BY: ONEAL

SAMPLE DESCRIPTION: SWIPE TMI #9 INS CAS
GEOMETRY DESCRIPTION: AIR FILTER 2.75 IN
SAMPLE SIZE: 1.0000E+00 EA // CONVERSION FACTOR: 1.0000E+00
STANDARD SIZE: 1.0000E+00 EA
ANALYSIS LIBRARY FILE: ANL000

COLLECT STARTED ON 19-OCT-82 AT 11:27:56

COLLECT LIVE TIME: 3000. SECONDS
REAL TIME: 3000. SECONDS
DEAD TIME: 00.00 %

DECAYED TO 0. DAYS, 0.0000 HOURS BEFORE THE START OF COLLECT

ENERGY CALIBRATION PERFORMED 13-OCT-82
EFFICIENCY CALIBRATION PERFORMED 18-OCT-82

RADIATION COUNTING LAB. (3313)

19-OCT-82 14:17:31

CHART B9

PK	CENTROID CHANNEL	ENERGY KEV	FWHM KEV	BACKGRND COUNTS	NET AREA COUNTS	ERROR %	NUCLIDES
1	1138.23	568.84	1.0	120.	40.	46.1	CS-134, BI-207
2	1208.98	604.20	1.7	119.	505.	5.6	CS-134
3	1322.98	661.19	1.7	72.	5663.	1.3	CS-137
4	1591.41	795.41	2.0	33.	353.	6.0	CS-134

ERROR QUOTATION AT 1.00 SIGMA
 PEAK CONFIDENCE LEVEL AT 80.0%

RADIATION COUNTING LAB. (3313) 19-OCT-82 14:17:31

SAMPLE: SWIPE TMI #9 INS CAS
 DATA COLLECTED ON 19-OCT-82 AT 11:27:56
 DECAYED TO 0. DAYS, 0.0000 HOURS BEFORE THE START OF COLLECT.

R A D I O N U C L I D E A N A L Y S I S R E P O R T

NUCLIDE	ACTIVITY CONCENTRATION IN UC/EA				
	MEASURED	ERROR	DECAY	CORRECTED	
CS-134	2.20E-04	+/-1.82E-05		2.20E-04	+/-1.82E-05
CS-137	3.12E-03	+/-1.85E-04		3.12E-03	+/-1.85E-04
TOTAL	3.34E-03	+/-1.85E-04		3.34E-03	+/-1.85E-04

ERROR QUOTATION AT 1.00 SIGMA

PEAKS NOT USED IN ANALYSIS

CENTROID CHANNEL	ENERGY KEV	NET AREA COUNTS	ERROR %	GAMMAS/SEC
1138.23	568.84	40.	46.1	5.99E-01

RNL>

CHART B10

CHART B11

Fiberglass Sample Locations

Each fiberglass sample was a right rectangle 4" x 3" x 2" in dimension. The count time was 600 seconds.

<u>Sample #</u>	<u>Location</u>
1	Area in Center of Bottom of Vessel where Fiberglass Contacted Vessel Bottom.
2	Area on Bottom of Vessel Near the Vessel Sides where Fiberglass Contacted Vessel Bottom.
3	Area Just Underneath Bottom of Detector.
4	Area in Center of Feberglass Packing Near the Detector Bottom.
5	Area in Contact with Vessel Side.
6	Area Just Above Detector Top.
7	Area in Contact with Upper Part of Detector.

G A M M A S P E C T R U M A N A L Y S I S

CANBERRA SPECTRAN-F V2.06 SOFTWARE

RADIATION COUNTING LABORATORY (3313)

25-AUG-82 09:47:13

A N A L Y S I S P A R A M E T E R S

MCA UNIT NUMBER: 3 / ADC UNIT NUMBER: 1.0
 DETECTOR NUMBER: 1 / GEOMETRY NUMBER: 10
 SPECTRUM SIZE: 4096 CHANNELS
 ORDER OF SMOOTHING FUNCTION: 5
 NUMBER OF BACKGROUND CHANNELS: 4 ON EACH SIDE OF PEAK
 PEAK CONFIDENCE FACTOR: 80.0%
 IDENTIFICATION ENERGY WINDOW: +- 1.00 KEY
 ERROR QUOTATION: 1.00 SIGMA UNCERTAINTY

MULTIPLER ANALYSIS NOT PERFORMED

SPECTRAL DATA READ DIRECTLY FROM MULTICHANNEL ANALYZER AND:

ANALYZED BY:

SAMPLE DESCRIPTION:¹

COLLECT STARTED ON 25-AUG-82 AT 09:15:16

COLLECT LIVE TIME: 600. SECONDS

RADIATION COUNTING LABORATORY (3313)

25-AUG-82 09:47:13

P E A K A N A L Y S I S

PK	CENTROID CHANNEL	ENERGY KEY	FWHM KEY	BACKGND COUNTS	NET AREA COUNTS	ERROR %	NUCLIDES
1M	1138.51	569.43	1.8	14394.	8359.	3.2	CS-134, BI-207
2	1209.32	604.82	1.7	6125.	35242.	0.6	CS-134
3M	1323.26	661.77	1.8	7969.	340016.	0.2	CS-137
4M	1591.73	795.98	1.8	1418.	25939.	0.7	CS-134
5	2077.47	1038.88	2.0	295.	262.	13.2	-I-135 CS-134
6	2335.77	1168.09	2.0	268.	280.	12.1	CS-134
7	2730.02	1365.37	1.9	25.	650.	4.2	CS-134
8	2800.56	1400.67	2.3	52.	248.	8.3	

CHART B12

GAMMA SPECTRUM ANALYSIS

CANBERRA SPECTRAN-F V2.06 SOFTWARE

RADIATION COUNTING LABORATORY (3313)

25-AUG-82 10:28:10

ANALYSIS PARAMETERS

MCA UNIT NUMBER: 3 / ADC UNIT NUMBER: 1.0
 DETECTOR NUMBER: 1 / GEOMETRY NUMBER: 10
 SPECTRUM SIZE: 4096 CHANNELS
 ORDER OF SMOOTHING FUNCTION: 5
 NUMBER OF BACKGROUND CHANNELS: 4 ON EACH SIDE OF PEAK
 PEAK CONFIDENCE FACTOR: 80.0%
 IDENTIFICATION ENERGY WINDOW: +- 1.00 KEY
 ERROR QUOTATION: 1.00 SIGMA UNCERTAINTY

MULTIPLET ANALYSIS NOT PERFORMED

SPECTRAL DATA READ DIRECTLY FROM MULTICHANNEL ANALYZER AND:
 ANALYZED BY: ONEAL

SAMPLE DESCRIPTION: #2
 COLLECT STARTED ON 25-AUG-82 AT 10:12:36

COLLECT LIVE TIME: 600. SECONDS

RADIATION COUNTING LABORATORY (3313)

25-AUG-82 10:28:10

PEAK ANALYSIS

PK	CENTROID CHANNEL	ENERGY KEY	FWHM KEY	BACKGND COUNTS	NET AREA COUNTS	ERROR %	NUCLIDES
1M	1138.42	569.39	1.6	1251.	946.	8.4	CS-134, BI-207
2	1209.28	604.80	1.6	557.	3548.	2.0	CS-134
3	1323.26	661.77	1.7	386.	33306.	0.6	CS-137
4M	1591.68	795.96	1.7	49.	2544.	2.1	CS-134
5	2335.47	1167.95	2.0	23.	26.	38.9	
6	2729.64	1365.18	2.0	5.	59.	14.6	CS-134

ERROR QUOTATION AT 1.00 SIGMA
 PEAK CONFIDENCE LEVEL AT 80.0%

M - POSSIBLE MULTIPLIFT

G *D* *E* *S* *R* *P* *E* *C* *T* *R* *C* *H* *A* *Z* *L* *J* *V* *I* *W*

CANBERRA SPECTRAN-F V2.06 SOFTWARE

RADIATION COUNTING LABORATORY (3313)

24-AUG-82 15:19:55

ANALYSIS PARAMETERS

MCA UNIT NUMBER: 3 / ADC UNIT NUMBER: 1.0
DETECTOR NUMBER: 1 / GEOMETRY NUMBER: 10
SPECTRUM SIZE: 4096 CHANNELS
ORDER OF SMOOTHING FUNCTION: 5
NUMBER OF BACKGROUND CHANNELS: 4 ON EACH SIDE OF PEAK
PEAK CONFIDENCE FACTOR: 90.0%
IDENTIFICATION ENERGY WINDOW: +- 1.00 KEY
ERROR QUOTATION: 1.00 SIGMA UNCERTAINTY

MULTIPLER ANALYSIS NOT PERFORMED

SPECTRAL DATA READ DIRECTLY FROM MULTICHANNEL ANALYZER AND
ANALYZED BY: ONEAL

SAMPLE DESCRIPTION: #3

COLLECT STARTED ON 24-AUG-82 AT 15:09:00

COLLECT LIVE TIME: 600. SECONDS

RADIATION COUNTING LABORATORY (3313)

24-0116-82 15:19:55

PEAK ANALYSIS IS

PK	CENTROID CHANNEL	ENERGY KEY	FWHM KEY	BACKGND COUNTS	NET AREA COUNTS	ERROR %	NUCLIDES
1	1323.04	661.66	1.9	2.	246.	6.4	CS-137

ERROR QUOTATION AT 1.00 SIGMA
PEAK CONFIDENCE LEVEL AT 90.0%

CHART B14

G A M M A S P E C T R U M A N A L Y S I S

CANBERRA SPECTRAN-F V2.06 SOFTWARE

RADIATION COUNTING LABORATORY (3313)

24-AUG-82 16:14:07

A N A L Y S I S P A R A M E T E R S

MCA UNIT NUMBER: 3 / ADC UNIT NUMBER: 1.0
DETECTOR NUMBER: 1 / GEOMETRY NUMBER: 10
SPECTRUM SIZE: 4096 CHANNELS
ORDER OF SMOOTHING FUNCTION: 5
NUMBER OF BACKGROUND CHANNELS: 4 ON EACH SIDE OF PEAK
PEAK CONFIDENCE FACTOR: 80.0%
IDENTIFICATION ENERGY WINDOW: +- 1.00 KEY
ERROR QUOTATION: 1.00 SIGMA UNCERTAINTY

MULTIPLET ANALYSIS NOT PERFORMED

SPECTRAL DATA READ DIRECTLY FROM MULTICHANNEL ANALYZER AND:
ANALYZED BY: ONEALSAMPLE DESCRIPTION: #4
COLLECT STARTED ON 24-AUG-82 AT 15:23:27

COLLECT LIVE TIME: 600. SECONDS

RADIATION COUNTING LABORATORY (3313)

24-AUG-82 16:14:07

P E A K A N A L Y S I S

PK	CENTROID CHANNEL	ENERGY KEY	FWHM KEY	BACKGND COUNTS	NET AREA COUNTS	ERROR %	NUCLIDES
1	1209.06	604.69	1.7	4.	48.	15.9	CS-134
2	1323.35	661.82	1.6	6.	387.	5.2	CS-137

CHART B15

GAMMA SPECTRUM ANALYSIS

CANBERRA SPECTRAN-F V2.06 SOFTWARE

RADIATION COUNTING LABORATORY (3313)

25-AUG-82 11:09:49

ANALYSIS PARAMETERS

MCA UNIT NUMBER: 3 / ADC UNIT NUMBER: 1.0
 DETECTOR NUMBER: 1 / GEOMETRY NUMBER: 10
 SPECTRUM SIZE: 4096 CHANNELS
 ORDER OF SMOOTHING FUNCTION: 5
 NUMBER OF BACKGROUND CHANNELS: 4 ON EACH SIDE OF PEAK
 PEAK CONFIDENCE FACTOR: 80.0%
 IDENTIFICATION ENERGY WINDOW: +- 1.00 KEY
 ERROR QUOTATION: 1.00 SIGMA UNCERTAINTY

MULTIPLET ANALYSIS NOT PERFORMED

SPECTRAL DATA READ DIRECTLY FROM MULTICHANNEL ANALYZER AND:
 ANALYZED BY: ONEAL

SAMPLE DESCRIPTIONS: #5
 COLLECT STARTED ON 25-AUG-82 AT 10:54:28

COLLECT LIVE TIME: 600. SECONDS

RADIATION COUNTING LABORATORY (3313)

25-AUG-82 11:09:49

PEAK ANALYSIS

PK	CENTROID CHANNEL	ENERGY KEY	FWHM KEY	BACKGND COUNTS	NET AREA COUNTS	ERROR %	NUCLIDES
1M	1138.52	569.44	1.6	203.	173.	19.1	CS-134, BI-207
2	1209.21	604.77	1.8	92.	534.	5.3	CS-134
3	1323.24	661.76	1.8	171.	5133.	1.5	CS-137
4	1591.71	795.97	1.7	44.	312.	6.8	CS-134

CHART B16

G A M M A S P E C T R U M A N A L Y S I S

CANBERRA SPECTRAN-F V2.06 SOFTWARE

RADIATION COUNTING LABORATORY (3313)

25-AUG-82 11:37:11

A N A L Y S I S P A R A M E T E R S

MCA UNIT NUMBER: 3 / ADC UNIT NUMBER: 1.0
DETECTOR NUMBER: 1 / GEOMETRY NUMBER: 10
SPECTRUM SIZE: 4096 CHANNELS
ORDER OF SMOOTHING FUNCTION: 5
NUMBER OF BACKGROUND CHANNELS: 4 ON EACH SIDE OF PEAK
PEAK CONFIDENCE FACTOR: 80.0%
IDENTIFICATION ENERGY WINDOW: +- 1.00 KEV
ERROR QUOTATION: 1.00 SIGMA UNCERTAINTY

MULTIPLET ANALYSIS NOT PERFORMED

SPECTRAL DATA READ DIRECTLY FROM MULTICHANNEL ANALYZER AND:
ANALYZED BY: ONEAL

SAMPLE DESCRIPTION: #6
COLLECT STARTED ON 25-AUG-82 AT 11:23:37

COLLECT LIVE TIME: 600. SECONDS

RADIATION COUNTING LABORATORY (3313)

25-AUG-82 11:37:11

P E A K A N A L Y S I S

PK	CENTROID CHANNEL	ENERGY KEY	FWHM KEY	BACKGND COUNTS	NET AREA COUNTS	ERROR %	NUCLIDES
1	1203.84	604.58	1.3	58.	246.	8.3	CS-134
2	1322.92	661.60	1.8	41.	2396.	2.1	CS-137
3	1591.47	795.85	1.9	10.	164.	8.5	CS-134

CHART B17

G A M M A S P E C T R U M A N A L Y S I S

CANBERRA SPECTRUM-F V2.06 SOFTWARE

DIATION COUNTING LABORATORY (3313)

24-AUG-82 15:01:12

A N A L Y S I S P A R A M E T E R S

A UNIT NUMBER: 3 / ADC UNIT NUMBER: 1.0
 DETECTOR NUMBER: 1 / GEOMETRY NUMBER: 10
 SPECTRUM SIZE: 4096 CHANNELS
 ORDER OF SMOOTHING FUNCTION: 5
 NUMBER OF BACKGROUND CHANNELS: 4 ON EACH SIDE OF PEAK
 PEAK CONFIDENCE FACTOR: 90.0%
 IDENTIFICATION ENERGY WINDOW: +- 1.00 KEY
 ERROR QUOTATION: 1.00 SIGMA UNCERTAINTY

MULTIPLER ANALYSIS NOT PERFORMED

SPECTRAL DATA READ DIRECTLY FROM MULTICHANNEL ANALYZER AND:
 ANALYZED BY: ONEAL

SAMPLE DESCRIPTION: #7
 COLLECT STARTED ON 24-AUG-82 AT 14:36:59

COLLECT LIVE TIME: 600. SECONDS

DIATION COUNTING LABORATORY (3313)

24-AUG-82 15:01:12

P E A K A N A L Y S I S

CENTROID CHANNEL	ENERGY KEY	FWHM KEY	BACKGRND COUNTS	NET AREA COUNTS	ERROR %	NUCLIDES
1 1209.93	605.12	0.9	6.	29.	23.0	CS-134
2 1323.37	661.83	1.8	14.	287.	6.3	CS-137

ERROR QUOTATION AT 1.00 SIGMA
 PEAK CONFIDENCE LEVEL AT 90.0%

CHART B18

Sandia National Laboratories

Albuquerque, New Mexico 87185

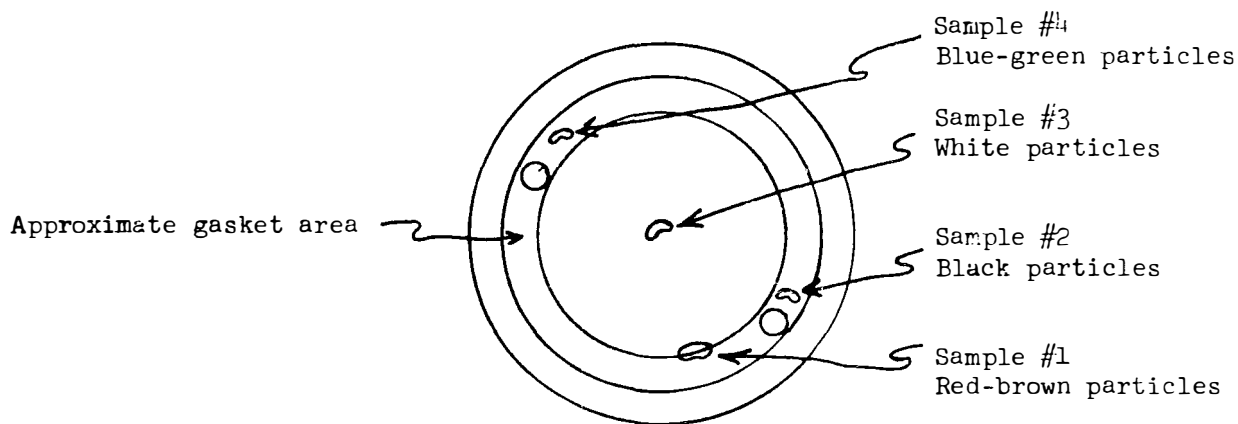
date: August 9, 1982

to: M. B. Murphy, 2341

S. F. Duliere
from: S. F. Duliere, 9453

subject: Analysis of Particulate from Three Mile Island Container

A radiation detector container from the Three Mile Island reactor facility was opened at Sandia's hot cell facility in order to check the detector and determine if its container had been breached during the TMI accident. When the detector was removed some particulate was found inside the container. Four samples of the particulate were stripped from the inside of the lid and examined by scanning electron microscopy and x-ray energy dispersive spectroscopy. The material was removed from the areas shown below.



Sample 1 (Figure 1) was stripped from the inner edge of the gasket area. The particles looked like rust. The elemental spectrum (Figure 2) supports this: the predominant element is iron. In addition to iron there are minor amounts of Mg, Si, Pb, Cl, Sn, Ca, Cr, Zn, and Zr.

Sample 2 (Figure 3), which was stripped from the area around the hole in the lid, was a black particulate. Its spectrum (Figure 4) reveals a composition of primarily Si, Zr, Pb, Cr, and Fe with minor amounts of Sn, Ca, and Ni.

Sample 3 (Figure 5), which was stripped from the center of the lid, consisted of a white particulate. It was primarily Al, Si, and Ca with minor amounts of Pb, Cl, K, Ti, and Fe (Figure 6).

August 9, 1982

Sample #4 (Figure 7), which was taken from the gasket area, was blue-green-white particulate. It was the most radioactive of the samples; swipes showed 78,000 dpm. Isotopic specie analysis by Health Physics Division 3312 showed that Cs-137 was the active isotope. X-ray analysis did not detect Cs but showed major elements to be Si, Ca, Ti with minors of Al, Pb, Fe.

Due to lack of positive background information, no conclusions were made as to how the particulate formed.

SFD:9453:j1



Figure 1 SEM 40X
"Rust" particles stripped from the inner
edge of the lid gasket area

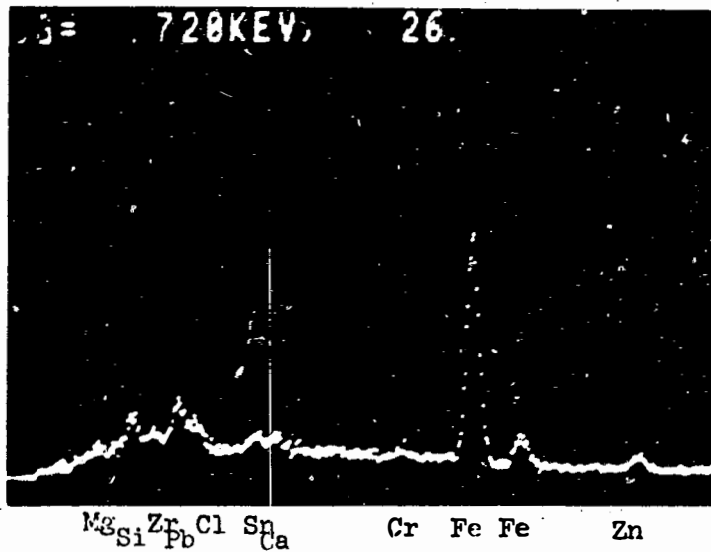


Figure 2
Elemental x-ray spectrum of particles in fig. 1



SEM 100X



SEM 1000X

Figure 3

Black particles stripped from around a hole in the lid

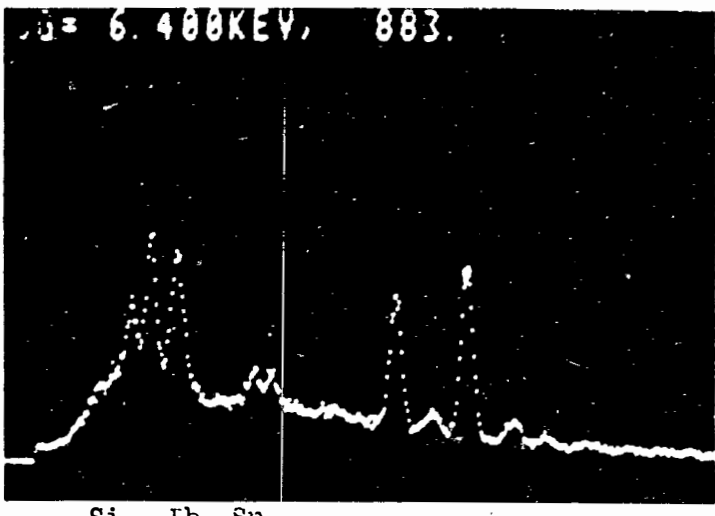


Figure 4

Elemental x-ray spectrum of particles in fig. 3



SEM 40X



SEM 1000X

Figure 5

White particles stripped from the center of the lid

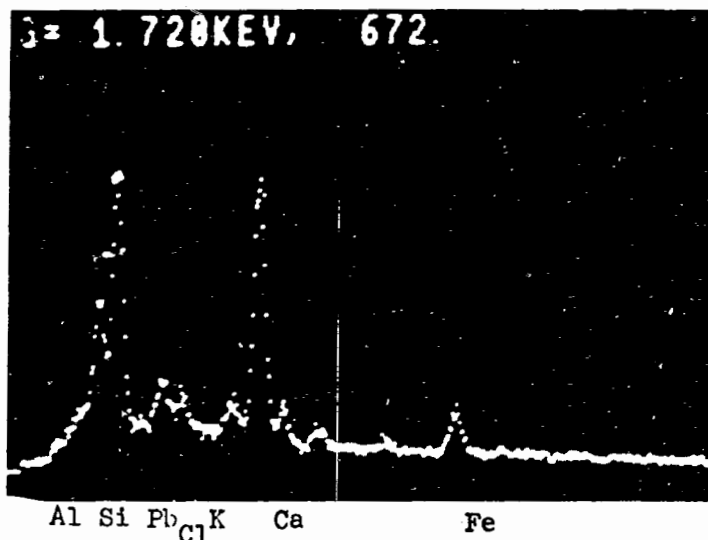


Figure 6

Elemental x-ray spectrum of particles in fig. 5

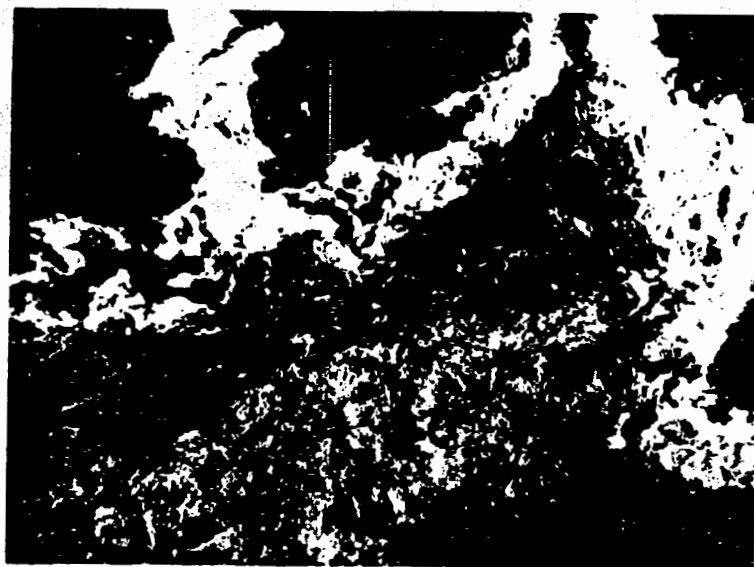


Figure 7

SEM 40X

Blue-green-white particles stripped from the
gasket area

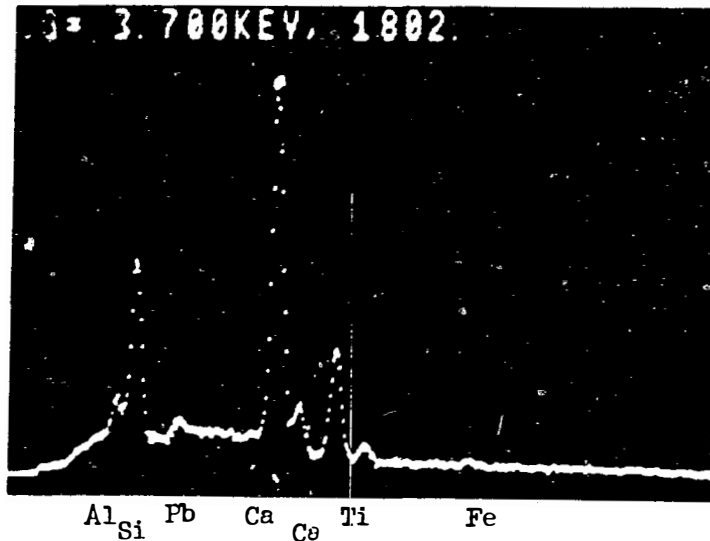


Figure 8

Elemental x-ray spectrum of particles in fig. 7

CHART B19

Boron Analysis Sample Locations and Procedures

Samples A1 through A5 were taken in various locations on the underside of the vessel lid. The cotton swabs were first moistened with de-ionized water and then swabbed over a 2" x 2" area. Sample A6 was done in the same way except that a swipe was used. Sample A7 was a swab of the outside top of the vessel after cleaning with toulene (done to see if boron was in the SS vessel itself). Samples P6, P7, and P9 were swipes taken for counting purposes in which no moisture was used to remove the chemical contaminants. Each sample was analyzed using emission spectroscopy techniques.

CHART B20

INDUSTRIAL HYGIENE SERVICES
Laboratory Data Sheet

File No.

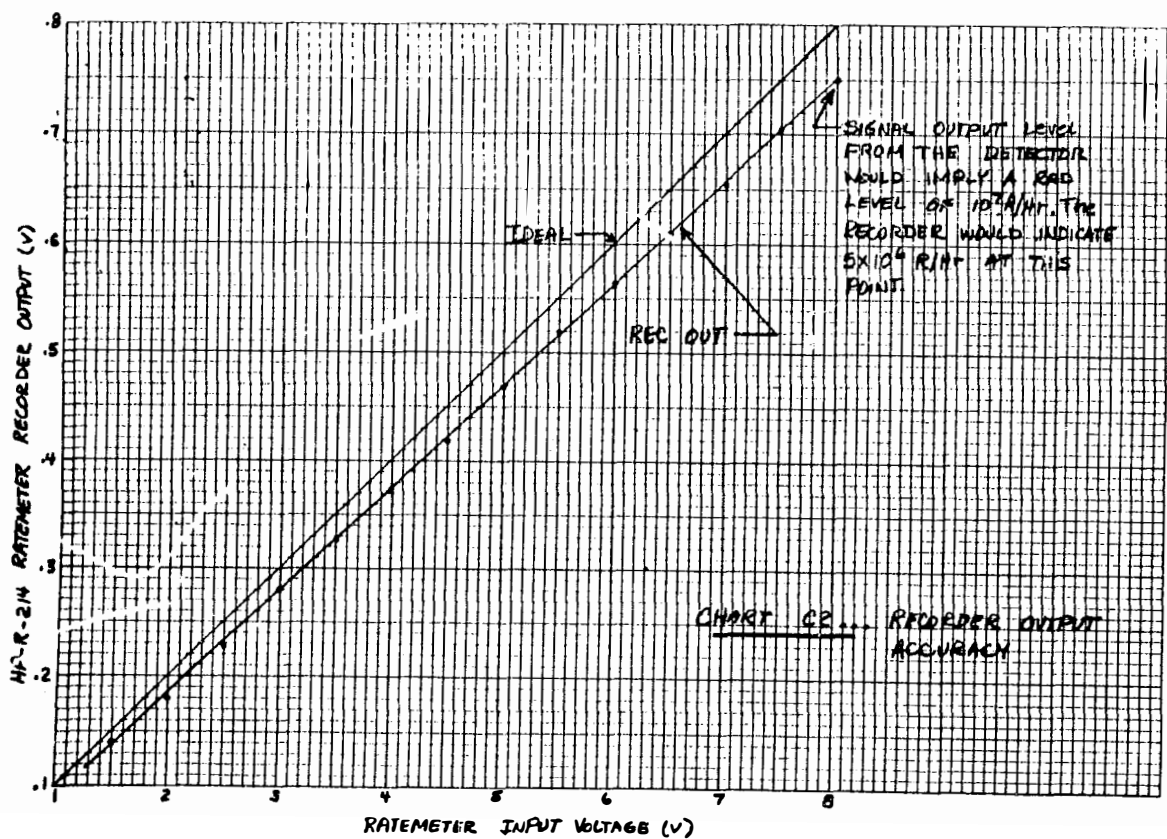
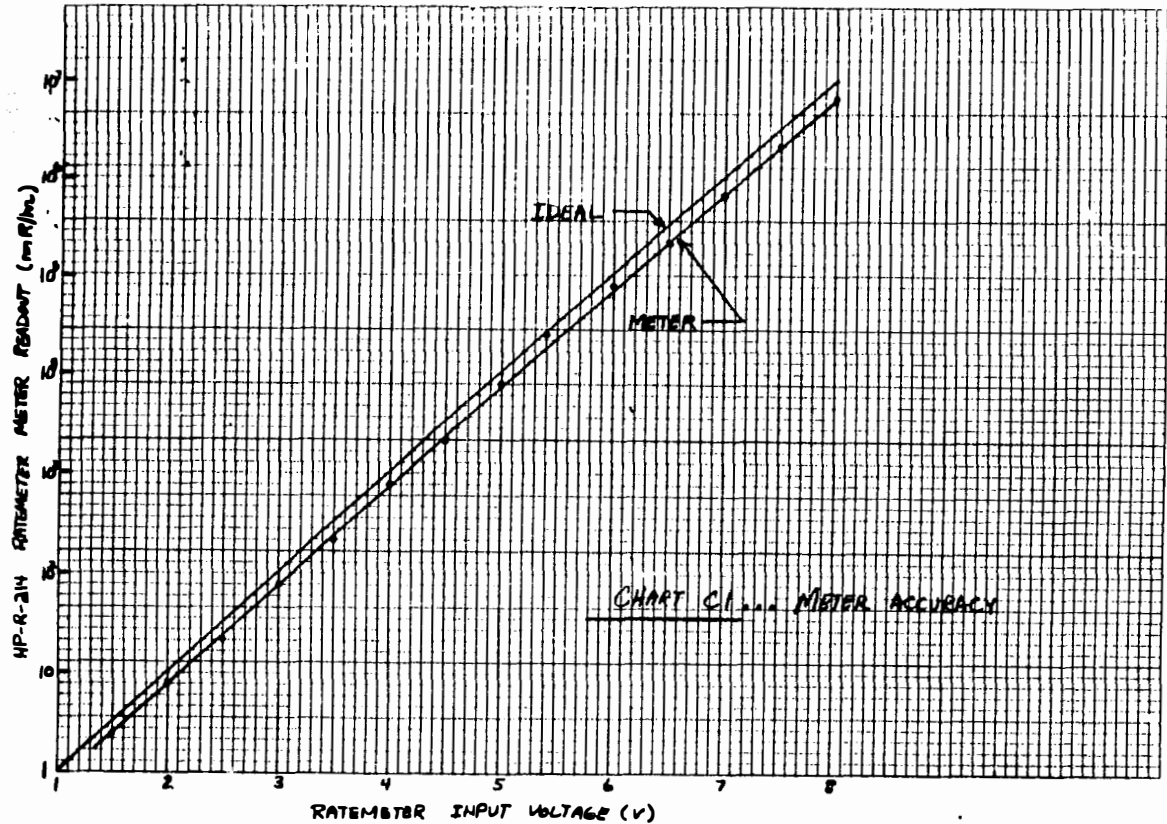
Submitted by <u>Murphy, M</u>	Org. <u>2341</u>	Analyst <u>G.R.A.Y.</u>	
Date Submitted <u>25-AUG-82</u> Day Mon Yr	Report Date <u>26-AUG-82</u> Day Mon Yr		
Lab Log No. <u>8.21.8.13 to 8.21.8.22</u>	Analytical Method No. (NIOSH) <u>Emission Spec.</u>		
Contaminant <u>PCP, O.D.N.</u>	Contaminant Code (CAS) <u> </u>		
Reference: Contact _____	Bldg/Rm _____		
Analysis Requested <u>Boron</u>	Priority Rush	Usual	
Log No.	Sample Description	Results	Units
8.21.8.13	A-1 Q-Tip	215 mg	
14	A-2 "	200 "	
15	A-3 "	210 "	
16	A-4 "	205 "	
17	A-5 "	200 "	
18	A-6 filter paper	ND - 4 ug	
19	A-7 Q-Tip	ND	
20	P6 filter paper Top of Detach	ND	
21	P7 " " Bottom of cash	ND	
22	P9 " " Cash Sides & Dents	ND	
(Continue entries on additional sheets; attach together.)			

A- Read by _____ Date _____

APPENDIX C

Ratemeter Accuracy

The data presented on Chart C1 and C2 were obtained by applying a DC input voltage ranging from 0 to 8.0 volts to the ratemeter input (which is the detector output) and observing the meter deflection (Chart C1) and measuring the recorder output (Chart C2).



HP UR 1901 Stripchart Recorder Accuracy and Corrected Data

The memo which follows to J. B. Logan/B. C. Rusche of Metropolitan Edison Co. from Donald Nitti of B&W provides a good summary of Dome Monitor observations made shortly after the accident. Among other things Nitti provides the only information we have regarding the accuracy of the stripchart recorder. He states, "There was a calibration error between the Dome Monitor indicator and the recorder such that the 8 decade signal was printed only over the first 3.78 decades of the 5 decade chart paper." The corrected HP-R-214 stripchart raw data follows Nitti's letter.

METROPOLITAN EDISON COMPANY

Subsidiary of General Public Utilities Corporation

Bechtel

Subject Containment Dome Radiation Monitor

Location TMI

To J.B. Logan/B.C. Rusche

Date June 27, 1979

This memo summarizes the present status of efforts to determine the radiation dose rates inside containment from the recorded dome monitor (HP-R-214) and other area radiation monitor readings and to use these dose rates to quantitatively determine the amount of fission product activity released into the Unit 2 containment building.

Background on the Containment Dome Monitor

1. The dome monitor is not located in the containment dome; it is sitting on top of the elevator/stairwell roof.
2. The containment dome monitor (HP-R-214) was designed and built to withstand the post-LOCA environment, i.e., 50.5 psig and 280°F for 50 minutes and 6 psig and 160°F for an additional 24 hours.
3. The detector and its pre-amplifier are housed within a cylindrical shield which is shown on the attached Figure 1 (Victoreen Dwg. No. 9041203).
4. The pre-amp is designed to perform within specifications up to 10^5 R of absorbed dose.
5. The instrument range spans eight (8) decades. If the detector were not in a shield, the normal range of the instrument would be 0.1 to 10^7 mr/hr. The shield was designed to provide an attenuation factor of 100 based on a Cs-137 source. Thus, the readout response over the range from 0.1 to 10^7 mr/hr is intended to be responding to in containment dose rates of 10 to 10^9 mr/hr due to the attenuation provided by the detector shield. Unfortunately, the attenuation factor is a function of the gamma energy, as can be seen by Figure 2 (attached). For gamma energies greater than 1 MeV, the attenuation factor would be only 10 or less, whereas for low energy gammas the attenuation factor would be 1000 or greater.
6. The monitor indicator (see attached Figure 3) can be read on either of two scales. The full range scale which spans all eight decades, or the expanded scale which spans only the 3 decades below the desired full scale reading set on the selector knob. (Since the meter is located about a foot above eye level, the meter is often read incorrectly due to the difficulty of seeing the position of the selector switch and due to parallax errors).

7. A multipoint recorder (HP-UR-1901) prints the dome monitor readings (point #12) on a 5 cycle log chart along with all the other area radiation monitors. (All the other radiation monitors are G-M tubes with a 5 decade response; whereas the dome monitor is a dual-ionization chamber with 8 decade response).

Problems Interpreting Dome Monitor Readings

There has been considerable confusion as to the dose rates in the containment due to the difficulty of interpreting the dome monitor readings. These difficulties are enumerated below:

1. The dome monitor shield attenuation factor is not known and cannot be determined without some knowledge of the source and then only with extensive calculations.
2. The recorder is a 5 decade log recorder, whereas the dome monitor is an 8 decade instrument which is linear within each decade. (Thus, the recorder was printing an 8 decade signal on 5 decade log paper).
3. There was a calibration error between the dome monitor indicator and the recorder such that the 8 decade single was printed only over the first 3.78 decades of the 5 decade chart paper.
4. The five decade chart paper placed on the recorder should always be marked from 0.1 to 10^4 mr/hr to correspond to the other area monitors, but at times chart paper marked 10 to 10^6 was used which further confused any casual attempts to analyze the radiation level within the containment. Furthermore, the chart speed is 8 inches per hour, but the chart paper is only marked for either 1 or 4 inches per hour.

Conclusions Regarding the Containment Dome Monitor

1. The dome monitor was designed to survive a post-LOCA environment and should have survived this accident provided that the gasketed cover on the shield had been properly sealed. The dome monitor electronics were designed to perform within specification up to 10^5 R (10^8 mr). The monitor's pre-amplifier, which is within the shield, would not have accumulated 10^5 R until sometime between April 7th and April 10th. The total accumulated dose through July 1st is estimated to be between 3×10^5 and 4×10^5 R. Victoreen has seen detectors of this type which have been used in hot cells and have failed due to very high radiation exposures; they usually exhibit very unstable signals. The dome monitor signal has been and continues to be extremely stable.

2. Any attempts to read the dome monitor readings (point #12) from the HP-UR-1901 recorder charts (at least for the period between March 28th and July 1st) must use a scale conversion curve similar to the one in Figure 4, (attached) and must bear in mind that full scale on the chart is always 10^4 mr/hr regardless of what is printed on the chart.
3. The dose rates that were measured by the detector within the shield of the dome monitor are shown in Figure 5(attached).

There is good agreement between the correctly interpreted dose rates from the HP-UR-1901 recorder charts and the operators readings of HP-R-214 which are logged in the Radiation Monitoring File (RM-0006) beginning on April 6th, 1979. (Certain operator readings which were obviously in error by a factor of 10 were not plotted). It should be noted that all the dome monitor readings of interest are spread over only about 1.3 inches of the recorder chart and that 1/16" could represent almost a factor of 2 in dose rate.

4. The dome monitor readings clearly reflect when the reactor building sprays came on by showing a marked decrease from 780 R/Hr to 36 R/Hr (inside shield) during the first day. The slow buildup between March 29(day-2) and April 6(day-9) is presently unexplained except for possibly the release due to venting the pressurizer. The sudden rise on April 6(day-9) is indicative of venting the waste gas decay tanks into the containment. Venting the waste gas tanks to containment continued through April 13th(day-16). Between days 16 and 33, the dose rate decreased with a 21 day half-life. Between days 34 and 36 (April 30-May 2), the dose rate decreased with a half-life of less than 2 days. Then, between 37 and 55 days, the dose rate reduction slowed to about a 13.4 day half-life (Cs-136 has a 13 day half-life).

Since this decay behavior is not characteristic of the decay of mixture of radionuclides nor of the decrease in gamma energy spectrum and since no fission products have these half-lives, it seems as though the dome monitor is measuring the rate of some fission product removal process occurring within the containment. It is rumored that some work was done on the containment cooling system around May 1st which necessitated shutting the coolers off for sometime; if true, it may explain the rapid decrease experienced during that period of time. Since mid-May, the dose rate has held steady at 40 R/Hr.

Recommendations for Additional Work

1. The post-accident events must be reviewed more carefully to:
 - a. Quantify the activity removal effectiveness of the containment sprays during their 5 minutes and 50 seconds of operation,

June 27, 1979

Page 4

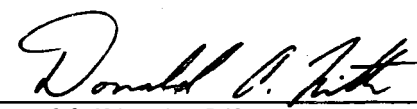
1. b. Explain the activity increase during the period May 29-April 6,
 - c. Quantify the activity source associated with the sudden increase in dose rate on April 6,
 - d. Explain the rapid decrease during the period April 30-May 2,
 - e. Explain the slow decreases during the periods April 13-30 and May 2-21, and
 - f. To explain the reason for the constant dose rate since May 21st.
2. The Task effort, presently in progress at B&W, to assess the radiation exposure to components within the containment should be expanded to include calculation of the dose rate to the shielded detector from synthesized fission product sources which produce the measured dose rates to the shielded detector. For example, the detector dose rate should be calculated for each of the following sources:
 - a. Airborne sources with:
 1. 50% of the Xe activity in core
 2. 50% of the Kr activity in core
 3. 50% of the I activity in core
 4. 50% of the Cs (+Ba) activity in core
 - b. Major plate-out sources on containment walls with:
 1. 50% of the I activity in core
 2. 50% of the Cs(+Ba) activity in core
 3. 5% of the Zr(+Nb) activity in core
 - c. Local plate-out sources on elevator shaft roof and monitor shield [using same $\mu\text{ci}/\text{cm}^2$ as in item (b)]
 - d. Direct radiation sources from sump water containing:
 1. 50% of the I activity in core
 2. 50% of the Cs(+Ba) activity in core
 3. 5% of the Zr(+Nb) activity in core
 - e. Detector leakage sources (assuming specific activity from item (a) leaked into the detector shield).

If the above recommendations are followed, not only will the radiation level in the containment be known, but we will improve our estimate of the amount of fission products released into the containment and will obtain valuable insight into how decontamination can be facilitated.

June 27, 1979

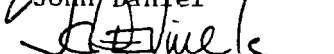
Page 5

Prepared by:


Donald Nitti

Donald Nitti, B&W

Approved by:


John Daniel

Jack Devine

DISTRIBUTION:

J.A. Daniel
E.A. Schlomer (B&W)
J.C. DeVine, Jr.
J.J. Barton
R.C. Arnold
R.J. McGoey
L.D. Garman (GAI)
M. Ross
D.C. Smith (TVA)
J.T. Collins (NRC)
R. Ely (GAI)
W. Hopkins (Bechtel)
J.D. Phinney (B&W)
G.R. Skillman (B&W)
J. Theissing (Bechtel)
J.A. Brummer
S.W. Porter
I. Green
D. Weaver
J.M. Putman (B&W)
B. Center (EI)
R.W. Heward, Jr.
J.G. Herbein
G.M. Staudt
T. Fisher

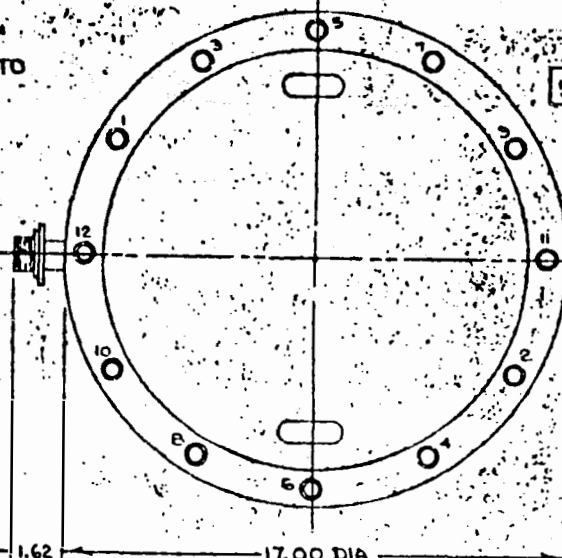
NOTES:

1. ALL DIMENSIONS ARE APPROXIMATE.

2. APPROX. WEIGHT ~ 550 LB

3. ATTENUATION 10^3 MR/HR TO
 10^2 MR/HR IN HOUSING4. THIS UNIT WILL MAINTAIN
NORMAL OPERATION AT
50.5 PSIG @ 280°F
FOR 60 MIN. (3000 SEC)
AND 6 PSIG @ 160°F
FOR AN ADDITIONAL
24 HOURS (86,400 SEC).5. TORQUE BOLTS TO
120 IN. POUNDS WITH
1-12 PATTERN.

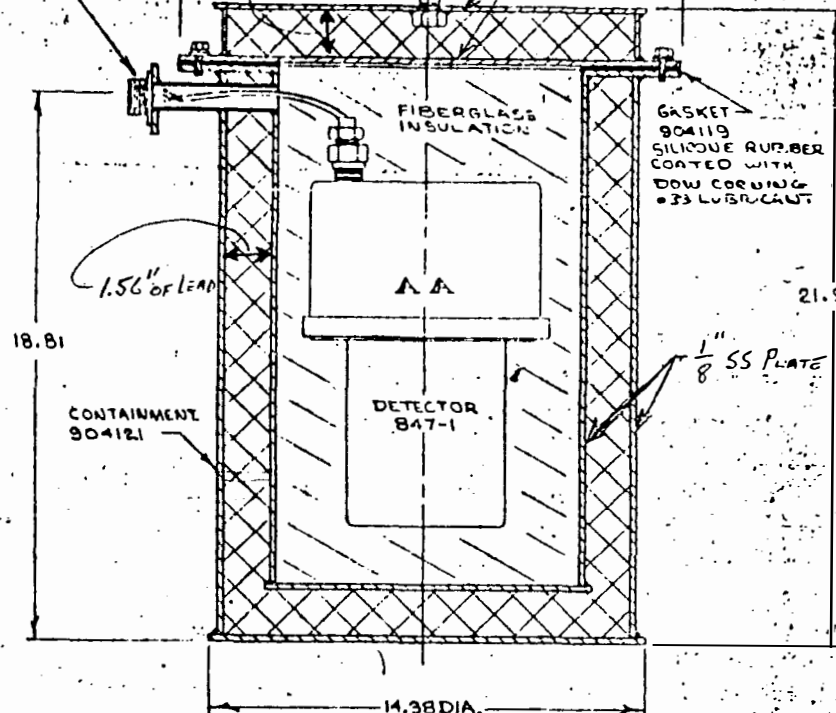
FIGURE 1



AMPHENOL CONNECTOR

1- 172-3165-1P2
1- AB3106A-16B-15
1- AN3067-B

904120



NAME	AREA	MONITOR	CONTAINMENT AREA	MATERIAL
VICTOREEN INSTRUMENTS INC.	E. 7120	DET. 847-1	CONTAINMENT AREA	LEAD
101 WOODLAND AVE. CLEVELAND, OHIO	WHERE USED	DET. 847-1	CONTAINMENT AREA	LEAD
DR. WJN	CHIEF	DET. 847-1	CONTAINMENT AREA	LEAD
SCALE	VA	DET. 847-1	CONTAINMENT AREA	LEAD
DATE 10-15-71	DRAWN BY	DET. 847-1	CONTAINMENT AREA	LEAD
	DWG. NO.	DET. 847-1	CONTAINMENT AREA	LEAD

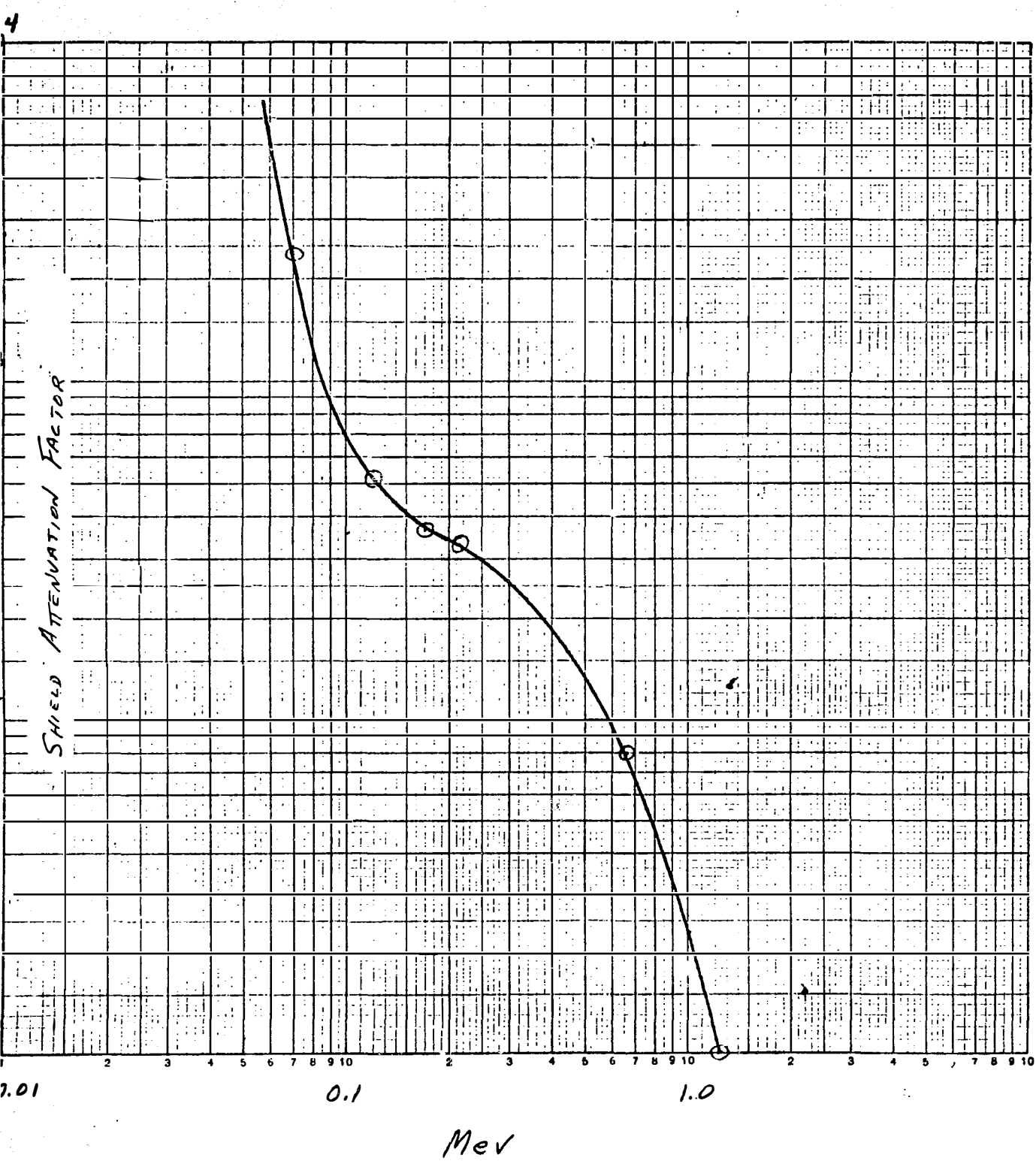
NOV 1 1976

REV. LET.	DESCRIPTION OF ITEM
A	PRE. EDITION REVISED AND READING BY DR. WJN

MICRO-TEK

ADDITIONAL TO THIS DRAWING
SEE SHEET 2

FIGURE 2 - Dome Monitor Shield Calibration



2.1.2 845 Series Area Monitor.

2.1.2.1 General Description. See Table 1-1.

The 845 Series Area Monitor is used to monitor gamma radiation levels in the reactor building dome. The 847-1 detector is installed in a special 904120 housing with stainless steel walls and a 2-inch lead shield for extended radiation level response. The 846-1 readout module is located in panel 12. The radiation alarm system of the readout module is connected into the evacuation alarm system. See drawing 905474.

The radiation level is presented on the readout module panel meter and also as recorder and computer outputs from the unit. The recorder output is 0 - 10mV and the computer output is 0 - 50mV.

The readout incorporates two independently adjustable electronic comparator type radiation alarm trips. The alarm trips actuate the audible annunciator system and a light on the readout module front panel.

The readout module front panel controls and indicators consist of the following:

A. The Panel Meter.

B. Function Switch - This is the only rotary switch on the front panel. It turns the unit on and off, selects the ranges to be displayed and activates the check source.

C. Amber Button/Indicator - Light on indicates alert radiation alarm trip. Button pressed causes meter to indicate alert alarm trip set point.

D. Red Button/Indicator - Light on indicates high radiation alarm trip. Button pressed causes meter to indicate high alarm trip set point.

E. Green Button/Indicator - Green light off indicates a power supply or collector supply voltage failure. Green light on indicates normal unit functioning. Green button pressed resets either or both radiation alarms.

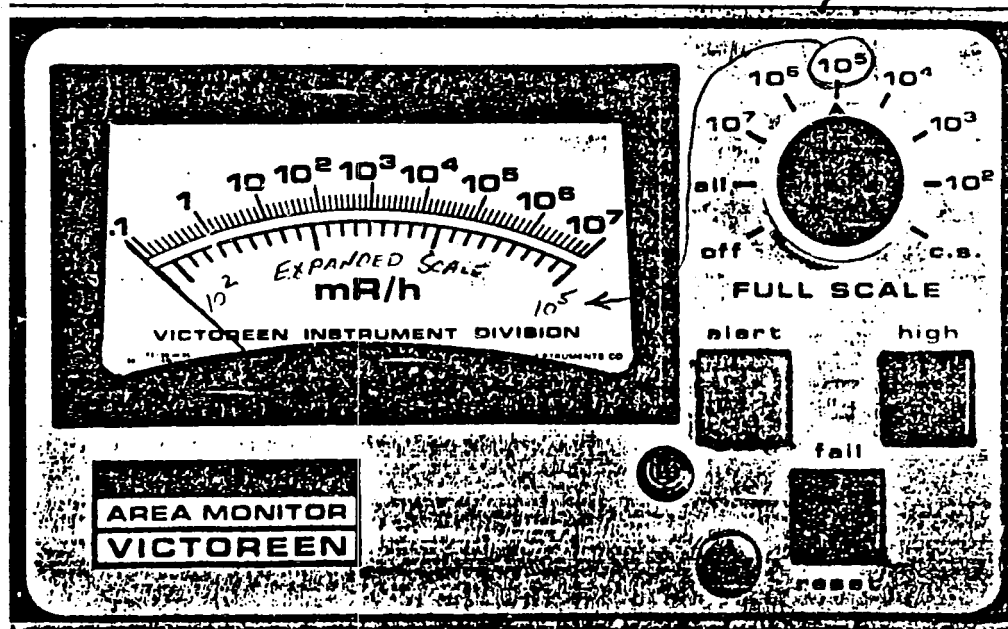


Figure 2-16 845 Series Model 845-1 Readout Module

KEY

Cx PRACTICED ON MAY 26, 1979
X ANESTERED C.V MAY 30, 1979

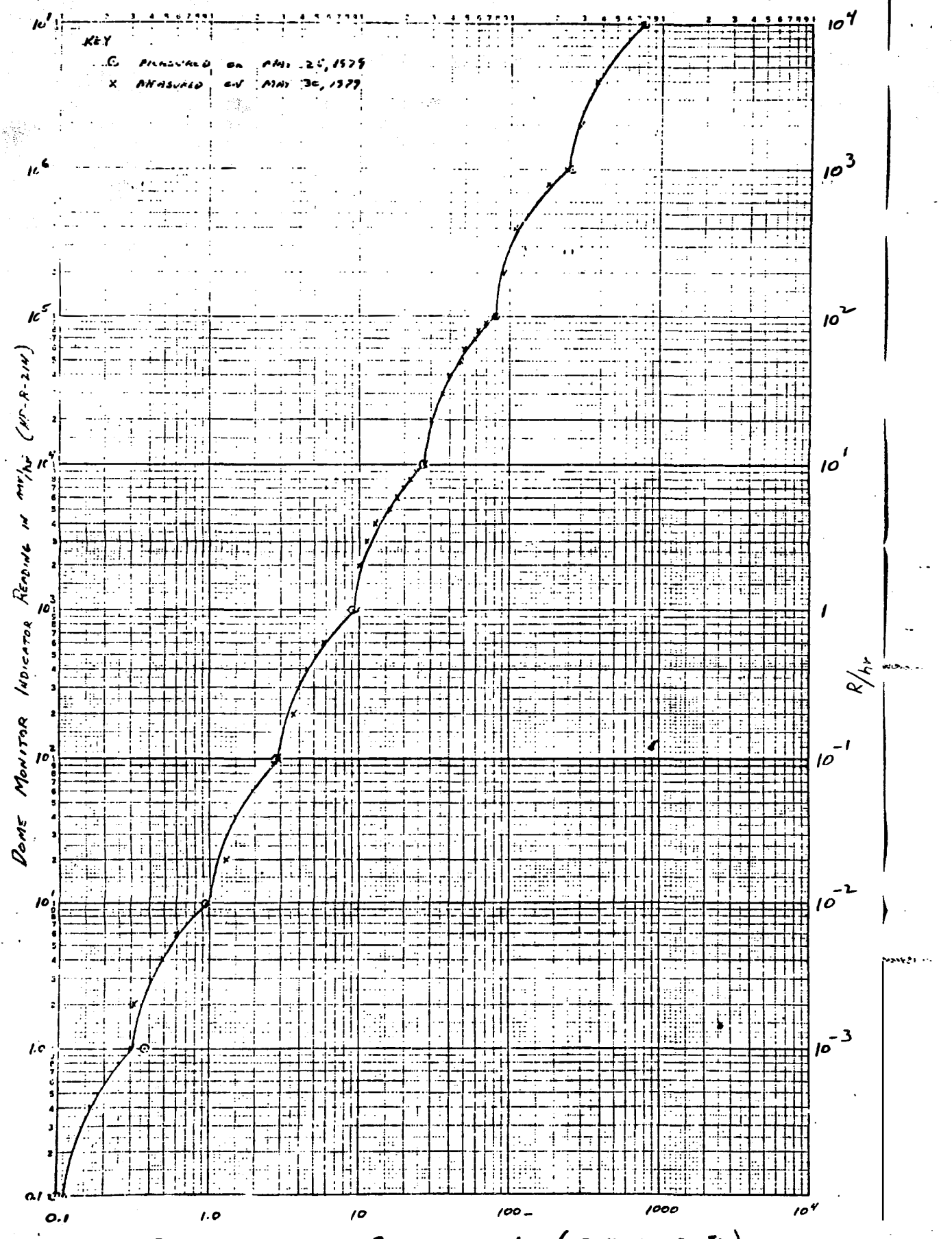
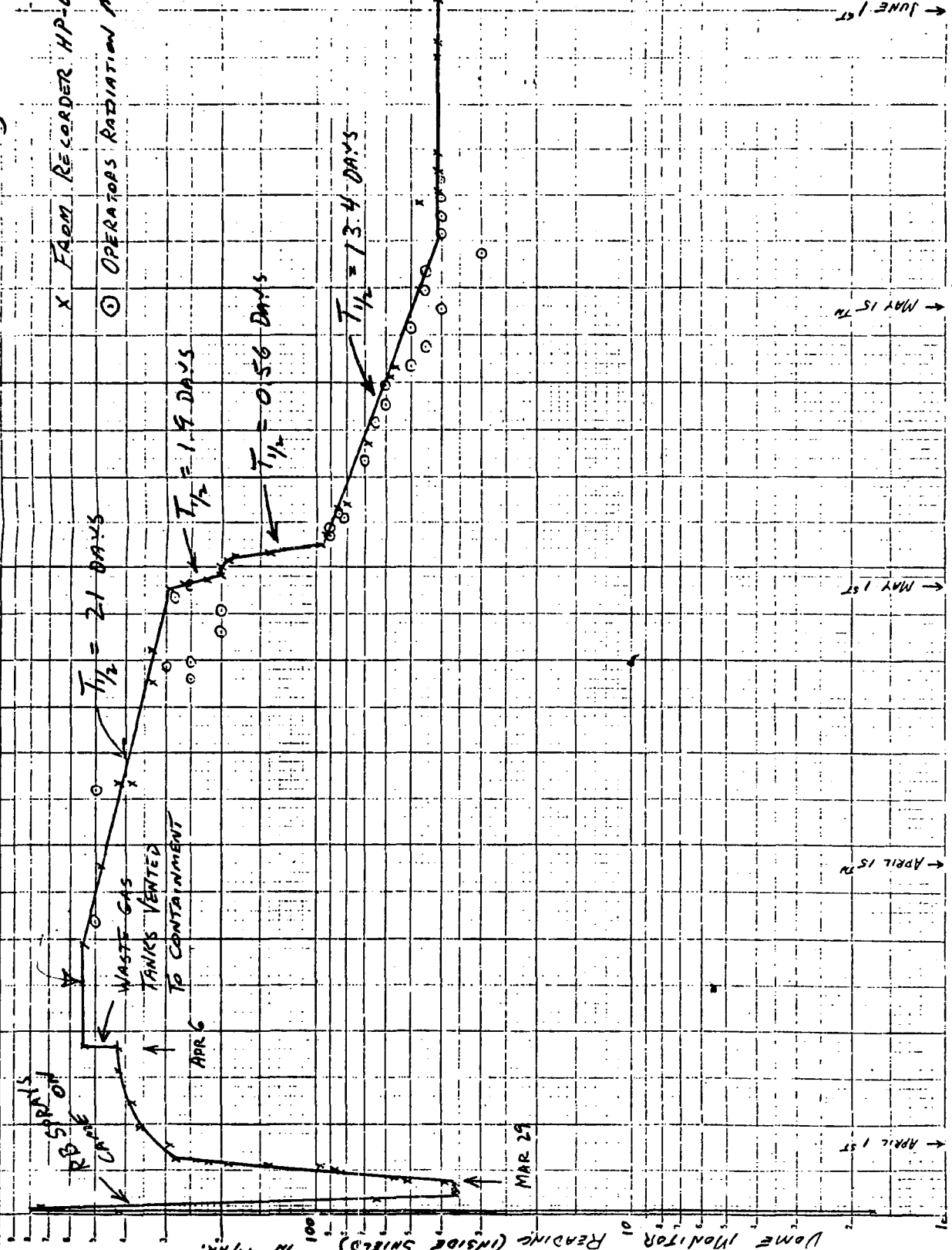


FIGURE 5 - Dose Monitor Readings (INSIDE SHELL)



HP-R-214 STRIPCHART CORRECTED DATA

These data have been derived from the actual TMI-2 stripchart readings. Correction factors have been applied to the stripchart readings to account for the improper scaling and log paper errors. The left-hand number of each set of data (A) is the time in hours since the beginning of March 28, 1979. The right-hand numbers (B) is the radiation reading in R/hr.

A	B
1. .00479	
3.75 .00479	
4. .001	
6.375 .001	
6.5 .00789	
6.625 .185	
6.75 .435	
6.875 .905	
7. 1.36	
7.117 1.46	
7.133 1.56	
7.15 1.66	
7.167 1.86	
7.183 24.3	
7.2 38.4	
7.217 100.	
7.233 252.	
7.25 349.	
7.375 517.	
7.5 590.	
7.625 590.	
7.75 658.	
7.875 722.	
8. .837.	
8.25 839.	
8.5 889.	
8.75 889.	
9. 939.	
9.25 939.	
9.5 889.	
9.75 889.	
10. 889.	
10.25 837.	
10.5 837.	
10.75 781.	
11. 722.	
11.25 722.	
11.5 658.	
11.75 658.	

A	B
12. 722.	
12.25 781.	
12.5 837.	
12.75 889.	
13. 839.	
13.25 889.	
13.5 837.	
13.876 837.	
13.9 590.	
13.95 590.	
13.967 517.	
14. 517.	
23.5 76.6	
23.583 74.8	
23.667 73.	
23.75 71.2	
23.8 71.2	
26.917 46.	
28.5 46.	
29. 43.5	
29.5 41.	
30. 38.4	
31. 38.4	
31.5 35.8	
32.5 35.8	
33. 38.4	
34. 38.4	
34.5 41.	
35.5 41.	
36. 43.5	
37. 43.5	
37.5 46.8	
38. 46.8	
38.5 48.3	
39.5 48.3	
40. 50.7	
40.75 50.7	

A	B	A	B
43.8	55.2	102.	385.
44.5	55.2	108.	385.
45.	57.3	114.	420.
46.	57.3	120.	420.
46.5	59.5	126.	453.
47.	61.5	132.	453.
47.5	61.5	138.	453.
48.	63.5	144.	486.
48.5	65.5	150.	517.
49.	65.5	156.	517.
49.5	67.5	162.	517.
50.	69.4	168.	576.
50.5	69.4	174.	618.
51.	71.2	180.	618.
51.5	71.2	186.	618.
52.	73.	192.	618.
52.5	74.8	198.	618.
53.	76.6	204.	618.
54.	76.6	210.	618.
54.5	78.3	216.	604.
55.	78.3	240.	597.
55.5	80.	264.	597.
56.	81.6	288.	611.
56.5	83.3	312.	618.
57.	84.9	336.	645.
57.5	86.4	360.	618.
58.	88.	384.	618.
58.5	89.5	408.	604.
59.	89.5	432.	604.
59.5	91.	456.	604.
60.	91.	480.	604.
60.5	92.5	504.	590.
61.	95.3	528.	562.
61.5	96.7	576.	590.
62.	98.1	672.	437.
62.5	99.5	768.	437.
63.	100.	864.	144.
63.5	100.	960.	88.
64.	100.	1056.	71.2
66.	121.	1152.	55.2
72.	252.	1248.	53.
78.	349.	1344.	50.7
84.	349.	1440.	53.
90.	385.	1920.	53.
96.	385.	2016.	57.3
		2304.	57.3

A B

**2400. 59.5
2496. 61.5
2976. 61.5
4512. 67.5
5232. 61.5
5952. 67.5
6048. 71.2
6696. 74.8
7440. 71.2
8136. 69.4
8880. 59.5
9600. 63.5
10296. 67.5**

APPENDIX E

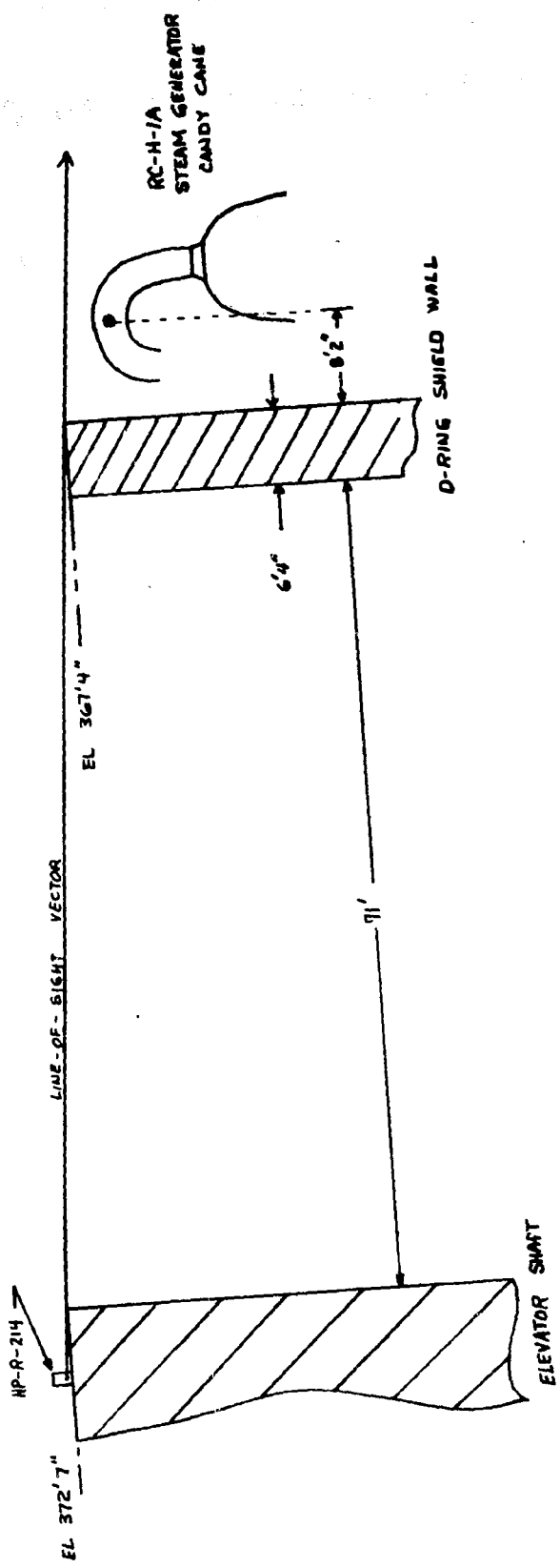
HP R 214 Line of Sight to Candy Canes

Charts F1 and F2 show the line of sight vectors from HP-R-214 to the steam generator candy canes A and B, respectively. As can be seen, there is probably a line of sight to the RC-H-1B candy cane, the nearer of the two. If we assume that the contamination in the liquid looks like a point source to the detector, we can make a very rough estimate of radiation level due to this source at the detector. We calculate this level to be approximately 675 R/hr using the following data and assumption:

1. Assume 1.173 and 1.333 Mev photons only
2. Neglect effects of attenuation of candy cane pipe
3. Assume volume of liquid is 2.35×10^3 liters
4. Assume aperature of detector is 75cm^2
5. Assume point source and $1/R^2$ radiation recuction where R is the distance to the source
6. No shielding by the SS vessel was assumed

Although this calculation is very rough, it should be conservative, i.e., radiation levels should be lower than calculated since high energy photons and no shielding was assumed.

CHART E1



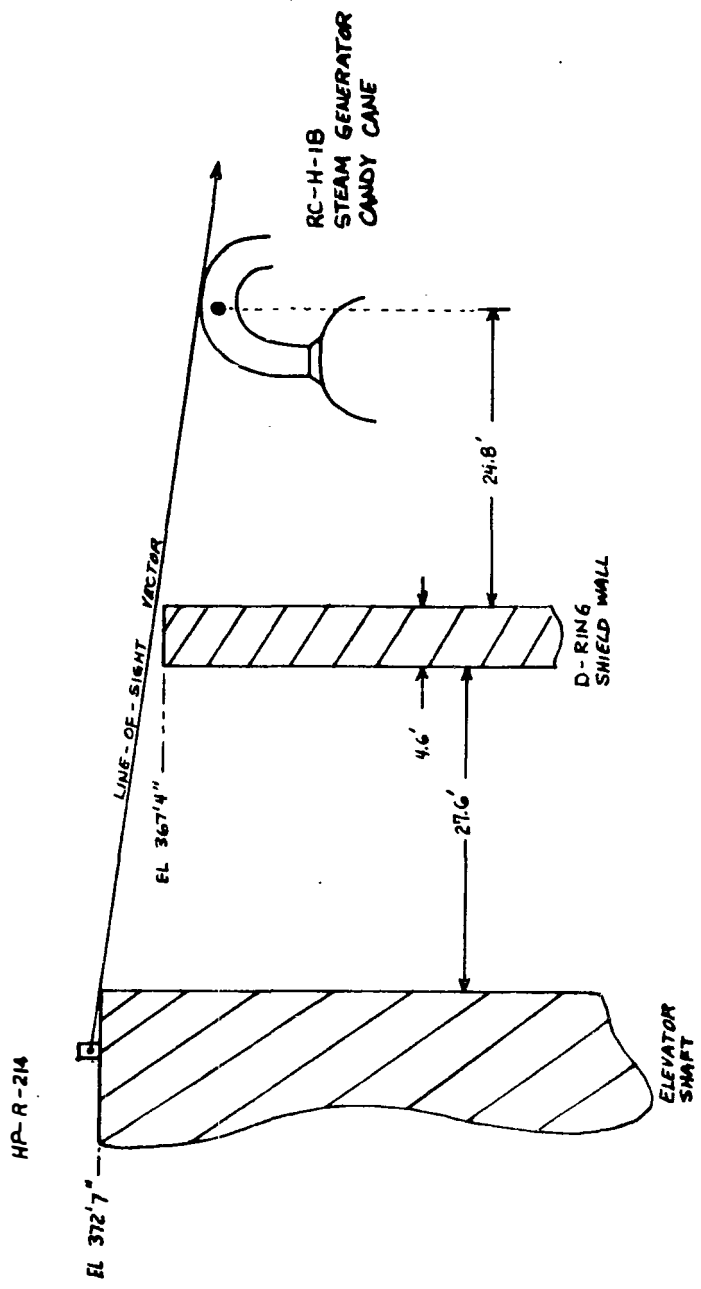
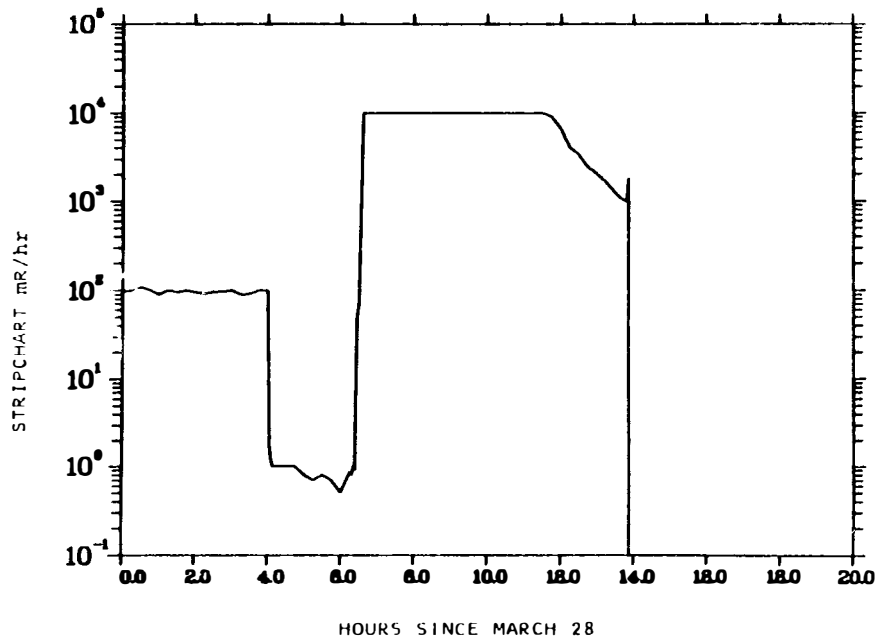
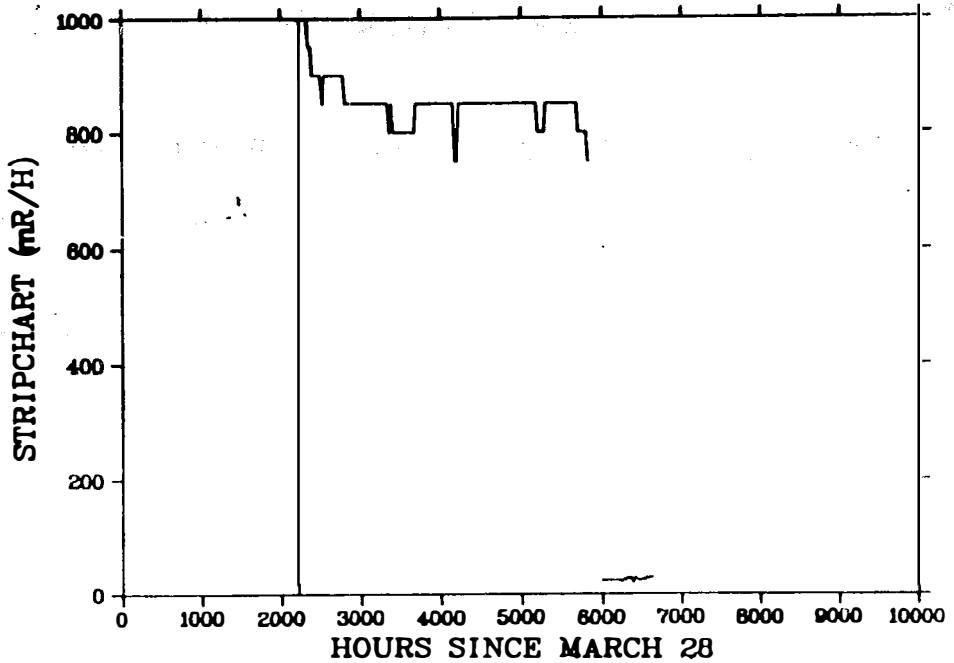


CHART E2

APPENDIX F

HP R 212 and HP R 213 Stripcharts



The top graph plots the stripchart from HP-R-212 as a function of hours since the beginning of March 28, 1979. The bottom shows similar information for HP-R-213. Note the difference in time scales. HP-R-213 failed early in the accident. HP-R-212 was not turned on until over 2000 hours after the accident began.

APPENDIX G

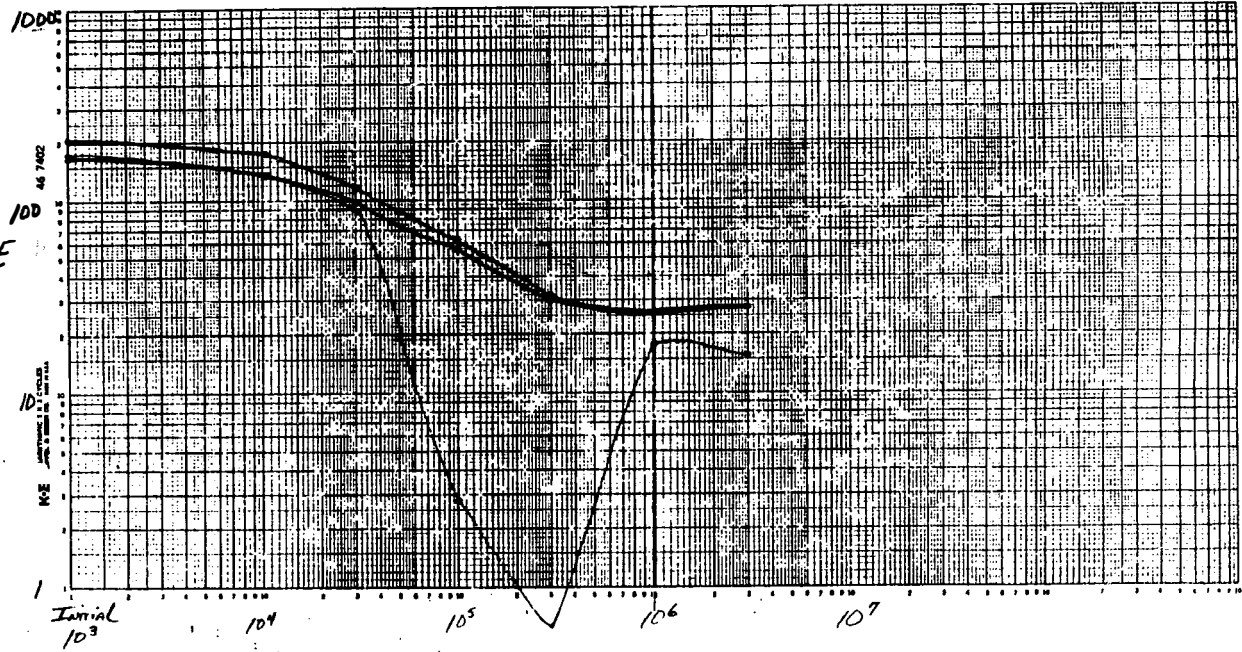
Radiation Total Dose Information

Appendix G contains the HFE vs. Gamma Dose characterizations which were used to estimate the total radiation dose to KP-R-214 transistors. Four transistor types from several manufacturers were exposed to a CO 60 source, both passively and actively, and the characteristic curves were measured at two collector currents. Optical density measurements of mylar wrap samples is also included.

2N3904

NPN
@ 100ma

Active
Fairchild



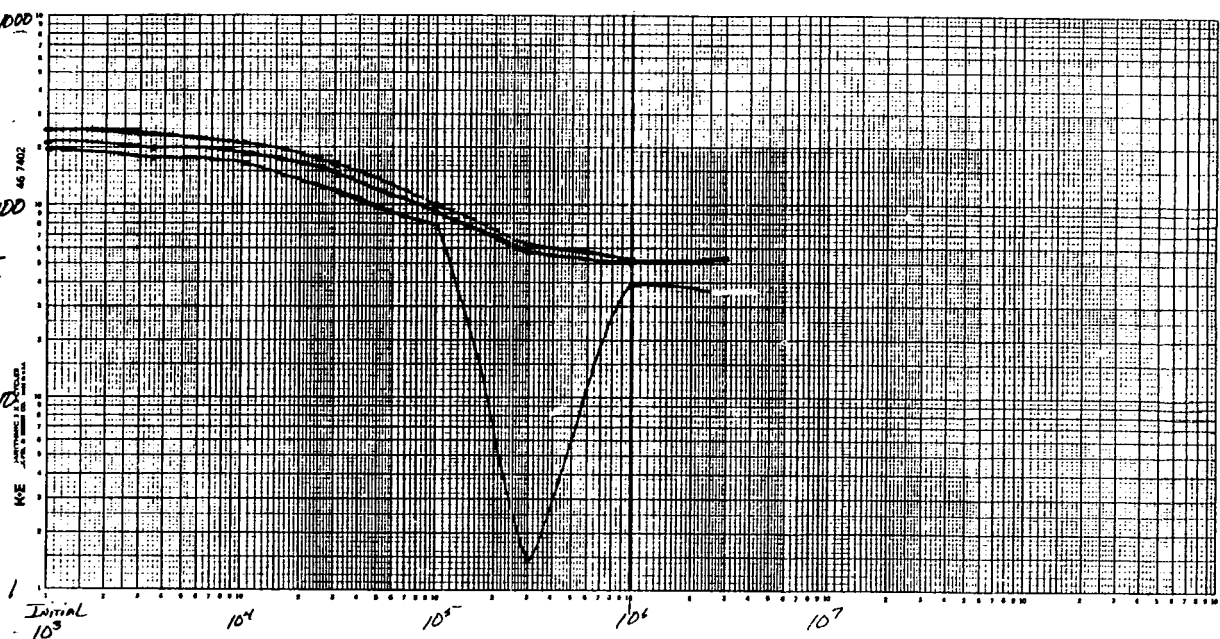
* 1, 2, AND 3

2N3904

NPN
@ 1ma

ACTIVE
Fairchild

HFE



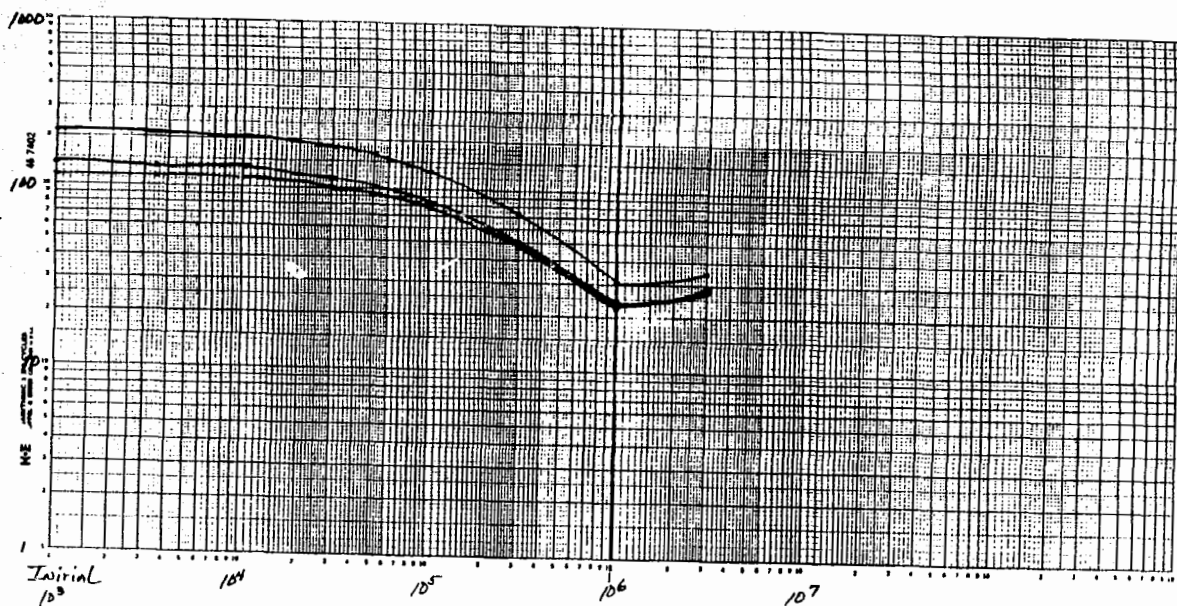
2N3904

NPN

@100μa

Active

GENERAL ELECTRIC



* 4, 5, AND 6

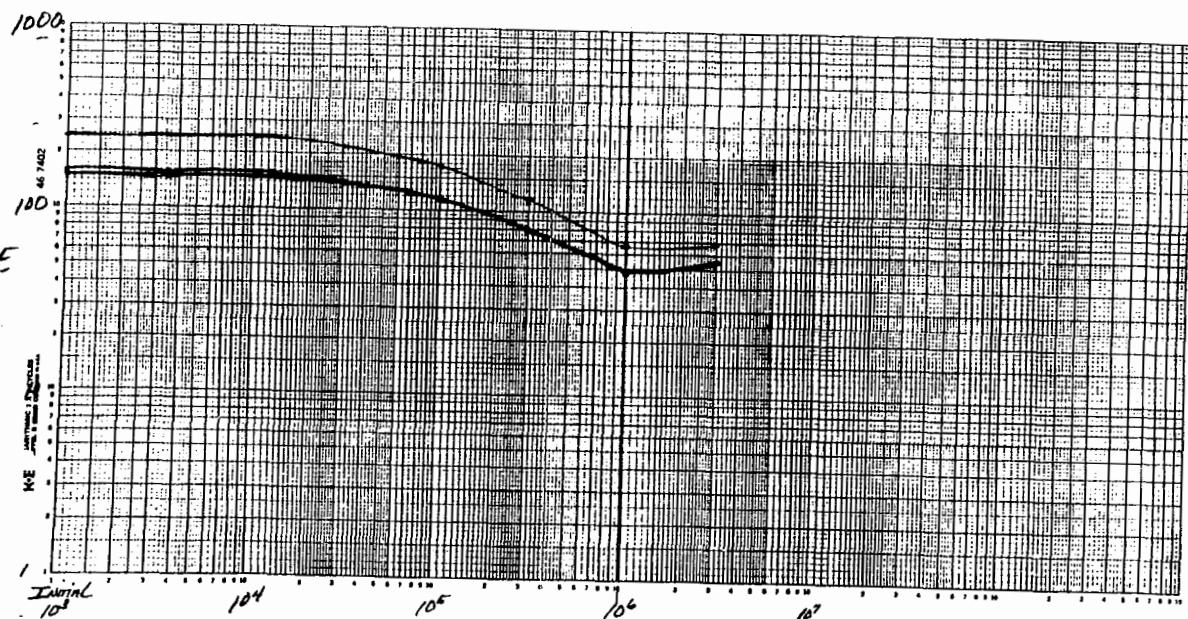
2N3904

NPN

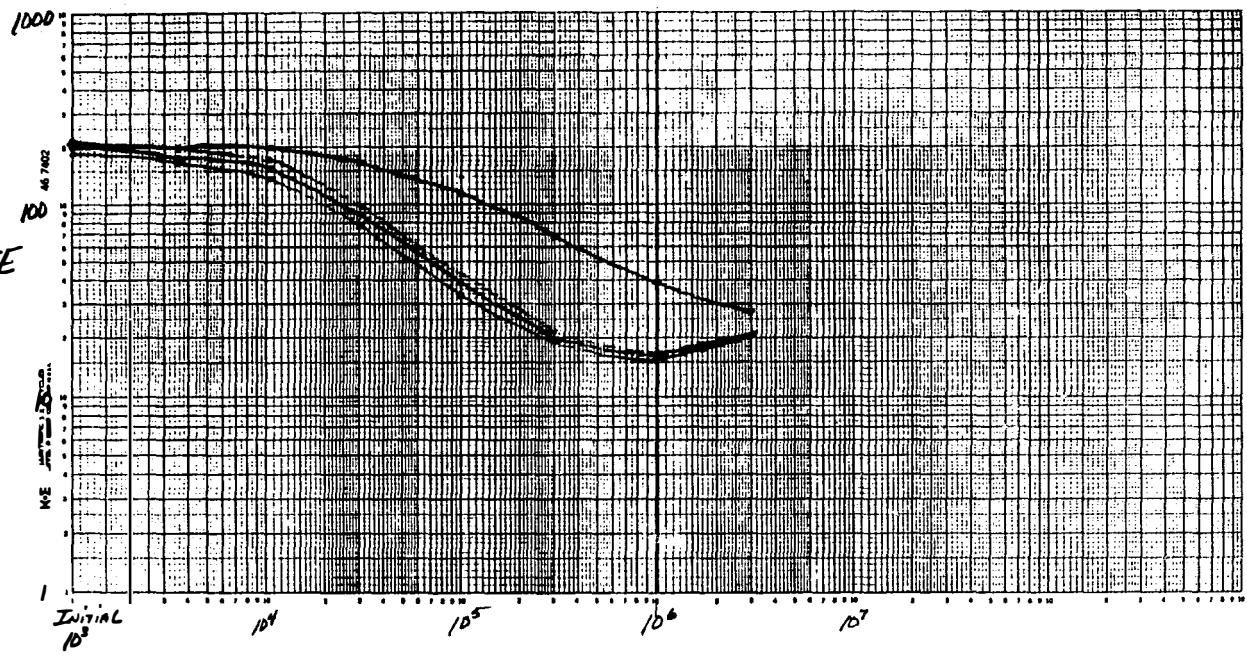
@1ma

Active

GENERAL Electric



Gamma Dose (Ra₀₅)



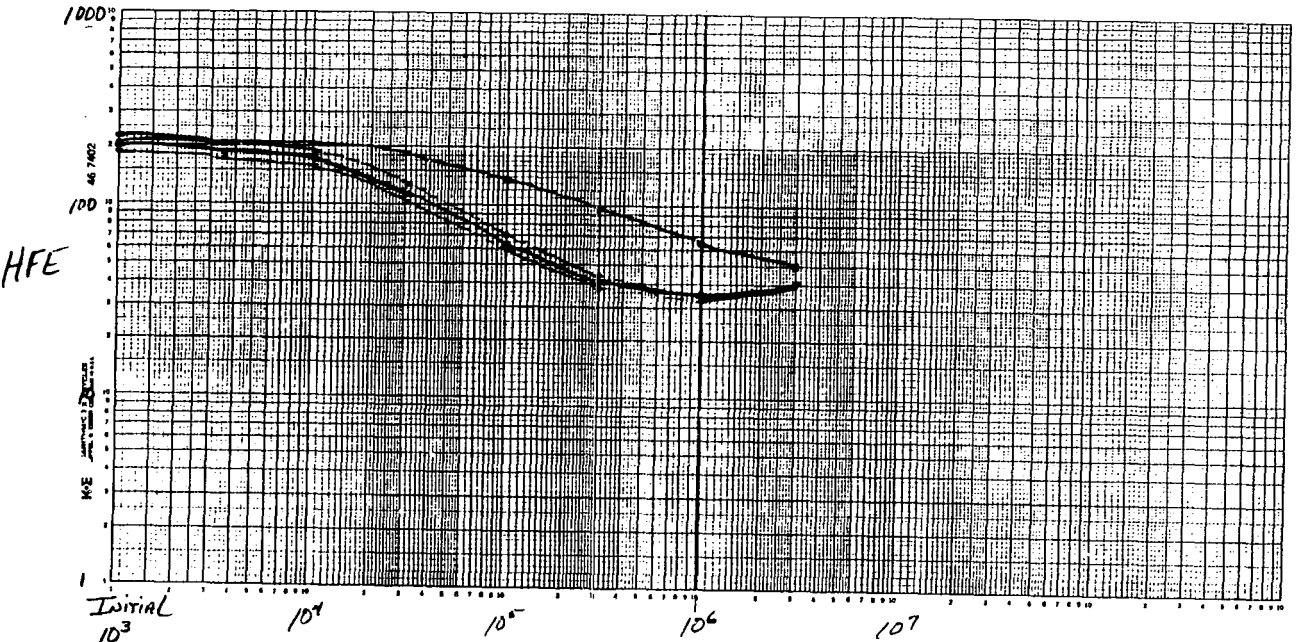
Gamma Dose (Rads)

*7,8,9, AND 10

2N3904

NPN
@1ma

ACTIVE
MOTOROLA



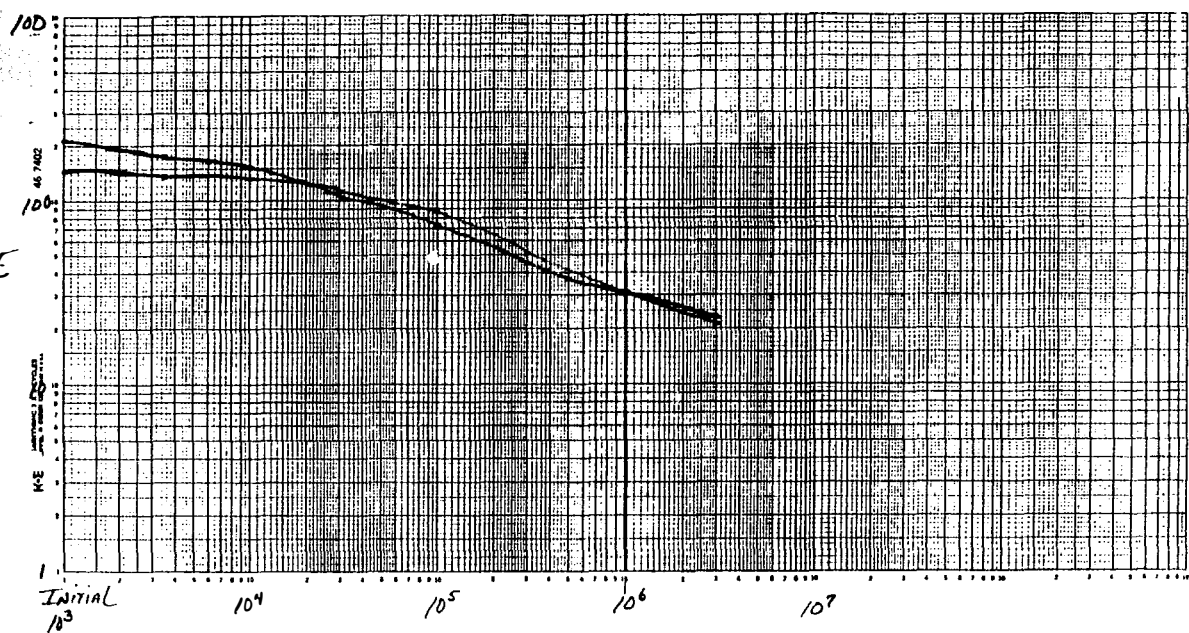
Gamma Dose (Rads)

#11, AND 12

ZN3904

NPN
@ 100ma

PASSIVE
FARNCHILD

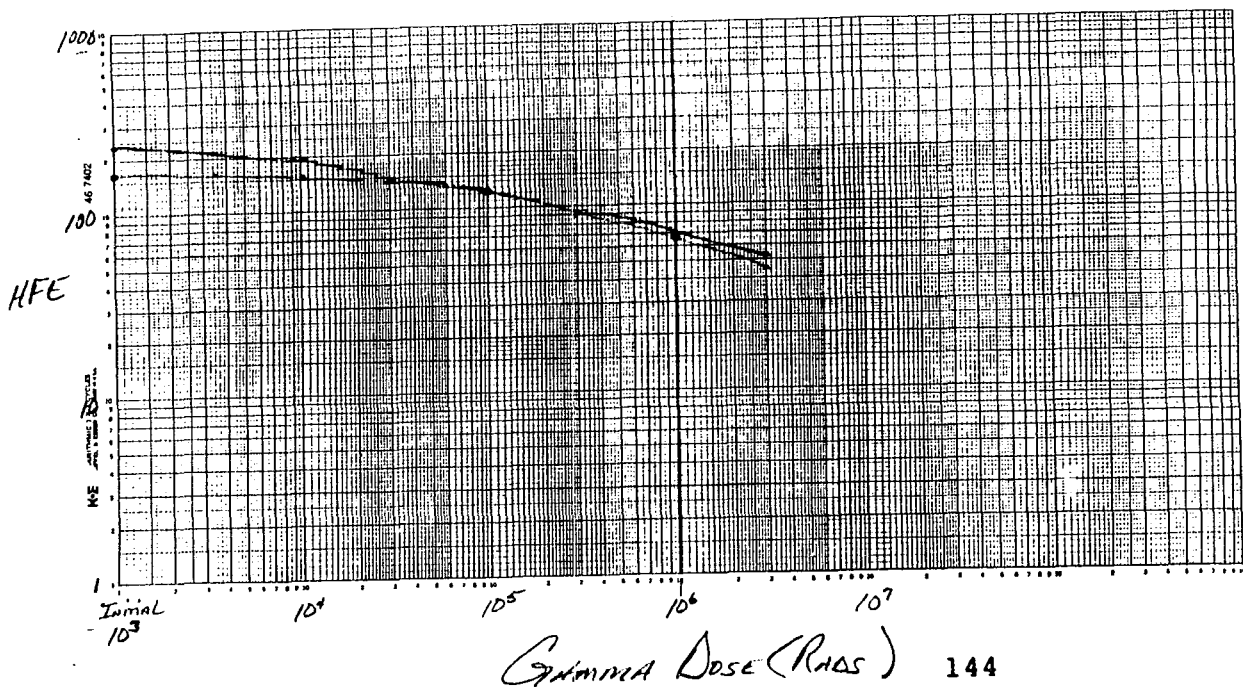


#11, AND 12

ZN3904

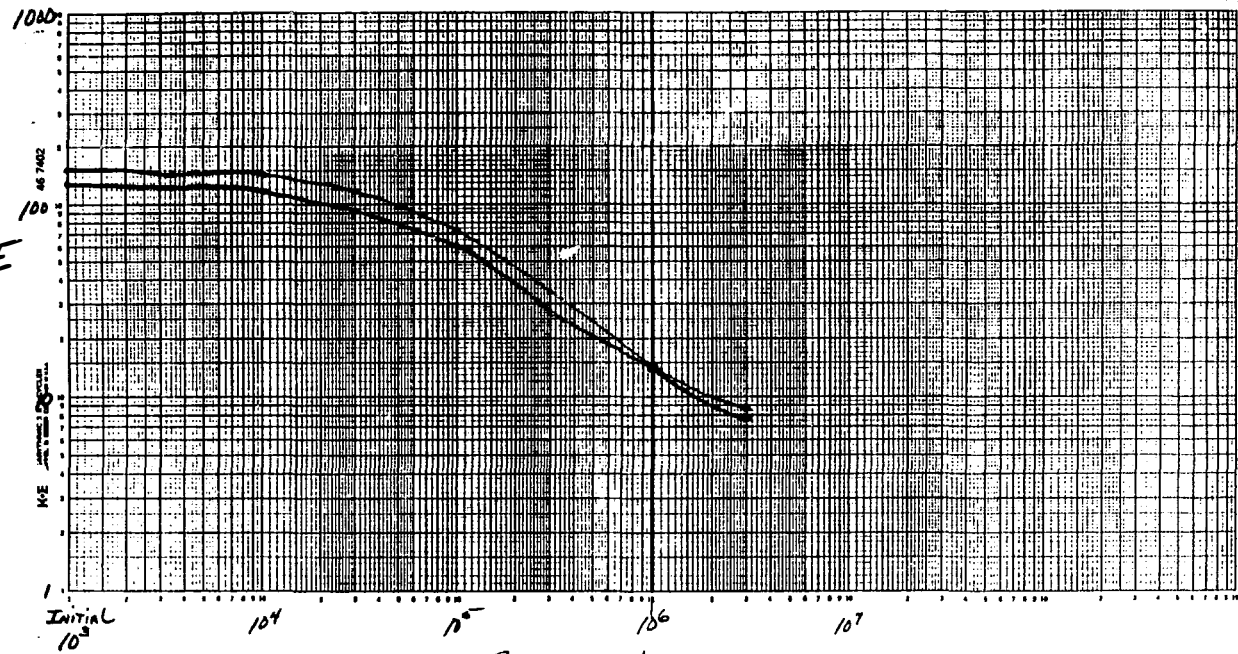
NPN
@ 1ma

PASSIVE
FARNCHILD



ZN3904

NPN
@ 100ma
Passive
General Electric

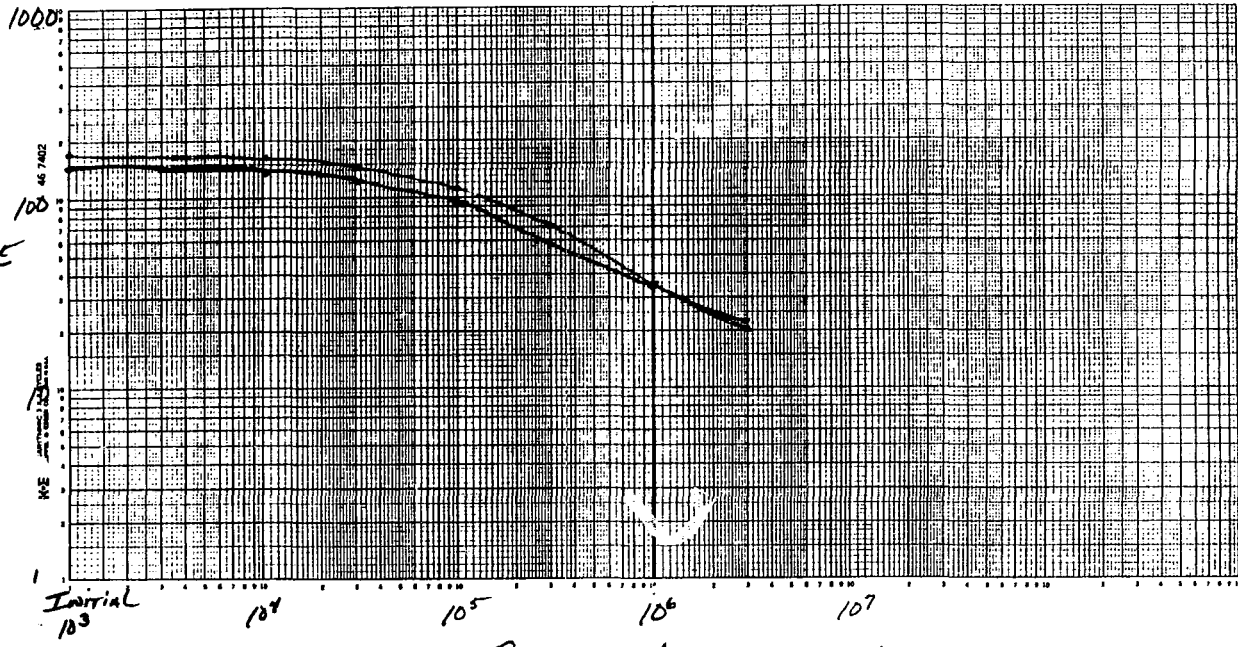


*13, mid 14

ZN3904

NPN
@ 10ma

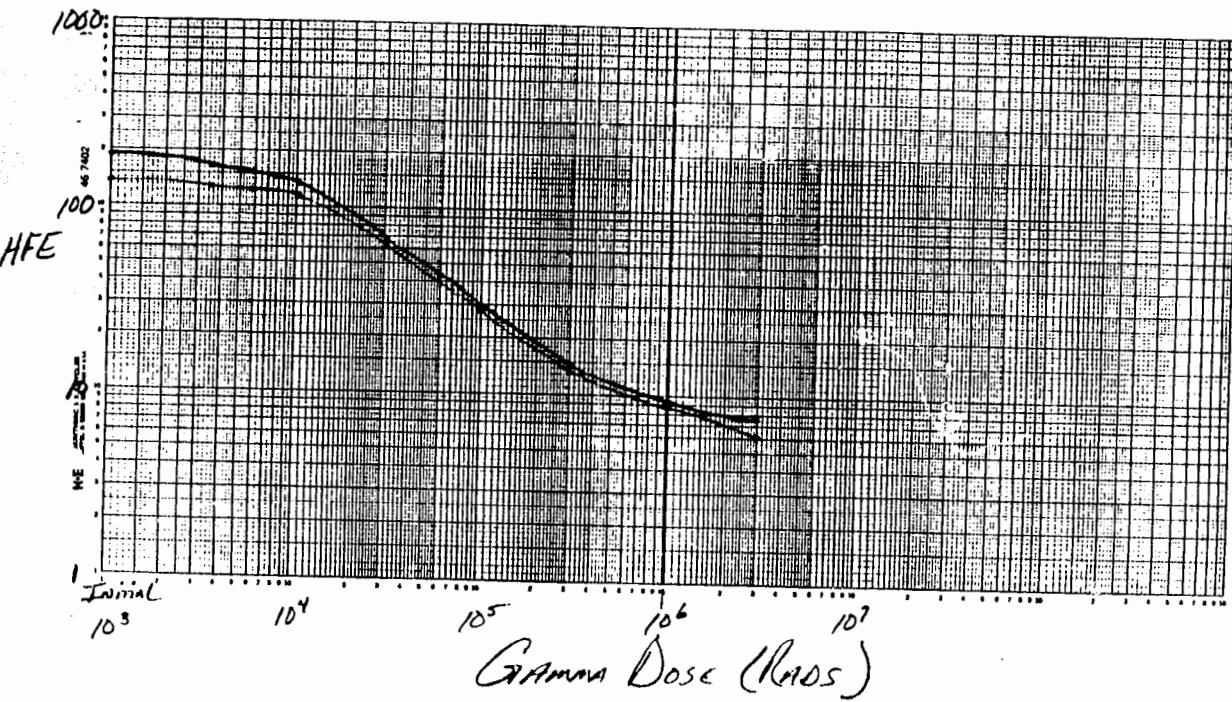
PASSIVE
GENERAL ELECTRIC



ZN3904

NPN
@ 100ma

PASSIVE
MOTOROLA

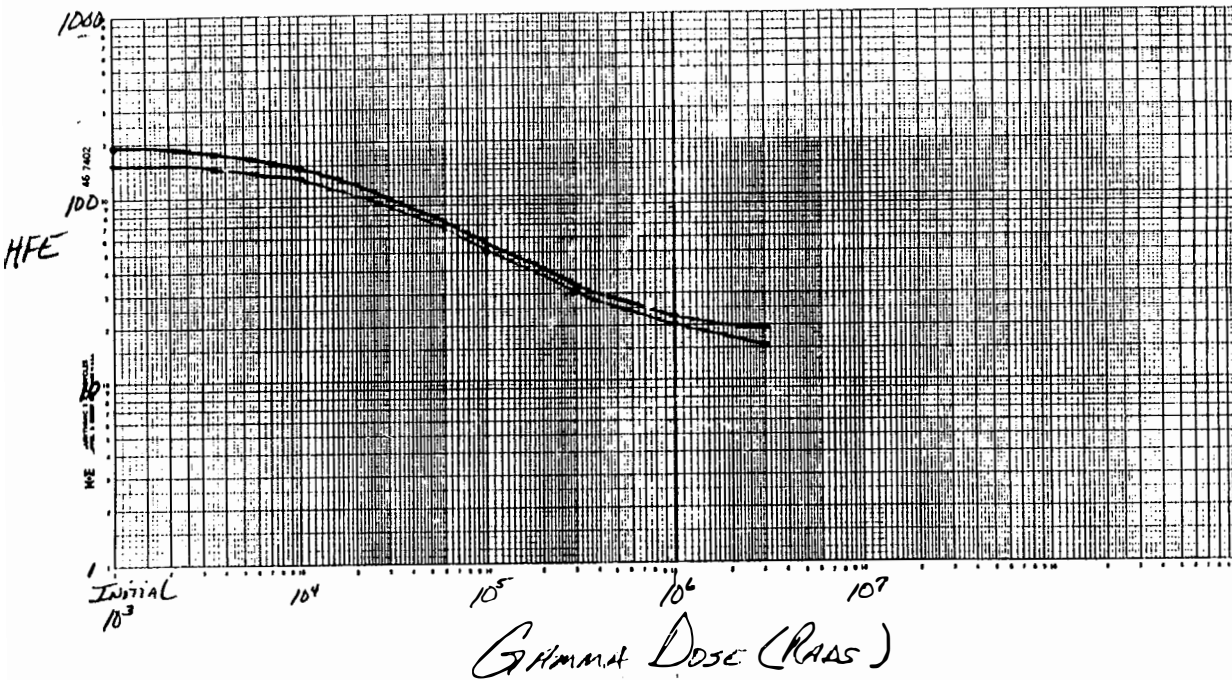


*15 and 16

ZN3904

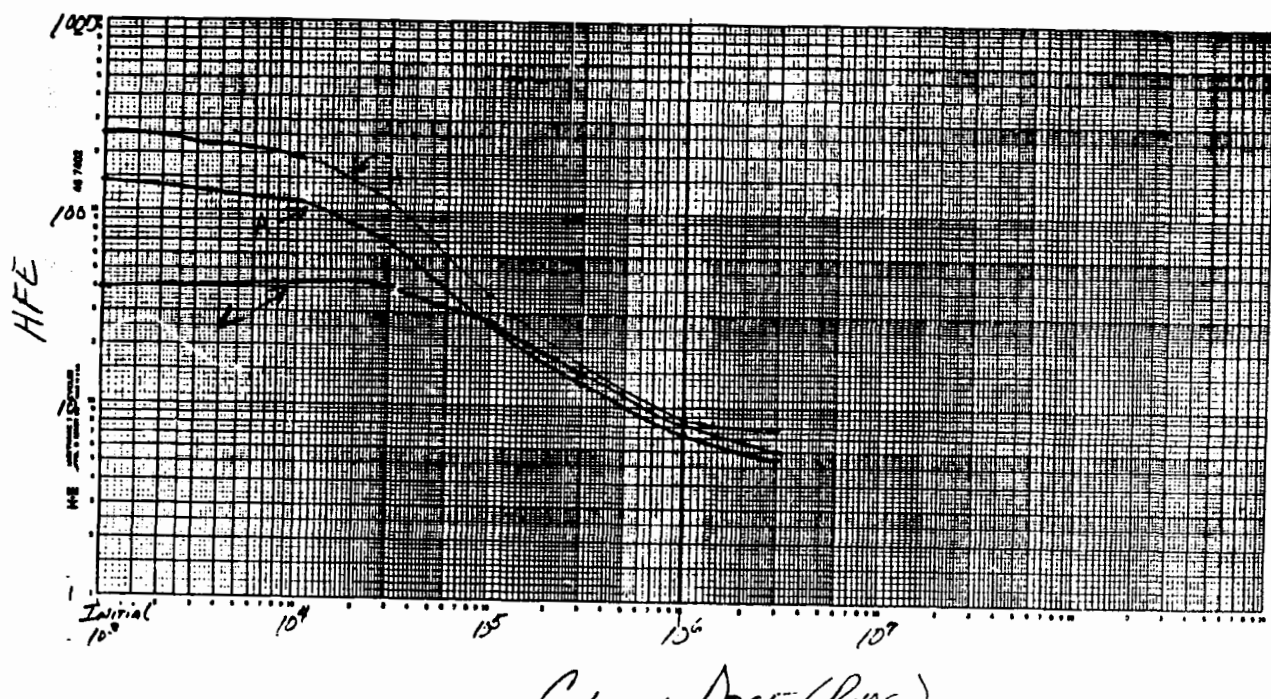
NPN
@ 1ma

PASSIVE
MOTOROLA



CUT Open

HIGH
LOW
AVERAGE

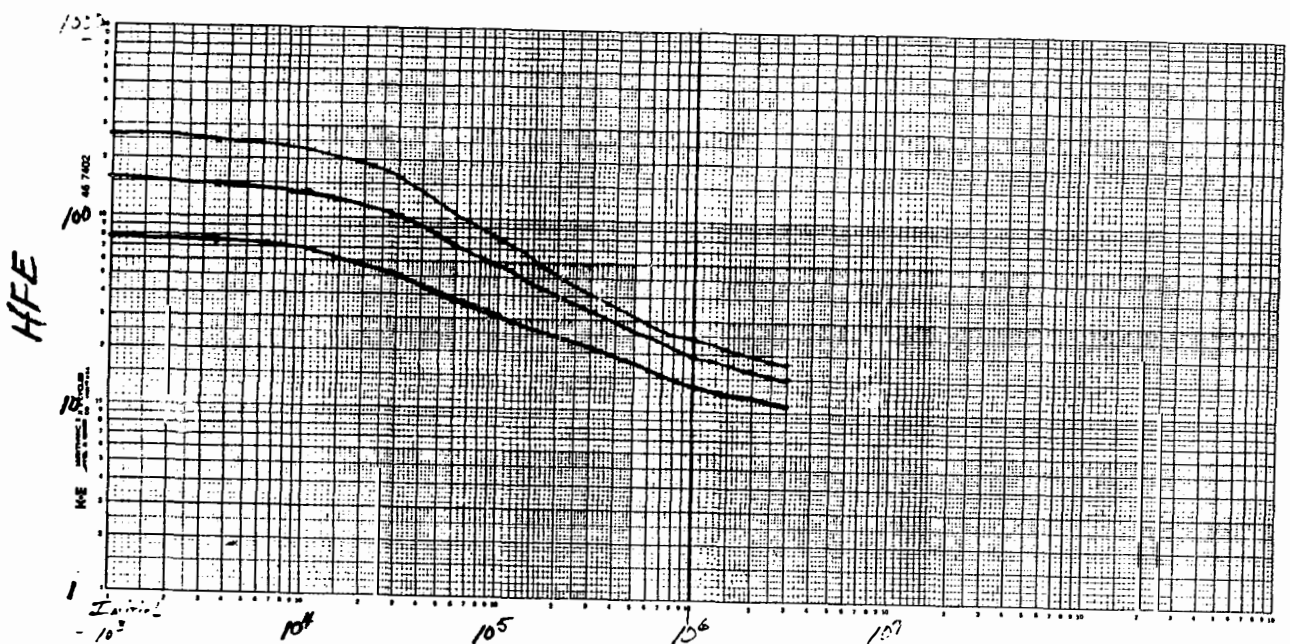


ZN3643

NPN
@ Ima

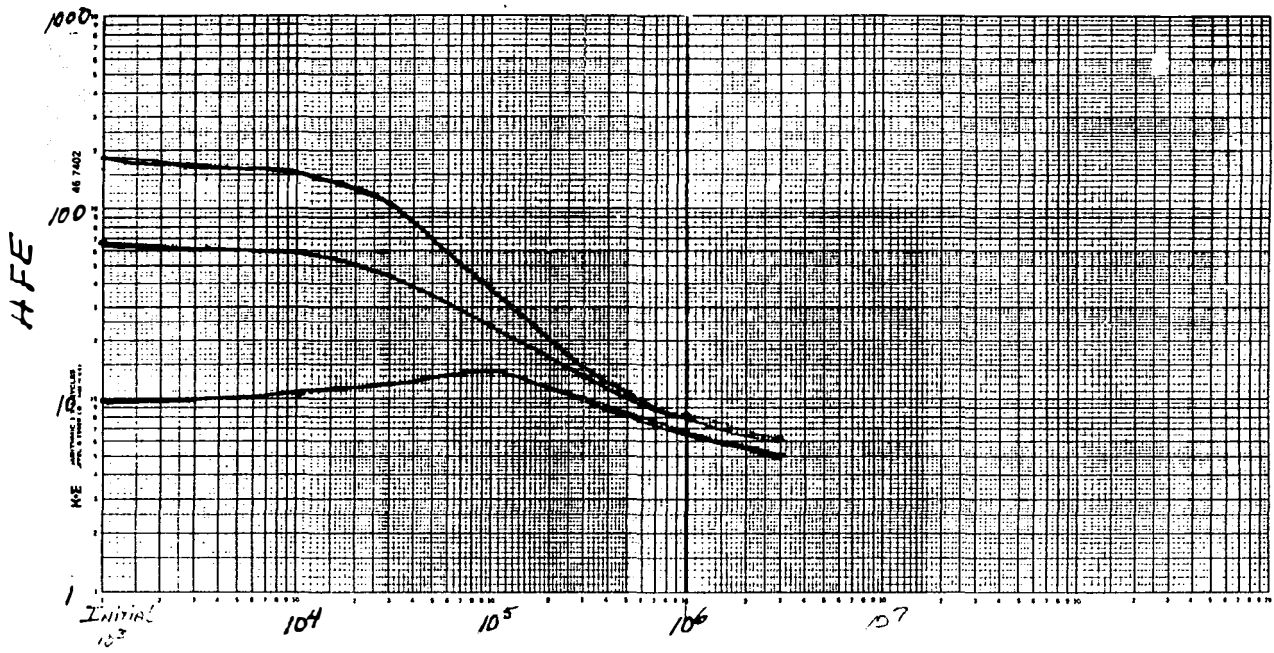
ACTIVE
FAIRCHILE

HIGH
LOW
AVERAGE



@ 100μa FRICCHILD

HIGH
LOW
AVERAGE



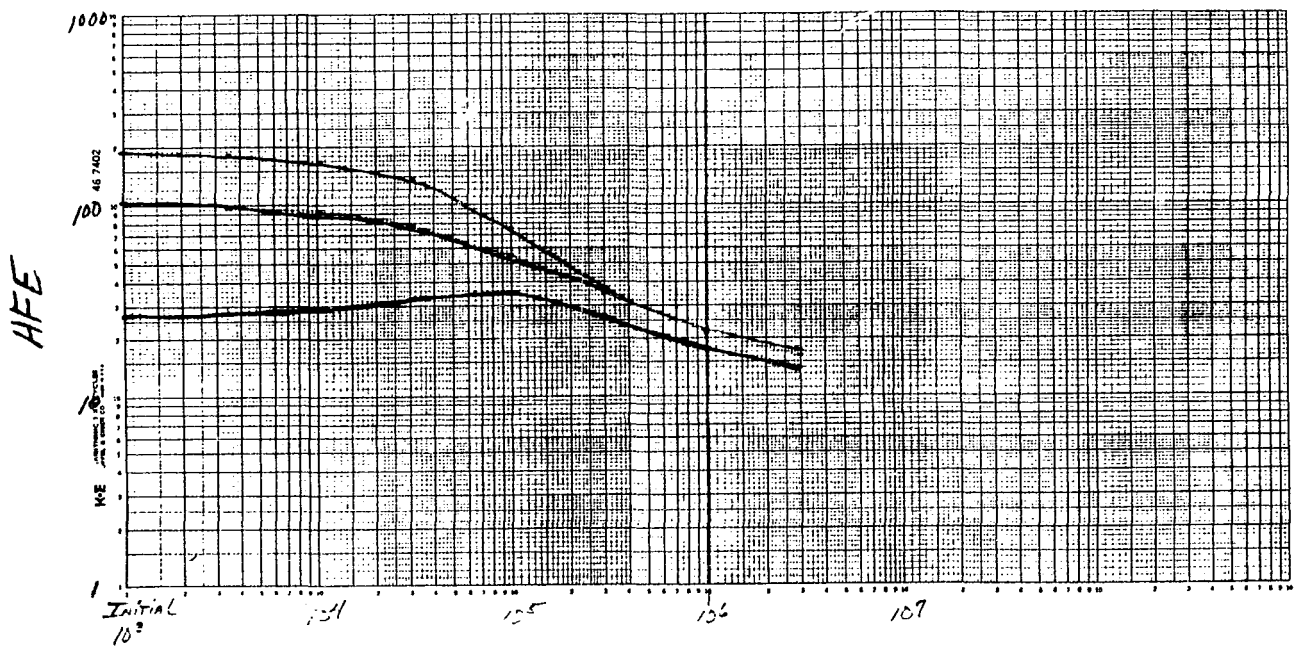
GAMMA DOSE (RADS)

ZN3643

NPN
@ 1mA

PASSIVE
FRICCHILD

F-34
LOW
AVERAGE

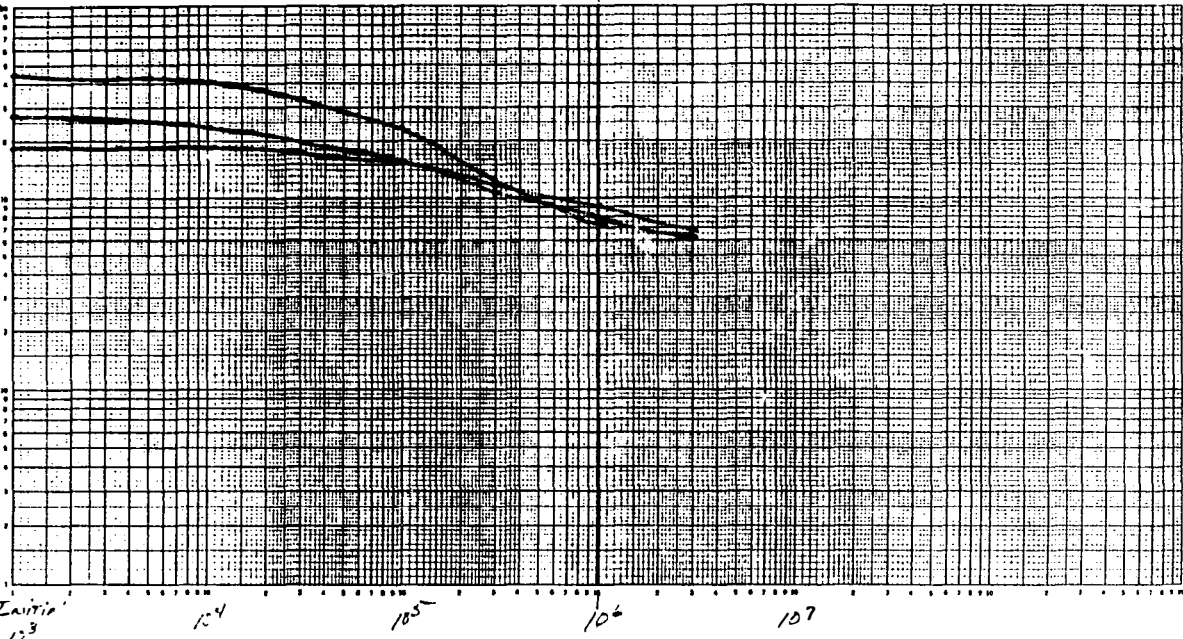


GAMMA DOSE (RADS) 148

@ 100μa Fairchild

HIGH
LOW
AVERAGE

HFE



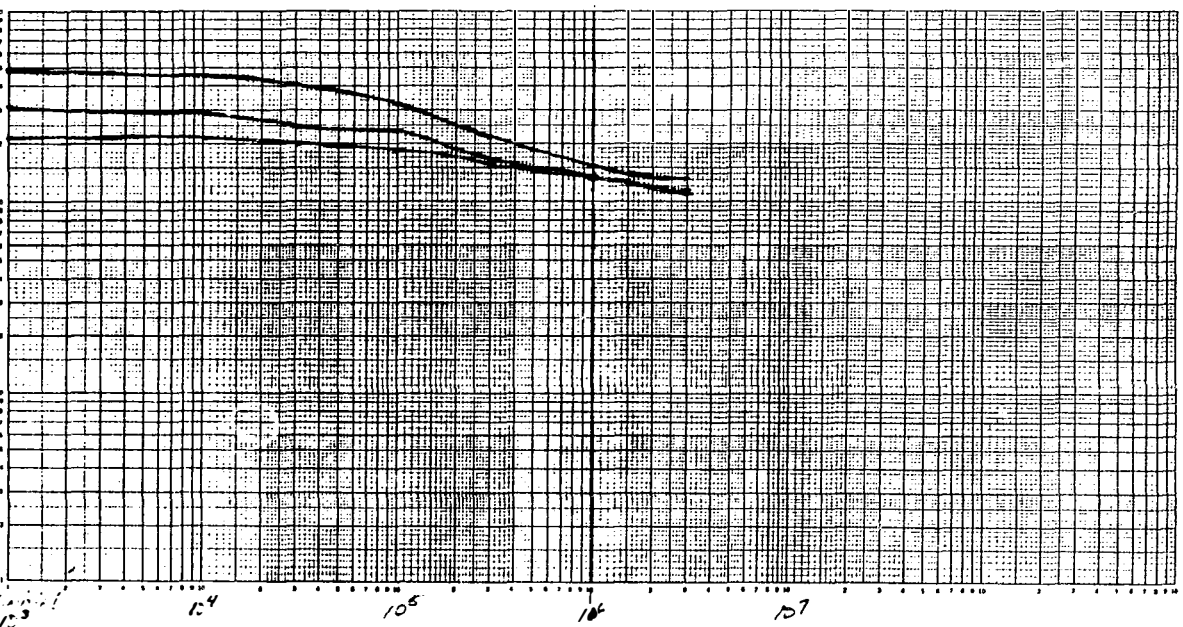
ZN3565

NPN
@ 100a

Native
Fairchild

HIGH
LOW
AVERAGE

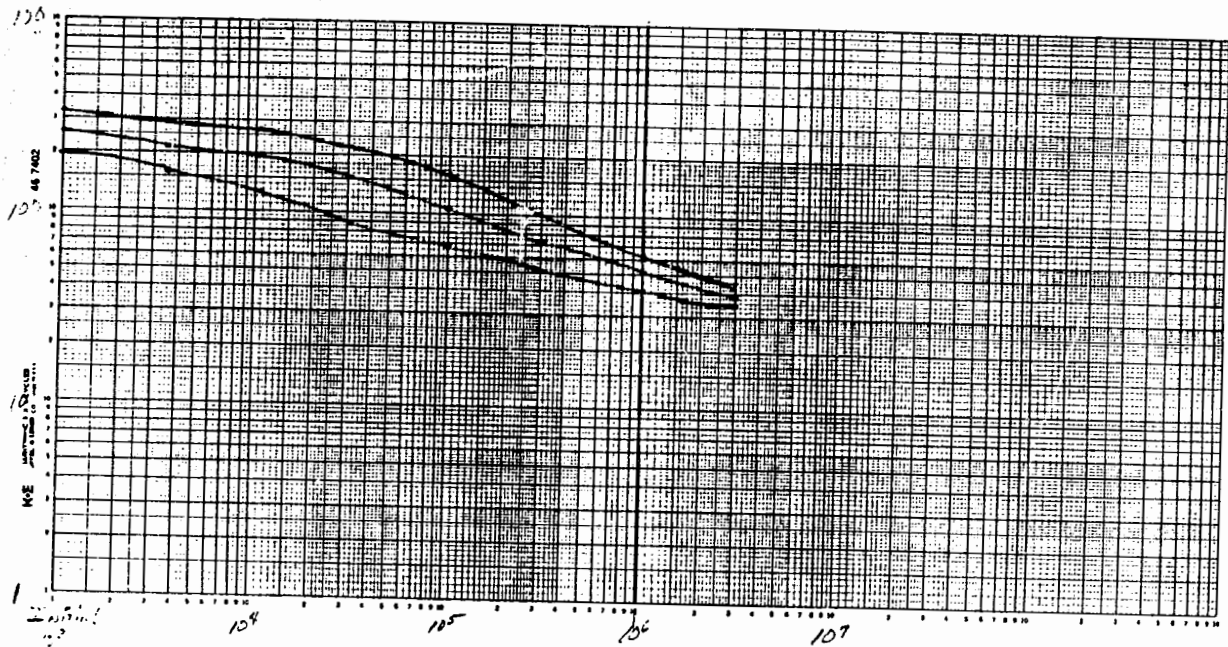
HFE



2N3565

NPN
@ 100ma FAIRCHILD

HIGH
LOW
AVERAGE

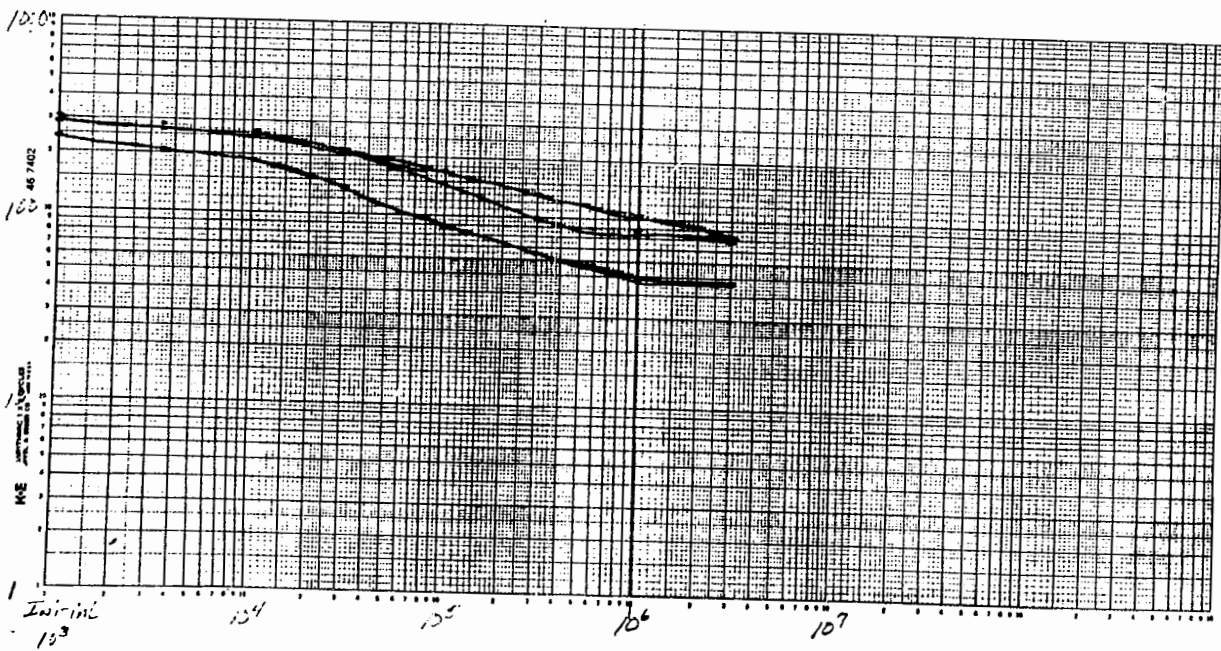


Gamma Dose (Rads)

2N3565

NPN
@ 100ma FAIRCHILD

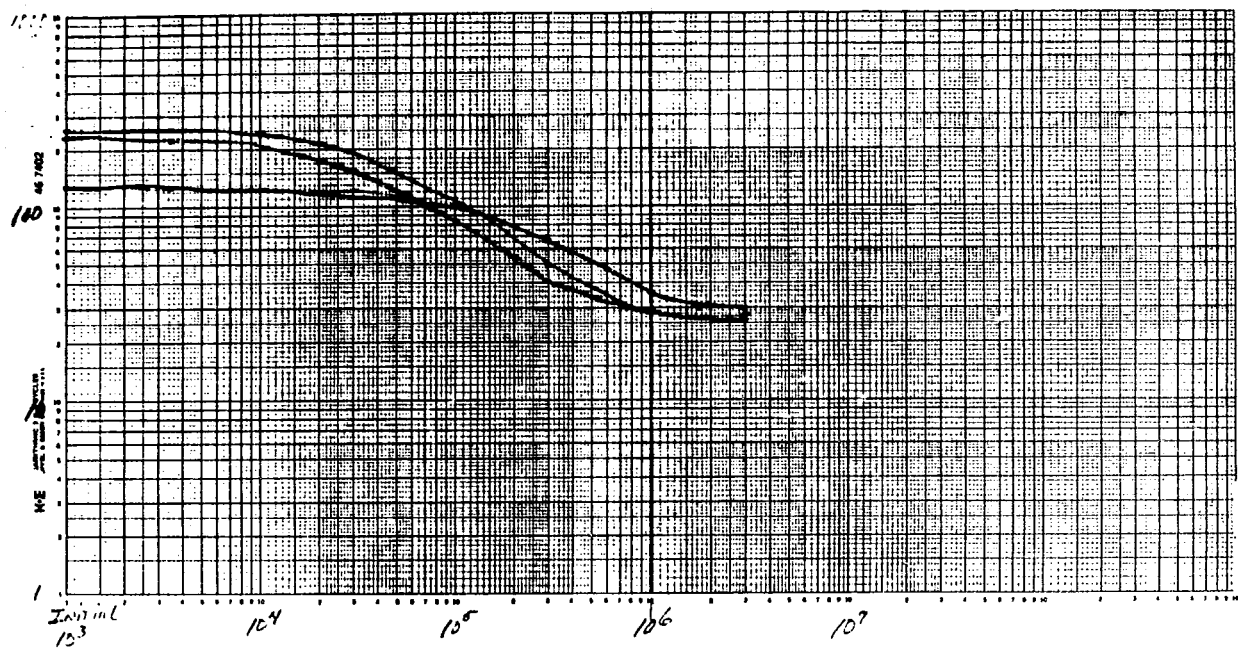
HIGH
LOW
AVERAGE



2N4249

PNP ACTIVE
@ 100ma Fairchild

HIGH
LOW
AVERAGE

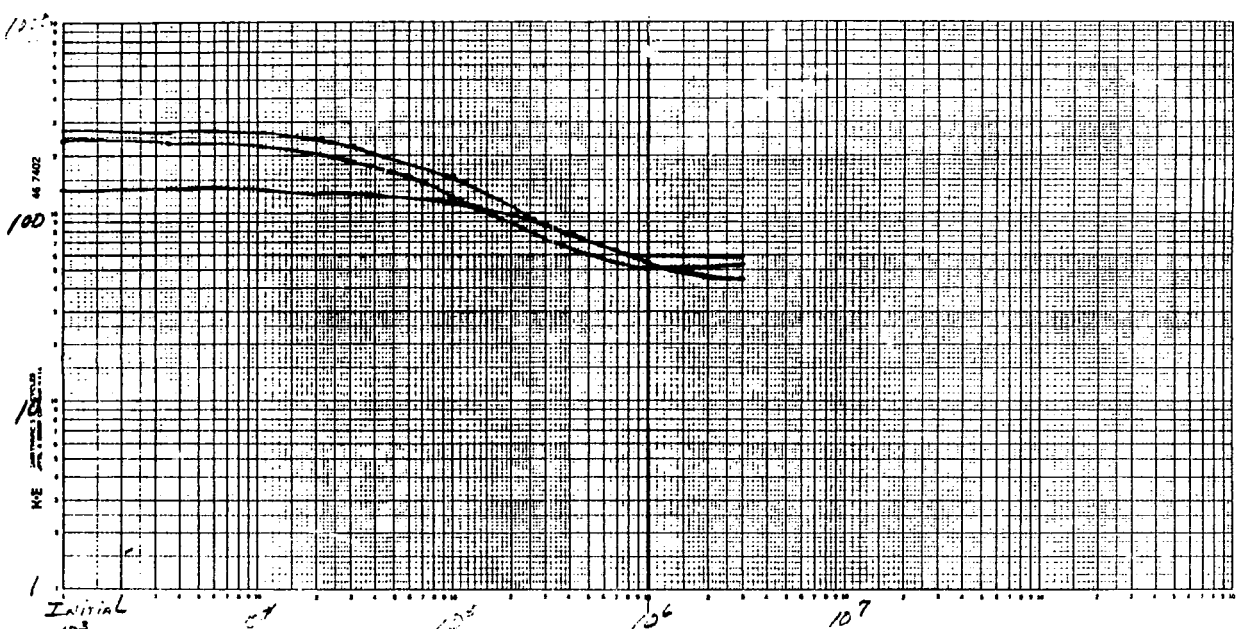


Gamma Dose (Rads)

2N4249

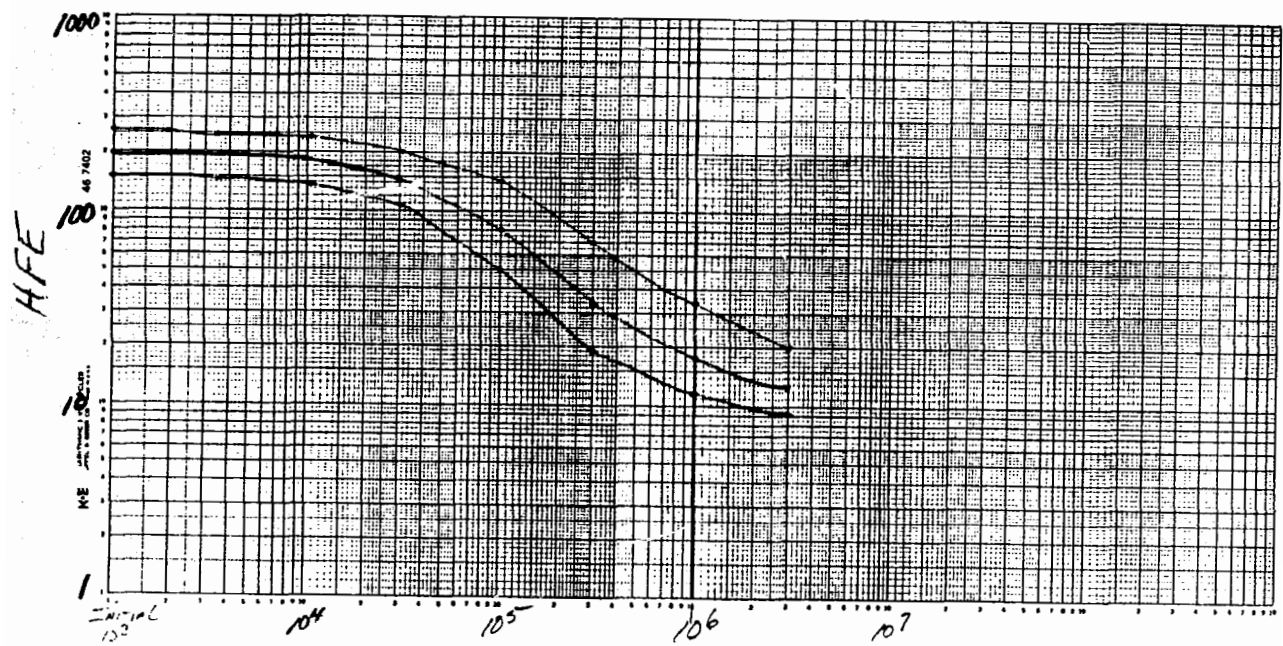
PNP ACTIVE
@ 1ma Fairchild

HIGH
LOW
AVERAGE



@ 100 μ A PHENICOL

HIGH
LOW
AVERAGE



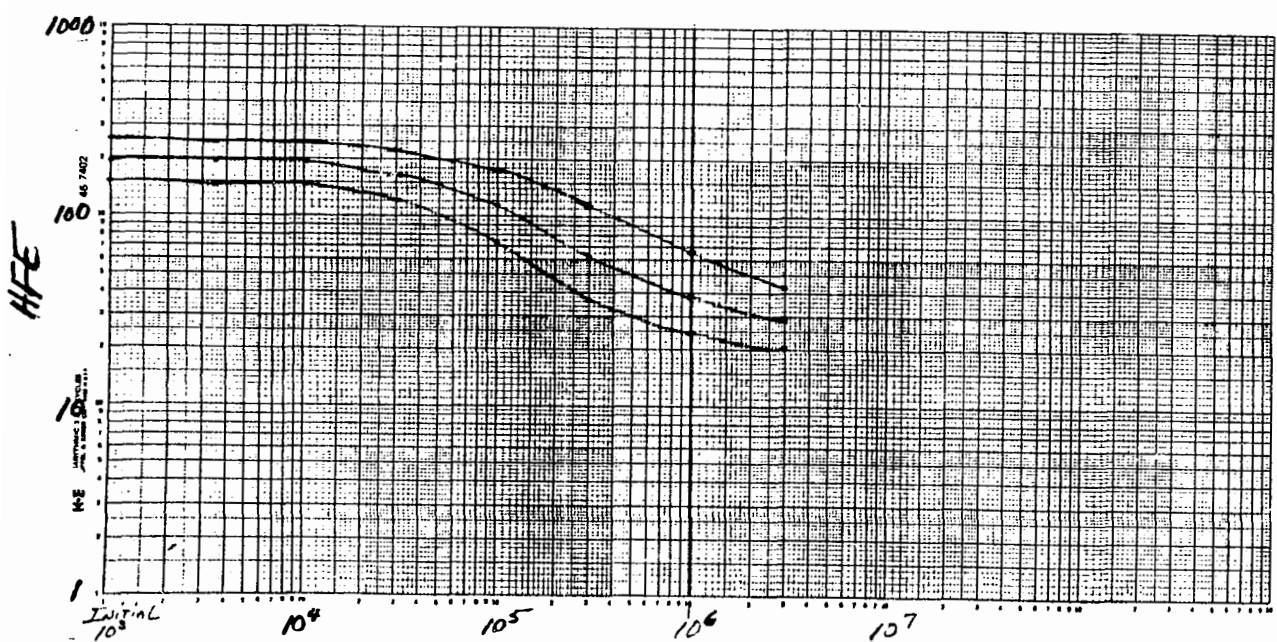
— Opinion Dose (Rads) —

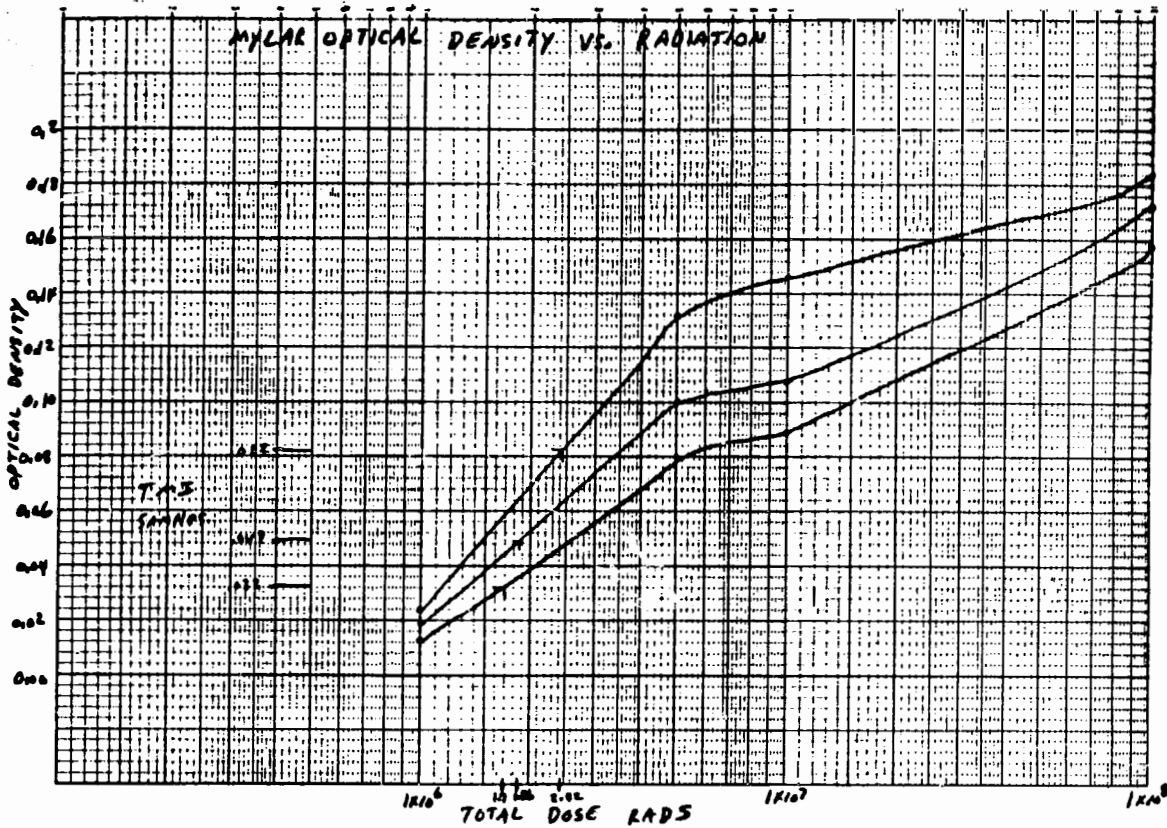
2N4249

PNP
@ 100 μ A

Passive
Fairchild

HIGH
LOW
AVERAGE





	MIN	\bar{X}	MAX
1×10^6	0.013	0.019	0.024
5×10^6	0.080	0.100	0.132
1×10^7	0.099	0.108	0.146
1×10^8	0.158	0.172	0.184
TMI	0.032	0.049	0.082

APPENDIX H

Transport Calculations and Results

- I. Calculate gamma rate at HP-R-214 location assuming upper containment is filled with noble gas

Here we assume the portion of containment above the 347.5 foot level contains a uniform mixture of noble gases. The volume of the upper dome is calculated to be 33189 m^3 . If this volume is made into an equivalent sphere the radius would be 19.93 m .

Hopkins in Reference 13 derives the flux density ϕ at the edge of a sphere containing a radioactive gas as:

$$\phi = \frac{Sv}{2\mu} \left[1 - \frac{1}{2\mu R} (1 - e^{-2\mu R}) \right] \quad (1)$$

where:

ϕ = flux density in photons $\cdot \text{cm}^{-2} \cdot \text{sec}^{-1}$

Sv = volumetric source strength in photons $\cdot \text{cm}^{-3} \cdot \text{sec}^{-1}$

μ = linear attenuation coefficient for air in cm^{-1}

R = radius of sphere in cm

Equation 1 accounts for the absorption of photons by air. The radiation dose rate is usually given as:

$$\dot{D} = \mu_{ME} \phi E_p \quad (2)$$

where:

\dot{D} = dose rate in $\text{Mev} \cdot \text{g}^{-1} \cdot \text{sec}^{-1}$

μ_{ME} = mass absorption coefficient for air in $\text{cm}^2 \cdot \text{g}^{-1}$

E_p = photon energy in Mev

In order to get the units in Mrad per hour for \dot{D} we must have a conversion constant:

$$D_K = 1.602 \times 10^{-13} \frac{\text{J}}{\text{Mev}} \cdot 3600 \frac{\text{sec}}{\text{hr}} \cdot 10^3 \frac{\text{gm}}{\text{Kg}} \cdot \frac{\text{rad-Kg}}{10^{-2} \text{J}} \cdot \frac{\text{Mrad}}{10^6 \text{rad}}$$

$$D_K = 5.7672 \times 10^{-11} \frac{\text{sec} \cdot \text{g} \cdot \text{Mrad}}{\text{Mev} \cdot \text{hr}} \quad (3)$$

Combining equations 1, 2 and 3 :

$$\dot{D} = D_K \mu_{ME}(\text{air}) \frac{SvEp}{2\mu} \left[1 - \frac{1}{Z_{MR}} (1 - e^{-Z_{MR}}) \right] \frac{\text{Mrad}}{\text{hr}} \quad (4)$$

Equation 4 gives the radiation rate as a function of $SvEp$ which is a measure of source strength or the energy deposited in 1 cm^3 of air on the edge of a sphere per second.

If we now place the detector on the edge of the sphere and place a lead and stainless steel shield around it, the dose rate D is found to be (Reference 16, Page 579):

$$\dot{D} = D_K \mu_{ME}(\text{air}) \phi Ep B(\mu, X) e^{-\mu X} \quad (5)$$

Where :

$B(\mu, X)$ = buildup factor as a function of the linear attenuation coefficient of the shield material μ and its thickness X

$e^{-\mu X}$ = exponential attenuation factor

Dose rate as a function of time into the accident can be calculated by using equation 4 for the outside of the HP-R-214 vessel. Hopkins give estimates of $SvEp$ as a function of time. The value of $SvEp$ is separated into 9 energy bins and equation 4 is used to calculate the rate for each energy bin. The total rate is just the sum of all 9 computations. The values of attenuation coefficients

are also functions of energy. The values used for these are given in Chart H1.

Equation 6 is used to calculate the radiation field inside the SS vessel. Here, even though the vessel is lined with both lead and steel, only a single buildup factor was used; that for lead. Lead was assumed to have the entire thickness of the container (4.597 cm). Table H1 lists the buildup factor as a function of energy as well as mass attenuation coefficients for lead and iron. The values of μ (linear attenuation coefficient for lead and iron) can be calculated using the densities also given in Chart H1. The thicknesses of lead and iron are 3.962 cm and 0.635 cm respectively. Equation 6 is given as:

$$\dot{D} = D_{\text{air}} \mu_{ME}(\text{air}) \phi E_p B(\mu_{Pb}, X_{Pb+Fe}) e^{-\mu_{Pb} X_{Pb}} e^{-\mu_{Fe} X_{Fe}} \quad (6)$$

If we wish to assume that the radiation release is not instantaneous, we multiply the values of $SvEP$ given by Hopkins by an exponential release factor having time constant τ :

$$\dot{D}_e = \dot{D} k (1 - e^{-t/\tau}) \quad (7)$$

Where :

\dot{D}_e = dose rate assuming an exponential release

t = time after initial release in hr

τ = time constant of release in hr

k = percent noble gas release

Our best estimates of dose rate used $\tau = 2$ hr. The value of k was varied until either curve matching was correct or total dose was correct. Hopkins' data was given for a 60% release. Chart H2 and H3 show typical computer output for inside and outside rates. Chart H4 shows SvEP data.

II. Calculate gamma rate inside the SS vessel due to radioactive gas trapped inside the vessel

In this section we estimate the gamma rate which the detector would measure in the event that the SS vessel were filled with the same atmosphere as the Containment Building. The volume inside the vessel is calculated to be $21.24 \times 10^3 \text{ cm}^3$. This is equivalent to a spherical volume having a radius of 17.17 cm.

Hopkins shows that the flux at the center of a sphere containing radioactive gas is:

$$\phi = S_v R \quad (8)$$

The dose rate in air at the center is:

$$D = D_K \mu_{ME}(\text{air}) S_v E_p R \frac{\text{Mrad}}{\text{hr}} \quad (9)$$

Equation 9 is then used as equation (5) to calculate the contribution to the HP-R-214 readout due to gas inside the vessel. This calculation should indicate higher levels than were actually there since it is unlikely that all the uncontaminated air inside the vessel could have been replaced by contaminated air. Also, in this case the detector fills up much of the inside of the vessel, and the spherical model hardly looks appropriate. Nevertheless we can get an order-of-magnitude answer. Chart I-4 gives the calculated D assuming an instantaneous release of 60% of the core's noble gas inventory.

Notice in chart H5 that the peak rate of 853 R/hr is approximately equal to that due to gas inside containment assuming a 20% release. Thus, since this approach is very conservative we conclude that gas inside was not an important factor. At 64 hours the level is 59 R/hr - much less than the plateau level on the stripchart between 60 and 800 hours.

III. Calculate radiation rate inside SS vessel due to beta emission from gas trapped inside vessel

In this section we calculate the rate produced by beta emission from gas that might be inside the vessel. Again we assume that the gas is of the same constituency as that in the containment atmosphere. This is a worst case since it is not possible for radioactive gas to permeate into the vessel and replace the non-radioactive gas there. In fact for a 2.5 psig pressure differential we calculate that in order to achieve equilibrium pressure the volume of gas inside would be increased by only at most 18%.

As before assume that the vessel is a sphere of radius 17.17 cm and ϕ is as given in equation 8. For electrons the energy of electrons emerging through a shield is given by:

$$E_B = E_0 - \rho \left(\frac{dE}{dx} \right) d \quad (10)$$

where :

E_0 = incident energy in Mev

ρ = density of medium in $\text{g} \cdot \text{cm}^{-3}$

dE/dx = linear stopping power of the medium in $\text{Mev} \cdot \text{cm}^2 \cdot \text{g}^{-1}$

d = thickness of absorber in cm

From Tait Page 153 (Reference 17) the dose rate is :

$$\dot{D} = k \phi \left(\frac{dE}{dm} \right) = k S_V R \left(\frac{dE}{dm} \right) \quad (11)$$

where :

dE/dm = mass stopping power for the medium in $\text{Mev} \cdot \text{cm}^2 \cdot \text{g}^{-1}$

S_V = Volumetric source strength in $\mu\text{Ci} \cdot \text{cm}^{-3}$

k = units conversion constant in $\text{g} \cdot \text{Mrad} \cdot \text{MeV}^{-1} \cdot \text{hr}^{-1} \cdot \mu\text{Ci}^{-1}$

R = Sphere radius in cm

Since in this case S_V is given in $\mu Ci \cdot cm^{-3}$ we must calculate a different conversion constant k .

$$k = \left(5.7672 \times 10^{11} \frac{\text{sec} \cdot \text{g} \cdot \text{Mrad}}{\text{Mev} \cdot \text{hr}} \right) \left(\frac{10^6 \text{Ci}}{\mu \text{Ci}} \right) \left(\frac{3.7 \times 10^{10} \text{electrons/sec}}{\text{Ci}} \right)$$

$$k = 21.33864 \times 10^7 \frac{\text{g} \cdot \text{Mrad}}{\text{Mev} \cdot \text{hr} \cdot \mu \text{Ci}} \quad (12)$$

The value dE/dx is a function of the incident beta energy and dE/dm is a function of the emergent energy E_B . In this case betas are being attenuated by the ion chamber walls which have a total thickness of 0.546 cm of Al. We have conservatively neglected the attenuation by air and fiberglass. Equations 10, 11 and 12 can be used to calculate the dose rate in the air of the ion chambers.

$$E_B = E_0 - P_{AL} \left(\frac{dE}{dx} \right)_{AL} d = E_0 - (2.7)(.546) \left(\frac{dE}{dx} \right)_{AL} \quad (13)$$

$$\dot{D} = (21.33864 \times 10^7)(17.17) S_V \left(\frac{dE}{dm} \right)_{AIR}$$

$$\dot{D} = 3.6638 \times 10^5 S_V \left(\frac{dE}{dm} \right)_{AIR} \quad (14)$$

In order to calculate \dot{D} from equation 14 we must have values of dE/dx for each beta emitter so that we can calculate E_B . Once we know E_B we can find a value for dE/dm for each emitter. Chart H.6 shows the values of these quantities. Chart H.7 gives the results of beta emission calculations for three radioactive gas concentrations inside the vessel. Very quickly Rb 88 becomes the primary source. The S_V data are from Hopkins. Chart H.8 gives a listing of some of the radioisotopes at 3.5 hours after reactor trip. The emission energies and decay chain information is also shown.

$E - B/n$ (MeV)	$\mu_M(\text{air})$ ($\text{cm}^2 \text{g}^{-1}$)	$\mu_M(\text{Fe})$ ($\text{cm}^2 \text{g}^{-1}$)	$\mu_M(\text{Pb})$ ($\text{cm}^2 \text{g}^{-1}$)	$\mu_M(\text{Al})$ ($\text{cm}^2 \text{g}^{-1}$)	$\mu_{ME}(\text{air})$ ($\text{cm}^2 \text{g}^{-1}$)	$B_r(\text{Pb})$ (units) $t = 4.597 \text{ cm}$
.04	.229	4.0	14.0	.55	.053	2.0
.15	.134	.183	1.84	.134	.0251	2.0
.40	.0953	.0919	.208	.0922	.0296	2.1
.80	.0706	.0664	.0836	.0683	.0289	2.2
1.30	.0557	.05218	.05576	.05	.02656	2.0
1.70	.04882	.04728	.049	.047	.02488	1.8
2.20	.04274	.04114	.0450	.0416	.02326	1.75
2.50	.0401	.03925	.0435	.039	.02245	1.75
2.80	.03746	.03736	.0428	.0372	.02164	1.7

161

$$\rho(\text{air}) = .001293 \text{ g cm}^{-3}$$

$$\mu_M = \frac{\mu}{\rho}$$

$$\rho(\text{Fe}) = 7.9 \text{ g cm}^{-3}$$

$$\rho(\text{Pb}) = 11.3 \text{ g cm}^{-3}$$

$$\rho(\text{Al}) = 2.7 \text{ g cm}^{-3}$$

μ data from : Etherington
Taft

B_r data from : Etherington
Reference 18

Chart H1 Attenuation Coefficients

CHART H2

***** GAMMA RATE THRU AIR AND PB *****

$$[0.333(1 - e^{-\frac{t}{2}})]$$

20%, Release total
wind

	ENERGY (MEV)	GAMMA RATE (MRAD/HR)
TIME 0.0 HRS		
	.04	0.
	.15	0.
	.40	0.
	.80	0.
	1.30	0.
	1.70	0.
	2.20	0.
	2.50	0.
	2.80	0.
TOTAL		0.
TIME 1.0 HRS		
	.04	.5659-284
	.15	.3230E-39
	.40	.6621E-07
	.80	.5737E-05
	1.30	.8252E-04
	1.70	.7590E-04
	2.20	.2905E-03
	2.50	.3124E-03
	2.80	.6443E-04
TOTAL		.8315E-03
TIME 3.0 HRS		
	.04	.1092-283
	.15	.6304E-39
	.40	.1013E-06
	.80	.5238E-05
	1.30	.1022E-03
	1.70	.9133E-04
	2.20	.3694E-03
	2.50	.3777E-03
	2.80	.6651E-04
TOTAL		.1012E-02
TIME 4.0 HRS		
	.04	.1204-283
	.15	.6978E-39
	.40	.1000E-06
	.80	.4235E-05
	1.30	.8835E-04
	1.70	.7932E-04
	2.20	.3210E-03
	2.50	.3290E-03
	2.80	.5358E-04
TOTAL		.8756E-03
TIME 5.0 HRS		
	.04	.1266-283
	.15	.7367E-39
	.40	.9454E-07
	.80	.3416E-05
	1.30	.7297E-04

CHART H2 (Cont.)

	1.70	.6576E-04
	2.20	.2661E-03
	2.50	.2734E-03
	2.80	.4181E-04
TOTAL		.7235E-03
TIME	7.0 HRS	
	.04	.1316-283
	.15	.7698E-39
	.40	.8013E-07
	.80	.2345E-05
	1.30	.4687E-04
	1.70	.4245E-04
	2.20	.1717E-03
	2.50	.1770E-03
	2.80	.2481E-04
TOTAL		.4652E-03
TIME	10.0 HRS	
	.04	.1319-283
	.15	.7757E-39
	.40	.6044E-07
	.80	.1538E-05
	1.30	.2290E-04
	1.70	.2082E-04
	2.20	.8416E-04
	2.50	.8696E-04
	2.80	.1139E-04
TOTAL		.2278E-03
TIME	14.0 HRS	
	.04	.1293-283
	.15	.7635E-39
	.40	.4188E-07
	.80	.1013E-05
	1.30	.8626E-05
	1.70	.7857E-05
	2.20	.3176E-04
	2.50	.3285E-04
	2.80	.4162E-05
TOTAL		.8631E-04
TIME	24.0 HRS	
	.04	.1220-283
	.15	.7241E-39
	.40	.1841E-07
	.80	.4379E-06
	1.30	.7457E-06
	1.70	.6797E-06
	2.20	.2747E-05
	2.50	.2843E-05
	2.80	.3551E-06
TOTAL		.7827E-05
TIME	44.0 HRS	
	.04	.1089-283
	.15	.6499E-39
	.40	.4529E-08
	.80	.9507E-07
	1.30	.5575E-08
	1.70	.5082E-08
	2.20	.2054E-07
	2.50	.2126E-07

CHART H2 (Cont.)

	2.80	.2653E-08
TOTAL		.1547E-06
TIME 64.0 HRS		
	.04	.9744-284
	.15	.5832E-39
	.40	.1529E-08
	.80	.2192E-07
	1.30	.4168E-10
	1.70	.3799E-10
	2.20	.1536E-09
	2.50	.1589E-09
	2.80	.1984E-10
TOTAL		.2386E-07
TIME 240.0 HRS		
	.04	.3692-284
	.15	.2231E-39
	.40	.8755E-10
	.80	.1563E-08
	1.30	0.
	1.70	0.
	2.20	0.
	2.50	0.
	2.80	0.
TOTAL		.1650E-08
TIME 480.0 HRS		
	.04	.9909-285
	.15	.5971E-40
	.40	.1123E-10
	.80	.1560E-08
	1.30	0.
	1.70	0.
	2.20	0.
	2.50	0.
	2.80	0.
TOTAL		.1571E-08

.292 CP SECONDS EXECUTION TIME.

LGO

 $[0.333(1-e^{-t/2})]$ 209. Balance Total
Outside

***** GAMMA RATE THRU AIR AND PB *****

	ENERGY (MEV)	GAMMA RATE (MRAD/HR)
TIME 0.0 HRS		
	.04	0.
	.15	0.
	.40	0.
	.80	0.
	1.30	0.
	1.70	0.
	2.20	0.
	2.50	0.
	2.80	0.
TOTAL		0.
TIME 1.0 HRS		
	.04	.2382E-03
	.15	.2416E-03
	.40	.5536E-03
	.80	.1536E-03
	1.30	.6507E-03
	1.70	.4794E-03
	2.20	.1530E-02
	2.50	.1524E-02
	2.80	.3106E-03
TOTAL		.5681E-02
TIME 3.0 HRS		
	.04	.4597E-03
	.15	.4716E-03
	.40	.8474E-03
	.80	.1402E-03
	1.30	.8058E-03
	1.70	.5769E-03
	2.20	.1946E-02
	2.50	.1842E-02
	2.80	.3206E-03
TOTAL		.7410E-02
TIME 4.0 HRS		
	.04	.5067E-03
	.15	.5220E-03
	.40	.8363E-03
	.80	.1134E-03
	1.30	.6967E-03
	1.70	.5010E-03
	2.20	.1690E-02
	2.50	.1605E-02
	2.80	.2583E-03
TOTAL		.6730E-02
TIME 5.0 HRS		
	.04	.5331E-03
	.15	.5511E-03
	.40	.7905E-03
	.80	.9144E-04
	1.30	.5750E-03

CHART H3 (Cont.)

	1.70	.4154E-03
	2.20	.1401E-02
	2.50	.1334E-02
	2.80	.2016E-03
TOTAL		.5893E-02
 TIME 7.0 HRS		
	.04	.5541E-03
	.15	.5758E-03
	.40	.6700E-03
	.80	.6277E-04
	1.30	.3696E-03
	1.70	.2682E-03
	2.20	.9043E-03
	2.50	.8634E-03
	2.80	.1196E-03
TOTAL		.4388E-02
 TIME 10.0 HRS		
	.04	.5555E-03
	.15	.5802E-03
	.40	.5053E-03
	.80	.4117E-04
	1.30	.1805E-03
	1.70	.1315E-03
	2.20	.4433E-03
	2.50	.4242E-03
	2.80	.5493E-04
TOTAL		.2917E-02
 TIME 14.0 HRS		
	.04	.5445E-03
	.15	.5711E-03
	.40	.3502E-03
	.80	.2713E-04
	1.30	.6802E-04
	1.70	.4963E-04
	2.20	.1673E-03
	2.50	.1603E-03
	2.80	.2006E-04
TOTAL		.1958E-02
 TIME 24.0 HRS		
	.04	.5135E-03
	.15	.5416E-03
	.40	.1539E-03
	.80	.1173E-04
	1.30	.5880E-05
	1.70	.4293E-05
	2.20	.1447E-04
	2.50	.1387E-04
	2.80	.1712E-05
TOTAL		.1261E-02
 TIME 44.0 HRS		
	.04	.4585E-03
	.15	.4861E-03
	.40	.3787E-04
	.80	.2545E-05
	1.30	.4396E-07
	1.70	.3210E-07
	2.20	.1082E-06
	2.50	.1037E-06

CHART H3 (Cont.)

	2.80	.1279E-07
TOTAL		.9854E-03
TIME 64.0 HRS		
	.04	.4102E-03
	.15	.4362E-03
	.40	.1278E-04
	.80	.5869E-06
	2.80	.1279E-07
TOTAL		.9854E-03
TIME 64.0 HRS		
	.04	.4102E-03
	.15	.4362E-03
	.40	.1278E-04
	.80	.5869E-06
	1.30	.3287E-09
	1.70	.2400E-09
	2.20	.8088E-09
	2.50	.7753E-09
	2.80	.9564E-10
TOTAL		.8598E-03
TIME 240.0 HRS		
	.04	.1554E-03
	.15	.1669E-03
	.40	.7320E-06
	.80	.4185E-07
	1.30	0.
	1.70	0.
	2.20	0.
	2.50	0.
	2.80	0.
TOTAL		.3231E-03
TIME 480.0 HRS		
	.04	.4172E-04
	.15	.4467E-04
	.40	.9392E-07
	.80	.4177E-07
	1.30	0.
	1.70	0.
	2.20	0.
	2.50	0.
	2.80	0.
TOTAL		.8652E-04

.289 CP SECONDS EXECUTION TIME.

CHART H4

RA /LNH, FN=TAPE4	7.0487E3 1.5096E6 1.0497E6 8.4200E4 3.9215E5 3.0146E5 1.07E2E6 1.0625E6 1.4210E5 14.0 7.6676E5 1.4773E6 7.2323E5 5.5158E4 1.4689E5 1.1312E5 4.0376E5 3.9905E5 5.1597E4 24.0 7.2247E5 1.3997E6 3.0 3.1753E5 2.3820E4 1.2686E4 9.7767E3 3.4895E4 3.4504E4 4.3993E3 44.0 6.4512E5 1.2563E6 7.8139E4 5.1707E3 9.4842E1 7.3093E1 2.6088E2 2.5796E2 3.2867E1 64.0 5.7715E5 1.1273E6 2.6379E4 1.1923E3 7.0908E-1 5.4648E-1 1.9505E0 1.9287E0 2.4573E-1 240.0 2.1869E5 4.3134E5 1.5103E3 8.5008E1 0. 0. 0. 0. 0. 480.0 5.8697E4 1.1543E5 1.9379E2	8.4856E1 0. 0. 0. 0. 0. 720.0 1.5882E4 3.0830E4 8.0309E1 8.4706E1 0. 0. 0. 0. EOI ENCOUNTERED.
0.0		
8.6379E5		
1.5959E6		
3.3253E6		
1.2402E6		
2.9768E6		
3.4087E6		
6.6778E6		
1.2312E7		
1.8691E6		
1.0		
8.5188E5		
1.5867E6		
2.9031E6		
7.9309E5		
3.5681E6		
2.7747E6		
9.3762E6		
9.6389E6		
2.0283E6		
3.0		
8.3259E5		
1.5687E6		
2.2506E6		
3.6670E5		
2.2378E6		
1.6910E6		
6.0392E6		
5.8996E6		
1.0605E6		
4.0		
8.2449E5		
1.5600E6		
1.9956E6		
2.6640E5		
1.7383E6		
1.3195E6		
4.7147E6		
4.6176E6		
7.6755E5		
5.0		
8.1711E5		
1.5514E6		
1.7769E6		
2.0240E5		
1.3524E6		
1.0305E6		
3.6815E6		
3.6144E6		
5.6425E5		
7.0		
8.0397E5		
1.5344E6		
1.4254E6		
1.3149E5		
8.2216E5		
6.2968E5		
2.2486E6		
2.2147E6		
3.1691E5		
10.0		

* TIME (hr)	GAMMA RATE (D) (Mrad/hr)
0	$.853 \times 10^{-3}$
1	$.8277 \times 10^{-3}$
2	$.5526 \times 10^{-3}$
4	$.4541 \times 10^{-3}$
7	$.2708 \times 10^{-3}$
10	$.1812 \times 10^{-3}$
14	$.1257 \times 10^{-3}$
24	$.8493 \times 10^{-4}$
44	$.6754 \times 10^{-4}$
64	$.5912 \times 10^{-4}$
240	$.2224 \times 10^{-4}$
480	$.5958 \times 10^{-5}$
720	$.1605 \times 10^{-5}$

* TIME = 0 CORRESPONDS
TO 2.5 HOURS AFTER
REACTOR TRIP

CHART H5 RATE INSIDE SS VESSEL DUE TO GAS
INSIDE VESSEL (60% INSTANTANEOUS RELEASE)

ISOTOPE	E_α Mev	$(dE/dx)_{AL}$ Mev · cm ² · g ⁻¹	E_β Mev	$(dE/dm)_{AIR}$ Mev · cm ² · g ⁻¹
Kr 85M	.841	1.514	- 1.39	
Kr 85	.687	1.55	- 1.59	
Kr 87	3.49, 3.89, ...	2.3 (Ave)	.26	2.24
Kr 88	.52	1.6	- 1.84	
Rb 88	5.34	1.72	2.80	1.77
Xe 133	.346	1.77	- 2.26	
Xe 135	.91	1.51	- 1.31	
Xe 137	4.2	1.65	1.77	1.7
Xe 138	.82, 2.4	1.55	.12	3.4
Cs 138	2.5, 3.5	1.58 (Ave)	.67	1.7

CHART H6 ISOTOPE CHARACTERISTICS

TIME (hrs past 6:30 AM)	RATE (R/hr) 100% Containment Atmos., 60% Release INSTANTANEOUS	RATE (R/hr) 10% Containment Atmos., 60% Release Exponentially ($\tau = 2 \text{ hr}$)	RATE (R/hr) 10% Containment Atmos., 20% Release Exponentially ($\tau = 2 \text{ hr}$)
0	9940	-	-
.46	21800	-	-
1	23400	-	-
2	20500	1055	352
3	18800	1880	626
4	10700	1070	356
7	4800	480	160
10	2260	226	75
14	800	80	27
20	200	20	7
56	.03	-	-
240			

CHART H7 Beta Dose Rates due to Radioactive Gas inside Vessel

CHART H8

ISOTOPE	ACTIVITY (μ Ci/cm ³)	HALF-LIFE	EMISSION (MeV)	%	DECAYS TO
Kr - 83M	6.16	1.86 h	.0094 γ		Kr 83
Kr - 85M	79.6	4.48 h	.841 β .151 γ .304 γ	75.5 14	Rb 85
Kr - 85	1.03	10.72 Y	.687 β .514 γ		Rb 85
Kr - 87	7.78	76 m	3.49 β 3.89 β .403 γ .846 γ 2.55 γ	48.3 7.2 12.95	Rb 87
Kr 88	104	2.84 h	.52 β 2.39 γ 2.19 γ 1.529 γ .196 δ	35 13 11 26.3	Sr 88
Rb - 89	116.8	17.7 m	5.34 β .898 γ 1.836 γ 2.67 δ	14.5 22.1 2	Sr 89
Xe - 131 M	3.81	11.92 d	.03 δ	34	Xe 131
Xe - 133M	31.4	2.19 d	.03 γ .233 δ	45 10.3	Xe 133
Xe - 133	1376	5.25 d	.346 β .63 δ .035 δ .081 γ	38 8.8 37.1	Cs 133
Xe - 135	140.7	9.09 h	.91 β .25 δ .608 δ	90.3 2.9	Cs 135
		3.85 m			
Xe - 137			4.2 β .455 δ		
Xe - 138		14.2 m	.82 β 2.4 β .258 γ .4345 δ	1.768 γ	Cs 138
Cs - 138		32.2	2.5 β 3.5 β 1.435 γ 1.0 δ		Ba 138

Specified External Distribution Only:

**Mr. Frank Tooper
Office of TMI Programs
N. E. 23
U. S. Department of Energy
19901 Germantown Road
Germantown, Maryland 20767**

**Mr. R. D. Meininger
EG&G Idaho, Inc.
P. O. Box 88
Middletown, Pennsylvania 17057**

**Dr. W. W. Bixby
U. S. Department of Energy
P. O. Box 88
Middletown, Pennsylvania 17057**

**Mr. Ronald Holton
U. S. Department of Energy
AL/ETD
Albuquerque, New Mexico 87185**

2340 J. G. Webb
2341 M. B. Murphy (5)
2341 G. M. Mueller (3)
2341 C. R. Alls
2360 T. L. Workman
6400 A. W. Snyder
6422 D. A. Powers
6440 D. A. Dahlgren
6445 J. H. Linebarger
6445 P. A. Bennett
6446 L. L. Bonzon
6446 F. V. Thome
6449 K. D. Bergeron
7541 W. C. Jernigan
3151 B. J. Tolman
3151 W. L. Garner (3) DO NOT ANNOUNCE
8024 C. M. Ostrander (5)